APPROACHES TO FUNCTIONAL ELECTRICAL STIMULATION INDUCED CYCLING AND APPLICATION FOR THE CHILD WITH A SPINAL CORD INJURY

A DISSERTATION
SUBMITTED TO THE DEPARTMENT OF MECHANICAL ENGINEERING
OF THE UNIVERSITY OF GLASGOW
FOR THE DEGREE OF
DOCTOR OF PHILOSOPHY

By
Calum George Alexander McRae
July 2006

Abstract

In addition to the primary effects normally associated with spinal cord injury (which can include a loss of volitional motor control and sensation), individuals who suffer one are also subject to many additional health complications which affect them throughout life. These secondary symptoms, which are fast becoming the leading cause of death in this population, occur because of a sedentary lifestyle. The technique of inducing paralysed muscle contraction through application of low-level electrical charges to intact motor nerves, known as functional electrical stimulation (FES), can be utilised in several different ways to return some measure of function to spinal cord injured individuals. One particular application which has the potential to improve general health and fitness in this population through facilitating exercise is cycling.

This modality (known as FES-cycling) is the common theme linking the two main research areas which this thesis describes. In the hope of more compact and user-friendly approaches to FES-cycling through the incorporation of modern sensor and computing technology, two new hip-angle-based strategies (both of which utilise a limb-mounted sensor) and a "traditional" crank-angle-based strategy have been developed and incorporated into a PDA-based multi-functional FES system. Through both simulation and tricycle-based experiments, all three approaches have been shown to provide practical stimulation activation timing.

The second research focus concerns the development of two FES-cycling systems which are suitable for a spinal cord injured child, and methods to facilitate the intended use of both devices. A standard child's tricycle has been modified with appropriate instrumentation for FES-cycling and testing involving its target population was carried out at a US-based paediatric research hospital. These experiments culminated in the demonstration of FES-cycling by an untrained seven year old T4/T6 (motor complete) subject, and the evolution of the device into one which should be able to meet the specific needs of spinal cord injured children.

A second system with integrated motor has also been developed. As well as offering motor assistance, this device incorporates additional instrumentation to allow investigation into exercise and training capabilities. Experiments have been undertaken to validate this equipment and it is now ready for future pilot work involving paediatric subjects.

The two research foci in this thesis represent what are, in our opinion. important routes that FES-cycling should take to progress into the home environment and also allow participation of a population who have potentially the most to gain from using it.

Acknowledgements

It is impossible to avoid printing a long long list of names, such as is usually found here, because what follows would undoubtedly never have been possible without the support and patience of the extremely dedicated and brilliant people I have worked with during the last four years.

Firstly, thanks to my supervisors, Ken Hunt and Henrik Gollee. Both have provided me with timely expert guidance and teaching throughout. More importantly, from a personal point of view, I doubt I would have been able to accomplish what I have without the relaxed and supportive environment they provided through times of illness. Thank you to all those at the CRE (and those who hold it together - Elaine!), most who have become good friends and some who have even become dedicated Redlines fans (Geraint). You all helped me so much during my time here. In particular, colleagues who assisted during experiments: Ben (remember to take the van back!!), Pedro (Cleopatra's misses you greatly!), Barry (for bringing articulate, witty banter and guidance!), Andrew and Georg. Also, those who helped an engineer understand some non-engineering things (Sylvie, Lindsay and Chiara).

There are many others in and around the department who aren't named here but I will miss greatly and wish all the best for the future. The guys in the two workshops are also due a huge thank you (in particular Brian, Gordon and George) for making square pegs fit in round holes on the trikes!.

To everyone at Shriners, thank you too for all your support! Especially, Therese, Rich and Brian. I can't wait to hop across the pond (if the VISA process ever ends!). Most importantly, I am deeply grateful to all the subjects/cyclists I worked with. Not only those at Shriners, who together with their families showed remarkable patience and enthusiasm, but also the "seasoned pro" I had the good fortune to spend time with on a weekly basis in Glasgow.

To all my other friends (even those from Gargunnock...) around and far away: thanks for being there and understanding my social abstinence during the past months. Gav and Marisa - I promise I'll make time for recording now! Mum, Dad, John, Eilidh and Barry, thanks so much for for you support and patience. Most of all (and trying not to get too sappy!), my biggest thanks to Alyssa for keeping me calm, focused, making grammar seem "less umpossible!" and making me smile always.

Contents

List of Tables

List of Figures

List of Abbreviations

ASIA - American Spinal Injury Association

BMD - Bone Mineral Density

BMX - Bicycle Motocross

CF - Compact Flash

CT - Computed Tomography

CNS - Central Nervous System

DAQ - Data Acquisition

DC - Direct Current

EMG - Electromyography

FES - Functional Electrical Stimulation

FF - Fast Fatiguable motor unit

FR - Fast Fatigue Resistant motor unit

LED - Light Emitting Diode

PC - Personal Computer

PDA - Personal Digital Assistant

PID - Proportional plus Integral plus Derivative

PNS - Peripheral Nervous System

RF - Radio Frequency

S - Slow motor unit

SCI - Spinal Cord Injury

SPI - Serial Peripheral Interface

SRM - Schoberer Rad Messtechnik

VFT - Variable Frequency Train

1 Introduction

The contributions presented in thesis pertain to two separate themes, both of which are associated with the technique of functional electrical stimulation induced cycling for persons with a spinal cord injury. The first concerns a novel approach to stimulation control for cycling using a limb-mounted sensor and hand-held computer system. The second involves the development of FES-cycling methods and equipment for the child with a spinal cord injury. The thesis outline and contributions are as follows:

1.1 Thesis Outline

Chapter 2

Background information on the topics of spinal cord injury and functional electrical stimulation (FES) are given here. In addition, the concept of functional electrical stimulation induced cycling (FES-cycling) is introduced, with a review and discussion of associated benefits which have been reported.

Chapter 3

The main literature review, presented here, encompasses a description of FES-cycling systems (and accompanying technology) developed to date, an introduction to paediatric spinal cord injury and the role of FES in this population thus far. In a discussion of these topics, arguments for the work reported in subsequent chapters are formed and presented.

Chapter 4

Investigations into utilising a limb-mounted sensor for control of stimulation activation timing during FES-cycling (including all methodology, results, discussion and conclusions), and incorporation of these (and "traditional") approaches into a new multi-functional PDA-based FES system are described here.

Chapter 5

Chapter 5 describes the development of new FES-cycling methods and equipment for use within the paediatric spinal cord injured population. Details on a new tricycle-based design, its evolution and testing within the target population are presented and discussed.

Chapter 6

Following on from chapter 5, the development of a paediatric FES-cycling system with integrated motor is described here. Experiments designed to verify additional instrumentation and complete system operation are also discussed.

Chapter 7

The final chapter presents conclusions based on the thesis' contributions and provides suggestions for relevant future work.

1.2 Thesis Contribution

New Approaches to FES-cycling Stimulation Activation Control Using a Limb-mounted Sensor (Chapter 4)

Two novel approaches which utilise a measured hip angle to govern muscle activation timing for FES-cycling stimulation control strategies have been developed. Both have been tested by employing simulated data, then verified using experimental data.

Utilising a new PDA-based FES System for FES-cycling (Chapter 4)

New hip-angle-based and "traditional" crank-angle-based FES-cycling strategies have been implemented into a multi-functional PDA-based FES system which is capable of both surface and implanted stimulation. We have shown that, providing there is accurate sensor measurement, practical stimulation activation patterns can be produced in realtime using each strategy.

Development of a Tricycle-based FES-cycling System for the Child with a Spinal Cord Injury (Chapter 5)

A standard child's tricycle has been modified with appropriate instrumentation and orthotic equipment for FES-cycling. Testing (carried out in collaboration with a US-based research hospital) involving 10 paediatric spinal cord injured subjects has been undertaken to evaluate the system's suitability for its target population. Assessment of participant comfort and safety whilst seated on the tricycle has resulted in further seating, orthotic and handlebar adaptations. These experiments have led to our conclusion that a modular based approach with a standard device at its heart can offer a low-cost and aesthetically pleasing route to FES-based exercise and recreation in this population.

Demonstration of FES-cycling by an Untrained Paediatric Spinal Cord Injured Subject (Chapter 5)

An untrained seven year old T4/T6 (motor complete) subject has successfully achieved a significant period of unaided stationary FES-cycling using our tricycle-based system. In addition, experiments involving a total of three spinal cord injured children have provided the basis from which to develop appropriate methods for FES-cycling within this population.

Development of a Motor-integrated FES-cycle Test Bed and Training Device for the Child with a Spinal Cord Injury (Chapter 6)

A second, motorised, paediatric tricycle-based system has been developed. Including all FES instrumentation, orthotic and safety equipment present on the non-motorised system, this device has been further modified by way of a hub motor, torque sensor and appropriate interface equipment for full laptop-based analysis and control. In addition to providing assistance during training, this setup should provide a platform from which to develop motor-integrated mobile cycling strategies and undertake detailed investigations into the target population's exercise capabilities.

1.3 Publications

C. G. McRae and K. J. Hunt, "Development of methods and equipment for functional electrical stimulation induced cycling for use within the paediatric spinal cord injured population", in *Proc. 4th Ann. Conf. IEEE EMBSS UKRI PG Biomedical Engineering and Medical Physics, (Reading, UK)*, pp. 7-8, July 2005.

2 Background

This chapter outlines background information in areas fundamental to the research delineated in this thesis. Spinal cord injury shall be discussed in section 2.1 followed by a basic description of mechanisms involved in the human nervous and muscular system in section 2.2. An introduction to functional electrical stimulation (FES) will be given in section 2.3 with the final topic of electrical stimulation induced cycling (or FES-cycling) and the efficacy of this technique as an exercise and rehabilitation tool introduced in section 2.4.

2.1 Spinal Cord Injury

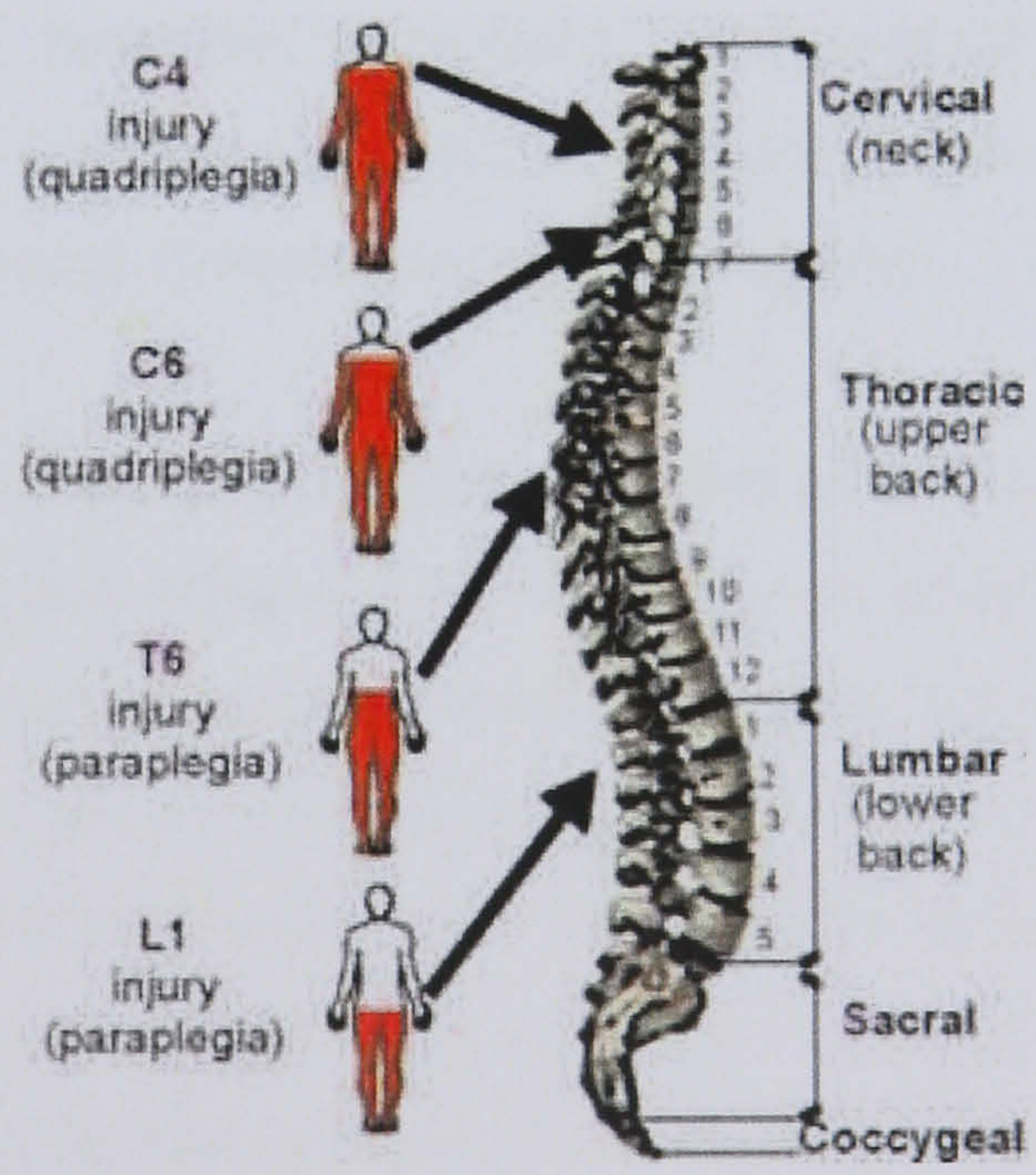

Figure 2.1: The spinal cord and areas affected at various injury levels. (Adapted from http://www.paraquad.asn.au/introduction/spinal/spinal.html)

The effects of spinal cord injury (SCI) can be detrimental to both general health and quality of life with many serious primary symptoms as well as subsequent secondary medical complications affecting the body. Annual Incidence in the UK is around ten to fifteen per million [1] compared with an estimated forty per million in the USA. This equates to approximately 40,000 and 230,000-250,000 people living with a spinal cord injury in each country respectively [2, 3]. Nearly all SCIs result from some kind of blunt trauma and although there is evidence to suggest that the chief mechanism varies in paediatric and adolescent age groups [4] (this will be discussed further in the sequel), motor vehicle accidents account for the majority of injuries in the adult population. The second and third highest proportions tend to vary, but are usually related to falls, sport or violence.

Although this population makes up only a small proportion of the total, social and economic costs are extremely high, thus warranting extensive research into rehabilitation.

The severity and range of primary symptoms endured depend on the level of injury, as determined by the point on the spinal cord below which function and sensory information is impaired. This effect and the position of these points is illustrated in figure 2.1 where each level is designated by the region in which it lies (cervical, thoracic, lumbar or sacral) and the spinal nerve number. Below the level of a lesion both afferent and efferent pathways (along with the information they carry) will be affected. The result can be a loss of volitional control over muscles and sensation of areas innervated below the lesion site, as the link between peripheral and central nervous system has been interrupted. Additionally, autonomic control of heart rate and blood pressure, along with regulation of bladder and bowel, may be disrupted.

Over time, these symptoms are often followed by secondary health complications, which arise from the aforementioned effects and consequent sedentary lifestyle forced upon SCI persons. Following a spinal injury, circulation may be poor in the region distal to the lesion, making the skin prone to deterioration. This, in combination with insensitive skin, can result in pressure sores if the person sits or lies in one position for long periods of time. There is also a reduction in bone mineral density post-injury, with a possible one-third being lost in the first year [5], leading to an increased risk of fracture. Susceptibility to heart disease may also increase as atrophied muscles (otherwise used to stress the cardiovascular system) are not applied to their full potential [6].

The extent to which a person's sensory and motor control is affected is described as "complete" or "incomplete", where a complete injury corresponds to a total loss of muscle control and sensation below the injury. The degree of impairment can be further defined through the American Spinal Injury Association[1] (ASIA) classification scale which uses a grading system from A to E (with A being the highest level of impairment).

When considering the effects of a spinal cord injury, it is immensely important not to overlook the social consequences. As well as managing all the primary and secondary health effects, the day-to-day life of an SCI person is confounded with extra challenges such as the access, transferring and transportation involved in simple tasks whose execution would ordinarily be taken for granted.

2.2 Mechanisms of the Nervous and Muscular Systems

To fully understand how tasks are performed in able bodied individuals, and consequently how the control systems and actuators employed are affected by spinal cord injury, the basics of the mechanisms involved should be discussed.

2.2.1 The Nervous System

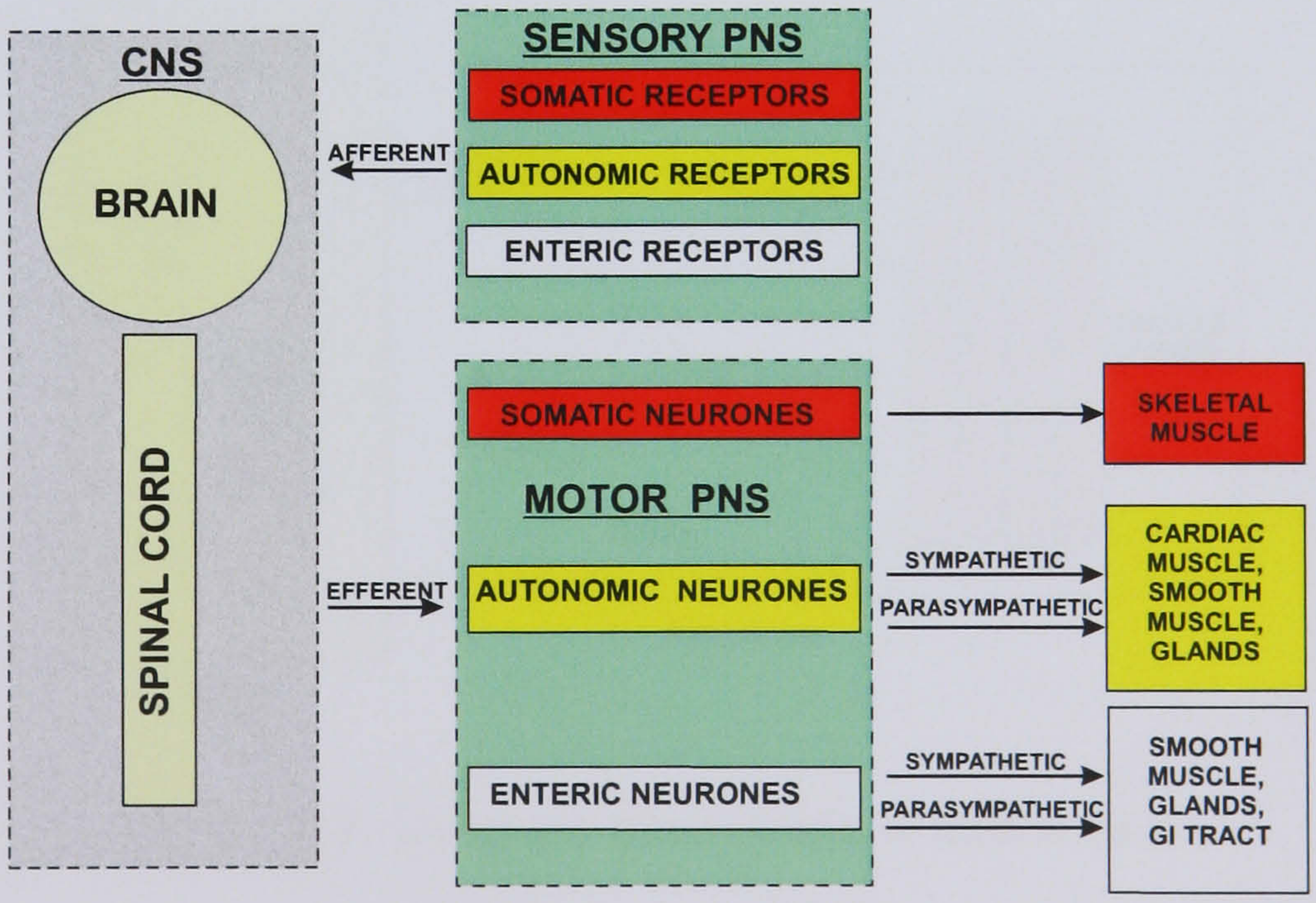

Figure 2.2: Divisions of the nervous system. CNS - central nervous system, PNS - peripheral nervous system, GI - gastrointestinal.

[1]American Spinal Injury Association, Atlanta, GA, USA. http://www.asia-spinalinjury.org/

Figure 2.2 illustrates the divisions of the nervous system, which can be divided into the central nervous system (CNS); consisting of of the brain and spinal cord, and the peripheral nervous system (PNS) [7]. Information is passed between the PNS and CNS via afferent and efferent pathways. The former carry action potentials to the CNS from sensory receptors while command information from the CNS to PNS is carried by the latter. The PNS can be subdivided into the somatic, autonomic and enteric divisions which are concerned with control of skeletal muscle, cardiac muscle, and the gastrointestinal tract respectively. The autonomic and enteric divisions, which have further sympathetic and parasympathetic subdivisions, are also responsible for smooth muscle and glands.

Voluntary motor control is achieved by action potentials being transmitted through efferent pathways from the CNS to the somatic part of the PNS. These action potentials are propagated via motor neurones which innervate the relevant skeletal muscles. Feedback for this process is obtained through somatic sensory receptors passing information to the CNS through afferent pathways. In conjunction with this, the autonomic division regulates involuntary systems using its receptors and neurones in a similar fashion.

2.2.2 Muscle Contraction

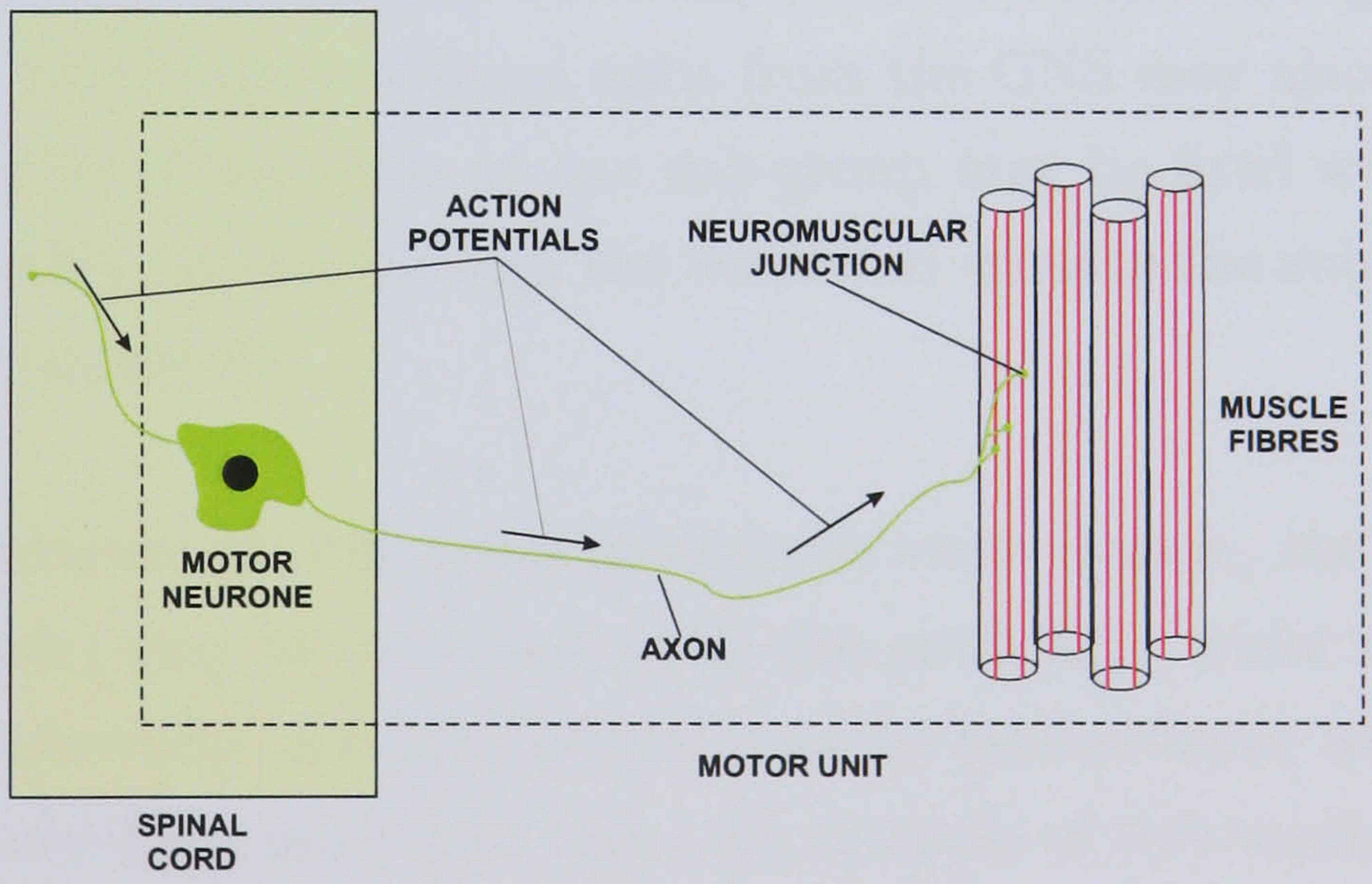

Figure 2.3: Diagram illustrating a motor unit.

The characteristics of muscle contractions largely depend on the motor units with which they are identified. Motor units (figure 2.3) consist of somatic motor neurones, their axons and the muscle fibres which they innervate [8]. There are three types of these units: slow, fast fatiguable and fast fatigue resistant. The individual properties of these, along with the proportion, dictate the behaviour of the muscle.

Slow units (S) innervate a small (relative to other unit types) number of muscle fibres. These fibres are of small diameter and are associated with low force generation but high fatigue resistance. The neurones of these units are relatively small, with small diameter axons extending from them. Both conduction velocity (of an action potential) and activation threshold for artificial stimulation (depolarisation beyond this will result in a contraction) are determined by the axon diameter with a larger diameter corresponding to a higher conduction velocity and lower threshold.

Fast fatiguable units (FF), as the name suggests, are associated with low fatigue resistance and the generation of high forces. Their neurones will be larger, with high conduction velocity/low threshold (for artificial stimulation) axons which have synaptic connections with large numbers of fibres. The last type of unit, fast fatigue resistant (FR), has characteristics which lie in between the other two in that it is associated with relatively high contraction forces and fatigue resistance. They have medium sized neurones and axons which innervate a lower number of fibres than the fast fatiguable type.

During volitional contractions, recruitment of motor units will generally follow a slow to fast-fatiguable (with FR units in between) order. This allows a gradual increase in contraction force. Stimulation of these units from the CNS may also be asynchronous, meaning a proportion of the units in one sub-group may be fired while the remaining recover. By selectively cycling through the recovered units in the sub-group, the effects of fatigue may be countered

By employing a mixture of unit types within the same muscle, the fatigue resistance (of the whole muscle) may be increased while also enabling a wider range of actions to be carried out. Conversely, one type of unit may be predominant within the muscle if it is consistently used for a particular task. An example of this would be those muscles used for posture, where slow fatigue resistant units are more desirable, and thus make up a higher proportion of the total.

2.3 Functional Electrical Stimulation

Functional Electrical Stimulation (FES) is a method for forcing muscle contraction through application of an electrical charge to intact peripheral or central motor nerves. Although it can be used for other purposes, including elimination of drop foot in stroke victims [9] and assistance for individuals affected by cerebral palsy [10], perhaps its most common use (and the main focus of this thesis) is in the restoration of function, and as a method of increasing general health and fitness in spinal cord injured persons.

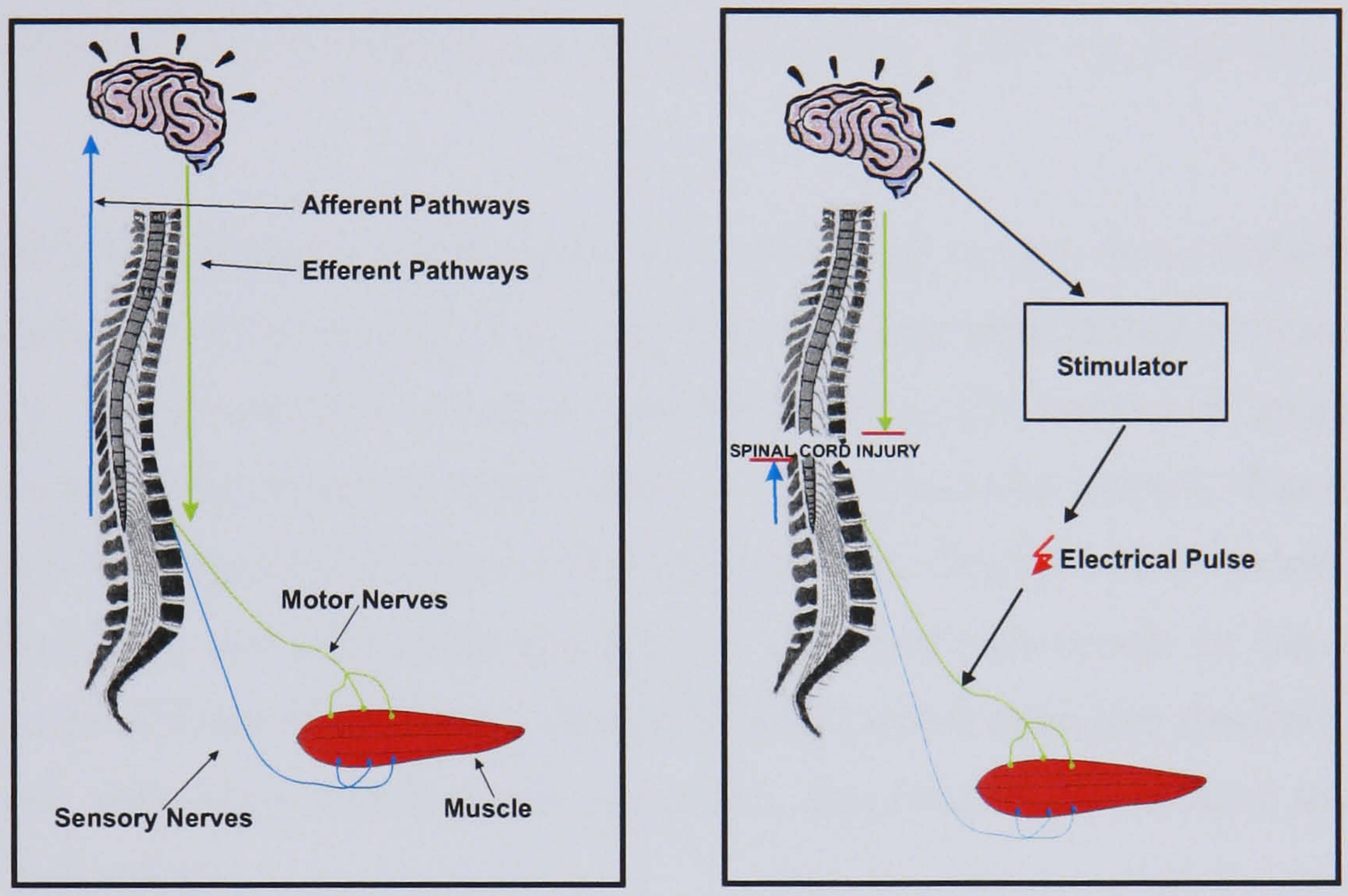

(a) Voluntary muscle contraction. (b) Muscle contraction with FES.

Figure 2.4: Muscle contraction through FES.

As described earlier, voluntary muscle contraction (figure 2.4(a)) is achieved while action potentials propagate from the CNS to PNS. With spinal cord injury, a lesion in the spinal cord interrupts this traffic in either direction. Thus to achieve controlled muscle contraction, an external stimulus in the form of an electrical charge may be applied to the appropriate motor nerves (figure 2.4(b)).

This charge may take the form of a unidirectional rectangular pulse, as shown in figure 2.5. Stimulation intensity, and therefore strength of contraction/number of muscle fibres recruited, can be controlled by varying the pulse width, amplitude or frequency. By implementing some form of control over these pulses, strategies may be formed whereby paralysed muscles are contracted sequentially to perform a desired action.

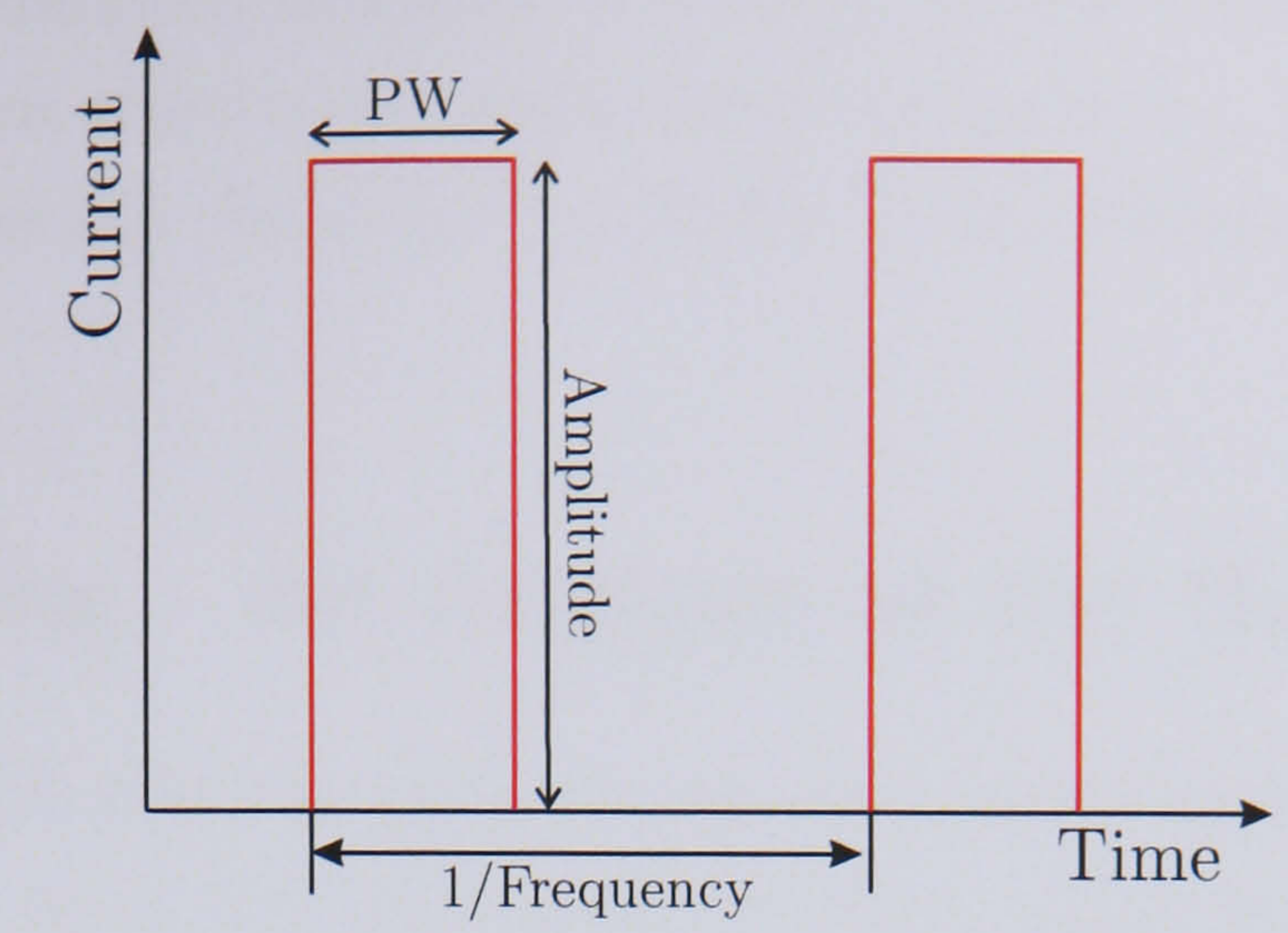

Figure 2.5: Unidirectional electrical pulse. PW - pulsewidth.

Delivery of electrical pulses to the nerve is carried out using three different methods: transcutaneously (where a charge is passed through the skin using surface electrodes), percutaneously (using electrode needles inserted close to the nerve) or implanted (where electrodes are surgically inserted either close to or around the nerve). Each have advantages and disadvantages depending on the application. Surface electrodes, for instance, are non-invasive, but are relatively inaccurate and use can result in the activation of unwanted muscles (those that might antagonise or counteract the desired motion). On the other hand, although much more accurate, implanted electrodes involve surgery and a risk of infection.

For FES to be possible, the lower motor neurones which are to be stimulated must be intact. In other words, an action potential must still be able to propagate to the muscle along the nerve from the point of external stimulation.

Bearing in mind the complex nature of the mechanisms involved in volitional control and the crude nature of FES, it is no surprise that muscle contractions initiated through artificial stimulation are relatively inefficient in terms of the strength of contraction and endurance. This is chiefly because of two reasons. Firstly, motor unit recruitment pattern differs from that described in section 2.2.2. The actual mechanisms involved are debatable but one idea, which has been widely suggested, is that the recruitment order under voluntary control is reversed during artificial stimulation conditions. More recently, however, this view has been contended with the suggestion that the process is in fact non-selective [11]. Secondly, unlike in voluntary control, where there is a measure of selection by the central nervous system as to the proportion of units being used at any given time, once a motor unit's threshold has been reached it will continue to fire until the artificial stimulation is ceased. The effect of these factors on FES applications may vary with different stimulation application methods (i.e. implanted versus surface stimulation), but generally the result is a faster onset of fatigue.

2.4 FES-Cycling - An Analysis of the Benefits

One application of FES with the potential for use as both an exercise and recreational modality is cycling. As a well established method which has been around for over twenty years, many studies have been performed to investigate the effects and potential benefits (health and social) it may bring to the spinal cord injured population. This section will attempt to summarise these findings in order to present the evidence for FES-cycling as a rehabilitative exercise training tool. A history of the technology involved, along with the state of the art, is discussed in chapter 3.

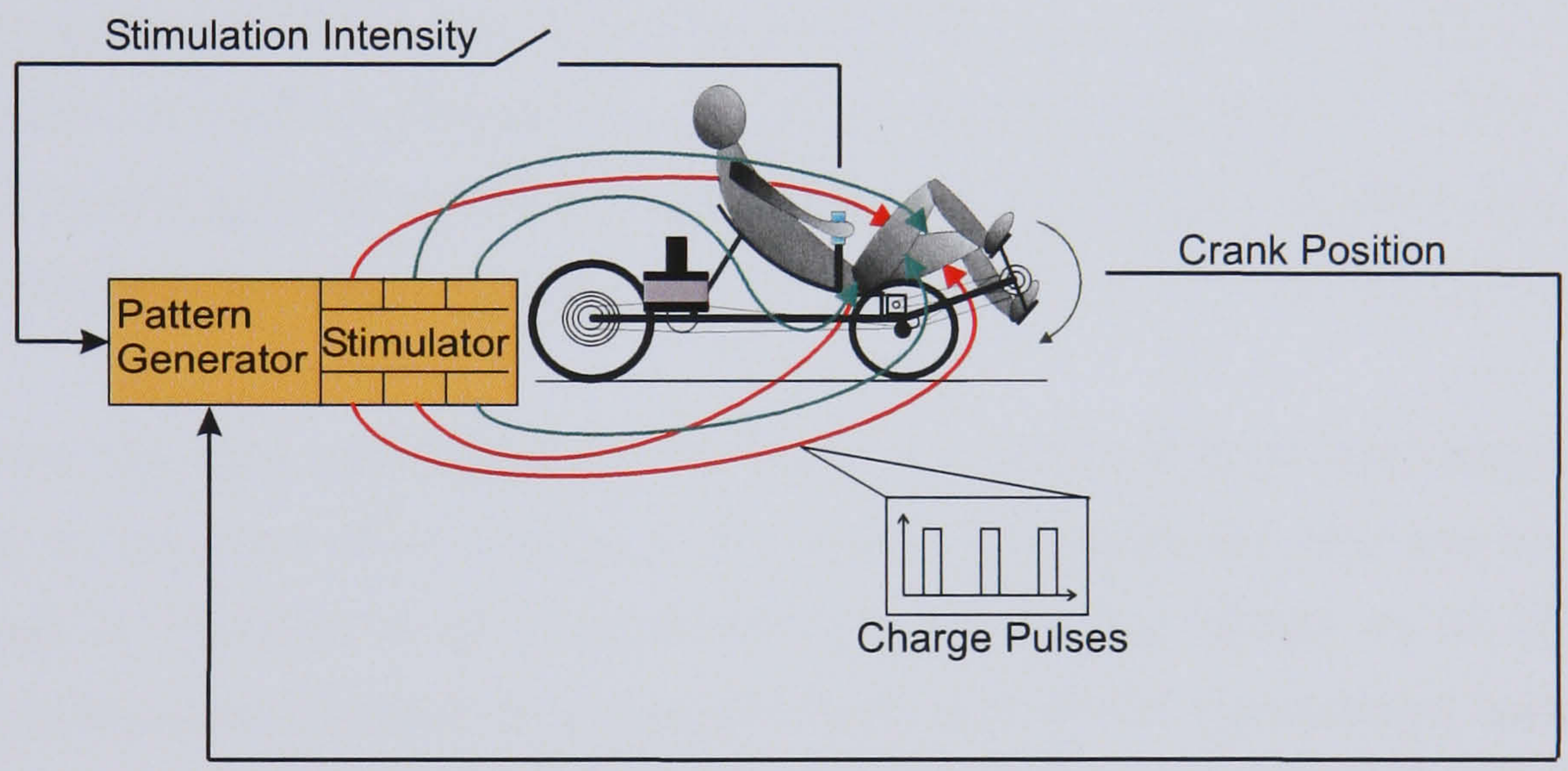

Figure 2.6: General FES-cycling setup.

Petrofsky et al. [12] developed what was probably the first FES-cycling system during the early eighties. Since then, several variations on the theme have been introduced, including both commercial ergometers (such as the ERGYS II[2] and Stimmaster Galaxy[3]) and systems capable of mobile cycling [13, 14]. Although these devices differ in their design and capabilities, there are a few themes which are common to all.

[2]Therapeutic Alliances Inc., USA. http:/www.musclepower.com/
[3]Electrologic of America, Inc., USA. http://www.stimmaster.com/

Broadly, the system (figure 2.6) will be based around some form of ergometer or modified cycle on which the rider is seated. Usually, the position of the pedals will be monitored in some way and this information may be used to dictate (through a control algorithm) which muscle contractions are required to enable a continuous pedal cycle. Control of the stimulation intensity (which depending on the system will either be automatic or via the rider) corresponds to a modulation of the charge being sent to the relevant muscle groups and consequently manipulation of pedal torque and cadence.

Following implementation of these concepts in systems which allow spinal cord injured persons to cycle using their own muscles, many feasibility studies have been conducted to investigate the potential medical benefits (which could counteract the secondary health complications described in section 2.1) this modality could offer.

In the majority of studies undertaken, the most commonly used muscle groups are the quadriceps, hamstrings and gluteal muscles, [15, 16, 17, 18, 19]. These are (certainly the quadriceps and hamstrings) the major force-producing muscles used during cycling. Importantly, they are also some of the largest muscles in the body, and thus are more likely to invoke a high cardiopulmonary response when contracted. The bulk of investigations involving FES-cycling focus on these three muscle groups and, therefore, most of the data reflecting a change in size or strength are connected to them.

In most cases the size, and isometric strength of the quadriceps and hamstrings have been shown to increase after a period of cycling. A significant increase in thigh girth was reported by Phillips et al. [15], Arnold et al. [16] and Sloan et al. [17] with the latter also showing an increase in cross-sectional area of the quadriceps using CT scanning techniques. In a separate eight week study, Hjeltnes et al. [18] describe combined, stimulated muscle cross-sectional area increases of 22%.

Janssen et al. summarise this, in a review of the clinical efficacy of FES exercise training [20], with their opinion that FES-cycling appears to reverse the disuse atrophy of paralysed muscle, or at least retard the rate of progression. In addition, both anecdotal and reported subjective evidence [21] by FES-cycling participants support this through claims of improvements in bulk and appearance.

Although in most setups only the muscle groups mentioned previously are stimulated during cycling, given the nature of surface FES (i.e. relatively inaccurate), other muscle groups, notably the calf, may be recruited indirectly through activation of non-targeted motor nerves. However, in cases where the size/bulk of calf muscles have been analysed [15, 16], no significant increase has been found following an FES-cycling training programme.

One of the biggest and most well documented benefits of FES-cycling is a raised level of cardiopulmonary fitness. Through inclusion of the body's largest muscle groups a high cardiac response can be invoked and following training central physiological adaptations may occur which result in an enhanced capability to transport blood and oxygen to peripheral areas, in particular to those muscles being utilised.

Increases in relevant outcomes such as heart rate and oxygen uptake, both over the course of a session and following extended training programmes, have been described by many investigators, [22, 16, 23, 24, 25, 26, 27]. Post-training peak oxygen uptake gains of 70% [18] and values as high as 1.77L/min [28] have been reported. However, the investigation which yielded a 70% increase involved a high intensity programme (7 sessions a week for 8 weeks) with eight tetraplegic subjects and final values of approximately 1.2L/min. The author attributes the massive gains in peak uptake to the intensity of training and low initial endurance capacity of the leg muscles. Indeed, the high level of injury in this particular subject population (C5-C7) and consequent low initial peak values of oxygen uptake (approximately 0.6L/min) reflect this. Studies involving both tetraplegic and paraplegic subjects have yielded more modest gains. Hooker et al. [23] describe peak oxygen uptake gains of 23% in theirs. In a much longer training programme involving both tetraplegic and paraplegic subjects, Mohr et al. [25] report an almost 20% increase in maximal values.

Janssen et al. [20] put the magnitudes of oxygen uptake seen during FES-cycling (around 1 - 2.0L/min) into perspective by remarking how these levels are akin to an able-bodied person walking or jogging. When compared with cycling under volitional control, cardiopulmonary responses seen during FES-cycling highlight an associated inefficiency. In a programme involving twenty able-bodied and twenty SCI subjects, Glaser et al. [29] showed that oxygen uptake for a given power output is significantly higher for FES-cycling than for able-bodied cycling. Also, a smaller (with 6 subjects in each group) investigation into cardiovascular responses during FES-cycling by Raymond et al. [26] showed a higher cardiac output for a given oxygen uptake (at equivalent power outputs) being displayed by SCI subjects when compared with able-bodied cyclists.

The influence of FES-cycling on the bone mineral density (BMD) of participants has been examined by several groups, producing mixed results. A study by BeDell et al. [30] where 12 SCI subjects cycled over a period of approximately 34 weeks (2 sessions per week) showed that BMD, measured at locations in the hip and thigh did not increase significantly. A further period of cycling undertaken by a portion of the subjects also failed to yield any significant increase, although a positive trend was found in measurements taken at the lumbar spine.

Conversely, in a long-term study undertaken by Mohr et al. [25] where 10 (T4-C6 complete) subjects cycled three times a week for 12 months (achieving a mean power output of approximately 10W), followed by one session a week for the following 6 months, BMD of the lumbar spine did not change significantly. However, analysis of the proximal tibia following the initial 12-month period showed a significant 10% increase. Encouragingly, Bloomfield et al. [31] also showed an increase (in this case, the distal femur) of 17.8% from baseline data by subjects who cycled above a level of 18 Watts for at least 3 months of a 9 month training programme. Also, in a case study involving a partial lesion subject, Perkins et al. [14] report bone density increases of 44% in the subject's more paralysed limb.

More recently, Chen et al. [32] carried out an investigation, involving 15 SCI males, into the effects on BMD after 6 months of FES-cycling training (5 days a week with a minimal resistance load) followed by a further 6 month period without. Their results show an 11% and almost 13% increase in BMD in the distal femur and proximal tibia respectively at the end of the first 6 months, then interestingly a return to levels close to baseline following the second, FES-cycle free, 6 month period.

In all of the above-mentioned investigations, the subjects were at least 2 years post-injury. A study by Eser et al. [33] set out to examine the effect of a cycling intervention on bone in recently injured patients. With a high level of participation including 38 subjects (19 FES and 19 control) who were between 4 and 8 weeks post-injury, bone density data collected from the tibial diaphysis before and following the programme (which involved a mean participation of 2.3 sessions per week for an average of 6 months whilst achieving a mean power output of approximately 12.7W) showed no significant attenuation of bone density loss.

Accounts of FES-cycling's effect on spasticity in the modern literature are limited and are generally based on the subject's perspective. A questionnaire carried out by Sipski et al. [21], which gives an insight into patient perception, shows 77% of the paraplegic contingent who responded felt an improvement in their spasticity. However, it is notable that over half of the tetraplegics (who made up the majority of the total responding population) felt no difference. In a study designed to evaluate the efficacy and safety of FES-included cycling, Arnold et al. [16] report a marked reduction in uncontrolled spasticity following the programme for all participants. Also, even though the intensity of spasms increased through augmented muscle strength, the subjects felt the frequency and duration were reduced.

In terms of the modality's functional performance as both an exercise and recreational tool, the two factors probably of most interest are the achievable workrate and how long a practical level can be sustained. Power outputs achievable through FES-cycling at present are generally a maximum of around 30-36 watts [31] while typical gains in capability range between 0 and 30 watts over a 6 week to 6 month period [20].

Power output variations, for a given level of oxygen uptake, between volitional and FES-cycling are considerable. In a study by Raymond et al. [26], the highest level achieved by a spinal cord injured individual is approximately 21% of that reached by the able-bodied subjects. An interesting paper by Kjaer et al. [34], where responses to electrically induced cycling in 8 able-bodied individuals with complete epidural anaesthesia (L3-L4) are studied, further emphasises this point with the workrate produced by the FES-cyclists being approximately one third of their impaired counterparts for a given oxygen uptake.

Regardless of maximum rates achievable, the ability to sustain a useful level is probably of more interest for recreation purposes. Using systems which have been designed as mobile devices [14, 13], complete lesion subjects have cycled up to 3km outdoors, while training sessions of up to 1 hour have been reported. However, as described in section 2.3, fatigue is still one of the biggest enemies of FES' ability to induce a target force from a muscle, thus endurance during cycling suffers from this. Workrate can be extremely variable over the course of a session (even with a constant stimulation intensity and oxygen uptake) with subjects being unable to maintain a set level. Theisen et al. [27] describe this behaviour over a 40 minute session in a study designed to investigate power output during prolonged cycling.

2.5 Discussion

Spinal cord injury is a severe condition which afflicts a significant number of people. The immediate and long term effects drastically alter quality of life for those who experience it while also posing a very serious threat to their health. With medical advancements extending the life expectancy of this population to near normal, the issues of rehabilitation and addressing secondary health problems (which arise as a result of a sedentary lifestyle) have become increasing prominent.

Considering the physiological mechanisms involved in what is effectively a new population are, as yet, not fully understood, functional electrical stimulation has succeeded relatively well in its mission to attenuate various neurological impairments. Although it has been implemented in systems designed to return function, its biggest role in the spinal cord injured population has increasingly become the promotion of health benefits through exercise. Its capacity to be both a training and recreational method to this end has rendered cycling one of the most popular applications of FES. In addition, the large number of well established stationary and mobile systems available mean there is much evidence to support this position.

On the whole, FES-cycling appears to increase bulk in those muscle groups stimulated. While systems which recruit additional or alternative muscle groups do exist [35, 36, 37], the majority of reported size increases concern those muscles which commercially available devices tend to employ (the quadriceps, hamstrings and gluteal muscles).

Significant increases in cardiopulmonary responses over time have been shown, indicating a training effect. Even though levels reported are quite low when compared to voluntary exercise, from the perspective of a sedentary population this could be quite beneficial [20]. Moreover, the ability for FES-cycling to induce high (compared with volitional cycling) responses at low workrates is important when there is a desire to avoid large forces being generated during exercise. Given the osteoporotic nature of the lower limbs belonging to SCI persons, this is extremely relevant.

Influence on bone mineral density has been contested by investigators, however one possible explanation for this may lie in the variation of measurement and training approaches used. Reported significant increases in BMD appear to be, for the most part, in areas around the knee joint and with subjects whose BMD had stabilised prior to beginning the study. Intensity and frequency of sessions performed during a cycling program appear to have the most impact on these site-specific increases. Reported significant improvements have involved either a high power output (over 18W approximately twice a week) or larger frequency of sessions at a lower power output (approximately 10W). There is also evidence to suggest this must be sustained to avoid a subsequent reduction.

As well as these three main outcomes, additional benefits such as a reduced incidence of pressure sores and improvement in spasticity and range of motion might be possible. Positive psychological effects from using this modality (in particular recreationally) may also occur. A majority verdict of improved perceived self-image and appearance reported by long-term users in a questionnaire designed to evaluate these factors [21] indicates this.

Performance capabilities reported indicate a maximum attainable power output of around 36 watts (higher values have been claimed [38], however in this instance the methodology used to reach them is not clear) and sustainable levels sufficient to propel a tricycle substantial distances. That said, the main limiting factor in improving on these achievements would seem to be the alternative, often inefficient, mechanisms involved in FES muscle contraction, chiefly the resulting fatigue. Thus, increasing endurance (at a range of workrates) is of particular importance if FES-cycling is to improve its performance (and hopefully health benefits for those who utilise it) as an exercise modality and further establish itself as a practical method for recreation.

In addition, it should ultimately be available to as many people as possible, particularly those who stand to benefit the most from using it. Until now, the target population of most FES applications has consisted mainly of adults, with the needs of spinal cord injured children receiving less attention. The reasons for this, along with the state of the art of FES-cycling technology shall be discussed in the sequel.

3 Literature Review

In the previous chapter, the concept of FES-cycling was introduced, while the evidence showing its potential as a rehabilitation, mobility and exercise tool within the spinal cord injured population was given. Leading on from this, the following chapter will focus on the background and reasoning for the main contributions in this thesis. In Section 3.1, the design of, and technology involved in FES-cycling systems during the last 23 years will be reviewed. Section 3.2 will introduce the topic of paediatric spinal cord injury, as well as delineating some of the unique issues involved and the role FES has played in this population. Finally, a discussion on these topics in section 3.4 will form the argument for the main contributions in this thesis; the implementation of a new sensor and multi-functional FES device in an FES-cycling system and the development of two novel FES-cycling systems for the spinal cord injured child.

3.1 FES-cycling - A Review of Design and Technology

As discussed previously, FES-cycling is an established technique used to promote health and fitness in the spinal cord injured population. Since the inception of this method over two decades ago, several different configurations and variations on the basic themes have been developed. This section will review the designs and technology incorporated into FES-cycling systems up to this point, giving the background necessary to argue the case for the introduction of a smaller control and sensor arrangement, as well as those design considerations which may be transferable to a system suitable for children.

3.1.1 System Design and Function

All FES-cycling systems can broadly be categorised into two main types which describe their layout: stationary ergometers and mobile devices. In addition, some may have an arm-cranking function (hybrids) or a motor to give assistance. Table 3.1 shows the configuration of selected systems over the past twenty three years.

Year	83	84	-	-	89	93	98	01	04	-	-	05	-
Source	[12]	[39]	[40]	E	[35]	[41]	[42]	[14]	[43]	[44]	[45]	B	R
Ergo		✓	✓	✓		✓				✓	✓		✓
Mobile	✓				✓		✓	✓	✓			✓	
Hybrid					✓					✓		✓	
Motor			✓		✓		✓		✓		✓	✓	✓

Table 3.1: Configuration of selected FES-cycling systems. Ergo - stationary ergometer, E - REGYS/ERGYS and Stimmaster™Orion, B - Berkel bike[1], R - RTI RT300-S.

Studies carried out by Petrofsky et al. [12, 39] in the early eighties describe what are probably the first cycle systems to utilise FES. Both are based on standard devices which are then modified with sensor, orthotic and stimulation equipment. In the case of [39], a standard stationary ergometer was altered through the addition of a continuous-turn potentiometer linked to the crank shaft and pedal replacements with Velcro™foot inserts (which enabled the rider's feet to be fixed). The other system developed by Petrofsky et al. around this time [12] is a tricycle based system capable of locomotion. Like its stationary counterpart, a potentiometer is linked to the crank shaft. Additionally, a second potentiometer connected to one of the brake levers allows the rider control over stimulation intensity. Chosen for its stability, low cost and available storage space (for stimulation control equipment), this tricycle was further modified using a high-back replacement seat (with waist and shoulder straps) more suited for paraplegic and tetraplegic riders.

These early prototypes were followed by the introduction of the REGYS system, which signalled the dawn of commercially available leg-cycling ergometers. A stationary design which incorporated the now proven FES-cycle technology, REGYS and its successors, ERGYS I and II, were used in several of the studies discussed in the previous chapter. In addition to this, a second, similar system, developed by Electrologic of America, called the Stimmaster™Orion (predecessor to the more recent Galaxy) was also introduced.

Some of the shortcomings of the earlier mobile system (instability during turns and a lack of assistance) were addressed by Petrofsky and Smith several years later with a second mobile device [46]. A two-person arrangement (side by side) offered superior

[1]BerkelBike BV, Nijmegen, Netherlands. http:/www.berkelbike.nl/

stability, while a second, able-bodied rider could offer assistance following fatigue. Unwanted adduction or abduction of the legs was restrained using stabiliser bars, that followed movement of the knees, and toe straps on the pedals.

A few years earlier, Pons et al. [35] developed a four-wheel system called the Paracycle. This device was also capable of locomotion and included several advancements from Petrofsky's designs. A more recumbent seat-back position was chosen to offer further stability while ankle braces on the pedals would restrict movement of the legs to one plane. Perhaps the most notable inclusion is that of a motor to drive the pedals, thus enabling passive exercise and assistance during stimulation-induced cycling. Instrumentation on this device included a potentiometer, to control the motor speed, a separate lever for stimulation control and braking, and optical shaft encoder to measure crank position (chosen for its reliability).

During the nineties, Gföhler et al. [42] introduced a tricycle system which also included an auxiliary motor. Rider position was upright, so several features were implemented to ensure stability while cornering and easy transfer. A specially designed rear axle, in the form of an articulated parallelogram, allowed inclination of the rear wheels. Also, a hydraulic saddle (which could incline), capable of easy height adjustment by the rider, allowed for independent transfer from a wheelchair. Around this time, another mobile design based around a standard wheelchair was introduced by Angeli et al. [47]. This system incorporates a quick-release attachment which contains a third wheel along with the equipment necessary for FES. As with previous devices, ankle braces, a crank-shaft position-reading sensor and motor are present. A coupler between each pedal and crank arm was added, resulting in a new cycling path which could improve efficiency through an optimised transfer of power from the legs.

In addition to "traditional type" cycling devices, a number of leg propelled wheelchair systems (which incorporate FES technology) also exist. Glaser et al. [48] modified a standard wheelchair with a ratchet drive system which incorporated two reciprocating footplates coupled to the wheels. Thus, forward motion could be achieved with the rider's feet attached to the footplates and raising the lower leg through contraction of the quadriceps only (with gravity lowering the leg). The wheelchair-based approach was developed further by Stein et al. [49] who utilised both knee flexion and extension for forward driving torque through a two-way clutch gearbox (on Glaser's design only knee extension contributed to this).

Until this point, prototype systems were mostly restricted to laboratory use while those commercially available were expensive, generally only certified to be used in the USA and limited to stationary cycling. In an effort to move FES-cycling into the home, with the hope of increased and more frequent use, Perkins et al. [14] describe the development of a modified recumbent tricycle for this purpose. The standard tricycle (chosen for its stability and low seating pressure) was altered by means of a 7-bit shaft encoder on the crank shaft, ankle/foot orthoses, throttle potentiometer for stimulation intensity control and compact stimulator (with internal cycling control software, which could be started and stopped from handlebar switches). Furthermore, as well as having mobile capabilities, the tricycle could be easily connected to a standard resistance trainer, thus converting it into an indoor stationary ergometer.

In an investigation into the design of motor-assistance control strategies for both exercise testing and approaches to recreational mobile cycling, Hunt et al. [43] developed the tricycle-based system even further. The two major additions were in the form of an auxiliary motor (positioned behind the seat and connected to both the drive wheel and pedals) and torque sensor (mounted on the crank shaft). In this configuration, control of the stimulator (and therefore, leg power) and motor were carried out via a laptop computer that contained software designed to distribute the contribution of both to the total power output at the pedals, such that the reference level (set by the throttle potentiometer) of a desired variable (eg. cadence) could be maintained.

In a separate study, with the design objective of creating a system capable of cycling over a large range of cadences, Fornusek et al. [45] utilised a commercially available ergometer which contained an in-built motor and was designed specifically for low intensity, passive cycling by SCI persons. The only major mechanical modification involved attaching a chair with passive leg braces (the standard ergometer was designed to allow a wheelchair to roll up to it). With data from the original system's crank shaft and motor readily available, the stationary FES system was completed with laptop-controlled stimulator hardware.

The effort to move FES-cycling into the home was explored further by Chen et al. [44], who describe the development of an inexpensive hybrid system with a design criterion and process based on interaction and feedback with both therapists and users. The system is based around an ergometer, which includes a shaft encoder, leg braces, hysteresis brake, and can be operated from the user's wheelchair. Stimulation was again computer-controlled. However, in this case the technology is miniaturised somewhat with the use of a pocket personal computer. A hand crank coupled to the leg-cycling pedals enabled assistance and/or independent upper-body voluntary exercise.

More recently, two new commercially available systems have been introduced. The first is a tricycle device called the Berkel bike [50]. Based around a wheelchair, this hybrid design is capable of both arm and leg cycling and may be used for mobile cycling. US-based company Restorative Therapies[2] have developed an FES stationary ergometer called the RT300-S. This device is based upon a Medica Thera Vital[3] motorised (for passive cycling only) ergometer which has been modified with a six channel stimulator and touch screen interface unit. Interestingly, the system is available in both adult and paediatric versions.

3.1.2 Stimulation Technology and Control Approaches

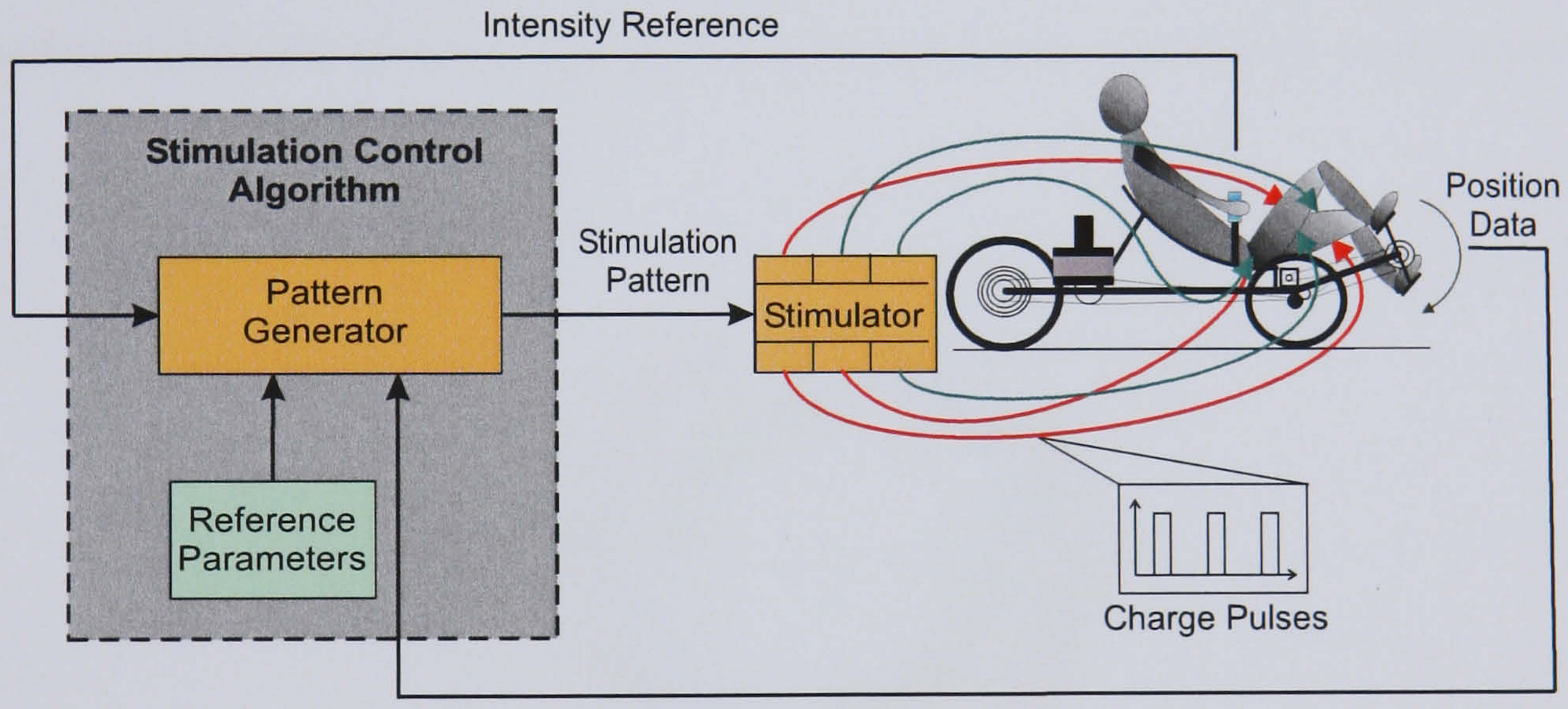

Figure 3.1: Simplified diagram illustrating stimulation control in FES-cycling.

The basic principles of FES-cycling control can be represented by the most basic, open-loop (from the rider's perspective) case as depicted in figure 3.1. In this setup, the status of the lower limbs/crank-shaft geometry is monitored in some way and fed into a control algorithm. This position data is compared with reference parameters (essentially a predefined pattern of stimulation activation times dependent on the position of the lower-limbs) in order to calculate which muscle group requires to be contracted

[2]Restorative Therapies Inc, Baltimore, USA. http://www.restorative-therapies.com/
[3]Medica Medizintechnik GmbH, Hochdorf, Germany. http://www.medica-medizin.de/

to continue the cycle. The generation of a new stimulation pattern is completed with a user-defined intensity level set to obtain a desired muscle-contraction strength (and hence torque at the pedals).

Although most of these basics hold true for all systems, approaches to data acquisition, stimulation intensity control, stimulation application and the origin of reference parameters may differ.

As motion is restricted by the pedals (and ankle orthoses) during cycling and is also symmetrical, the geometry of both lower-limbs may be defined by one angle (usually that of the crank) which, when measured, gives the position data required for control of stimulation. Typically, this has been achieved through the use of either a continuous-turn potentiometer [12, 39, 46] or optical shaft encoder [35, 41, 14] coupled to the crank shaft. In addition to the position of the crank, its rotational velocity is sometimes also recorded (or derived from the angle) [14, 42] and used as an extra timing parameter to allow for a fixed time delay (created by action potential propagation velocities and the mechanical speed of muscles) between stimulation and muscle contraction.

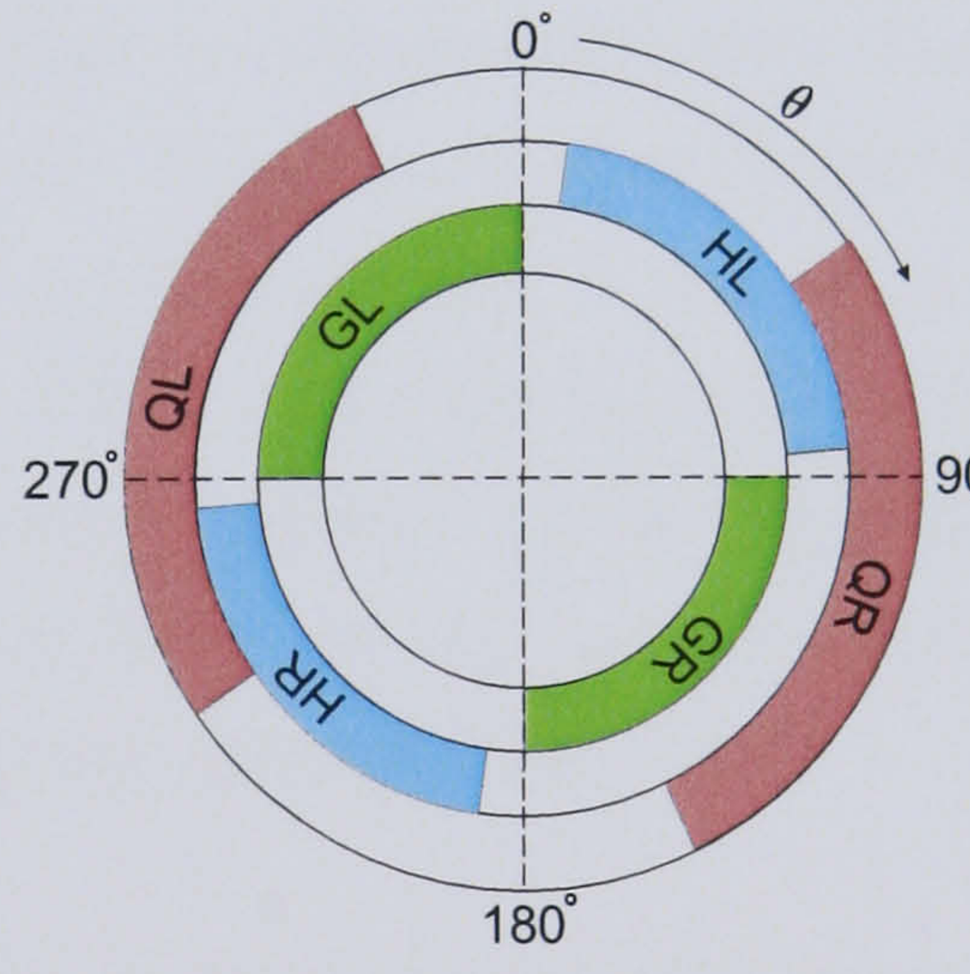

Figure 3.2: Example of a reference stimulation pattern. θ - Crank Position, QR - quadriceps right, QL - quadriceps left, HR - hamstrings right, HL - hamstrings left, GR - gluteal right, GL - gluteal left.

Reference timing parameters (that constitute what is essentially a "static" stimulation pattern, such as that shown in figure 3.2) have been generated in several different ways, primarily due to the varying bio-mechanical layouts of each system. Many studies have based them on surface electromyography (EMG) measurements from the muscles of able-bodied cyclists [35, 46, 41], although Pons et al. [35] note that the final sequence used for FES-cycling correlated poorly with that determined using able-bodied EMG measurements. Other approaches have included indentification through modelling the rider-trike system [51, 52], and simply monitoring the crank angles through which a positive torque is produced for each muscle group [53, 43].

Aside from contracting the appropriate muscle group at the correct time, an FES-cycling system's ability to obtain or maintain a desired power output or cadence depends, in part, on the control of stimulation intensity. In the setup illustrated in figure 3.1, this is set by the rider. This open-loop (from the point of view of the rider) approach has been adopted by many systems (mostly mobile-capable) where a reference intensity is set from either a throttle potentiometer [12, 46, 42, 14, 13, 43], lever [35] or computer based paddle buttons [39].

In stationary, commercially available systems and those orientated around development or exercise testing, direct control of the stimulation intensity is taken away from the rider and governed internally. In this scenario, the stimulation control algorithm is usually designed to maintain a target cadence (typically 50rpm) and will therefore modulate intensity appropriately to achieve this.

The ERGYS II and Stimmaster^{TM}Galaxy systems appear to implement a strategy whereby intensity is ramped up to a maximum over time in order to counter fatigue and maintain a target of 50rpm. When this can no longer be held and the cadence drops below 35rpm, stimulation is terminated [45]. Chen et al. [54] designed a proportional plus integral plus derivative (PID) controller for FES-induced free-swing movement of the lower leg, then subsequently applied it to their cycling system for cadence control. This approach was succeeded later by the introduction of a model-free, fuzzy logic controller to improve cycling smoothness [55].

As discussed in the previous chapter, muscle fatigue is one of the largest problems facing FES-cycling. The resulting low (when compared to able-bodied persons) capability for endurance (as well as a possible, impractical muscle force production during the early stages of training) limits both the practical nature of mobile systems and precise function of exercise test-beds. To compensate, a few devices designed for those purposes include an auxiliary motor [40, 35, 42, 45, 43].

In addition to cadence control, the objective here may alternatively be to maintain a target power output with the contribution from motor and stimulated muscle being varied according to level of fatigue. In most cases, torque at the pedals is monitored in some way (usually with appropriate sensors mounted on the pedals or crank shaft) and fed back into the stimulation control algorithm along with position and velocity data.

Source	*Stimulation Application*	*Muscle Groups/Nerves Employed*
[48]	Surface	Q
[12]	Surface	Q, G
[39]	Surface	Q, I
[40, 41, 49, 44]	Surface	Q, H
[35]	Surface	Q, G, Gas
[46, 42, 13, 45]	Surface	Q, H, G
ERGYS II	Surface	Q, H, G
Stimmaster^{TM}Galaxy	Surface	Q, H, G
Berkel Bike	Surface	Q, H, G
RTI RT300-S	Surface	Q, H, G
[47]	Surface	Q, H, G, Per
[36, 14]	Surface	Q, H, G, Ta, Gas
[53]	Implanted	Roots - L2, L3, L4, L5, S1, S2

Table 3.2: Stimulation application approaches and muscle groups/nerves employed by selected systems. Q - quadriceps, H - hamstrings, G - gluteus maximus, I - iliacus, Ta - tibialis anterior, Gas - gastrocnemius, Per - peroneal nerve.

Table 3.2 shows the stimulation application technique and muscle groups/nerves employed by various systems. In nearly all reported studies, stimulation is applied transcutaneously using adhesive electrodes. Usually, two electrodes (active and passive) are assigned to each muscle group, however some studies such as Petrofsky et al. [39] include a second active electrode in order to alternate stimulation across the muscle in the hope of improving fatigue characteristics.

Although incurring the disadvantages discussed in section 1.3, the benefits of increased accuracy and substantially decreased time for donning and doffing of equipment mean stimulation through use of implanted electrodes is an exciting option for FES-cycling. In a case study reported by Perkins et al. [53], a complete T9 lesion subject was able to propel a tricycle for up to 1.2km at a time through use of an implanted anterior spinal nerve root stimulator. In this system, stimulation commands are transmitted to an R.F. coupled, multiplexed receiver located in the right costal margin of the subject. From there, subcutaneous wires lead to intradural cuff electrodes attached to the nerve roots.

3.2 Paediatric Spinal Cord Injury

Although only making up a small percentage of the total spinal cord injured population, when compared to adults the paediatric contingent represent a group that is unique, not only anatomically, but also in terms of the required approaches to care and rehabilitation. This section shall review some of the pertinent background information concerning this population and the specific needs involved in their care and rehabilitation.

3.2.1 Demographics and Etiology

Spinal cord injury in the general paediatric population is, thankfully, a rare event (although some researchers note that the reported low frequency may be due in part to a high mortality rate in this group [4, 56]). Data on incidence is varied, not always age-group specific, based on admittance to the author's particular institution and mainly from US sources. In general though, approximately 3-5% of total annual SCI cases will be children under the age of fifteen with a further 15-17% younger than twenty years old [57, 2]. Males tend to make up a larger proportion of the total and this trend becomes more pronounced as age increases [57, 4].

Several authors report that, as with adults, motor vehicle accidents are responsible for perhaps the largest proportion of injuries [58, 57, 2]. However, when the distribution of causes across different age groups is analysed, the more prevalent injury mechanisms vary. For example, in toddlers and school age children, falls are one of the main causes while sports-related trauma tends to make up the biggest proportion in adolescents.

The majority (as high as 80%) of spinal injuries (across all ages) in this population occur in the cervical region [4, 59, 60], a fact that is even more pronounced in the younger age groups [56]. Data on the distribution of injury levels in children who go on to suffer some form of motor or sensory depravation suggests, however, that this trend does not apply to those with paraplegia and tetraplegia. Both Triolo et al. [58] and Vogel et al. [57] found that while the youngest children (infants and toddlers) still suffered the majority of the highest cervical-level lesions (C1-3), and are also most likely to be complete, thoracic and lumbar lesions were significantly more prominent in those children between one and ten years old while lower cervical cord injuries were more prevalent in older children (above age ten). Data reported by Cirak et al. [4] indicate that cervical level injures account for the majority across all age groups. However, the proportion of the sample studied with a neurological deficit (as oppose to vertebral injury alone) is unclear.

The disparity of predisposition to certain injury levels and injury mechanisms across different age groups may be attributed, in part, to the unique anatomical make up of a child and how this changes during growth. Factors such as a disproportionate head to body ratio and under-developed muscles in the neck are the main contributing factor to the high cervical-level injury incidence in the youngest age groups [4, 59, 60]. In addition, an under-developed skeletal structure which has an increased cartilage to bone ratio in the spine means that children are more susceptible to spinal injury in general. A disproportionately large head in pre-school children, which results in a higher centre of gravity, coupled with relatively poor coordination may explain why this age group is more prone to falls. On the other hand, it is the behavioural characteristics of adolescents that most likely account for the high proportion of sports related injuries in their sub-group.

3.2.2 Medical Issues

There are several anatomical and biomechanical features that are either unique to, or are more pronounced in, the paediatric spinal cord injured population and lead to additional or confounded problems in comparison to their adult counterparts. Many of the medical issues encountered arise because a child may be skeletally immature at the time of injury. This means that as they grow (without use of the affected limbs), the natural development of what is now a substantially weakened frame will itself create problems.

As discussed in the previous chapter, there is a significant reduction in bone mineral density in the limbs of adults who suffer a spinal cord injury and this is no different for children. There is little data on this subject pertaining to the paediatric population but in one study by Moynahan et al. [61], where bone mineral density was compared in 51 children at areas around the hip, losses in those greater than one year post-injury were comparable to data reported for adults (approximately 35-45%). However, although the percentage of reduction may be similar to adults, because their bones are often not fully developed at the time of injury (and do not develop properly in the time following), there is an increased risk of bone fracture [62, 63].

Another common problem is hip joint instability, to which this population are more susceptible, due to the more cartilaginous nature of their joints. Spasticity of the muscles around the hip joint can aid in the formation contractures (a usually permanent shortening of the muscle, it is another ailment to which this group is predisposed) and ultimately, over time, dislocation. Even without the presence of spasticity, dislocation of the hip often occurs as the lack of muscle force impairs joint development. Incidence appears to be predominately in those with thoracic level injuries. Based on a review of 72 patients, Miller et al. [64] found that the latter were twice as likely to develop hip instabilities than those with cervical or lumbar level injuries.

Skeletal immaturity at the time of injury can also greatly increase the risk of spinal deformities, chiefly scoliosis, throughout growth. Other than issues concerning the fracture or surgery induced problems, the main catalyst is a lack of muscle force combined with growth forces [65].

3.2.3 Care and Rehabilitation

Special consideration should be given to the rehabilitation process of a child/adolescent as the approach must differ from that of the adult [66]. As the child grows cognitively, emotionally and socially, the approach must be modified appropriately with each person in the rehabilitation team aware of the special needs at every level of development.

Yarkony et al. [67] suggest that the fact that children learn through play means that including play in the rehabilitation process will be more productive than a regimented exercise programme alone. Participation in sport, in this population in particular, is important. Johnson et al. [68] state that children of all abilities should be exposed to as many different types of sport as possible and that the physical wellbeing and sense of accomplishment from this can help alleviate the depression that accompanies spinal cord injury.

As mentioned, spinal cord injured children have a high risk of developing spinal deformities and muscle contractures. This can interfere greatly with seating systems and orthoses. In an evaluation of wheelchairs and seating systems, Gonzalez et al. [69] note that all seating systems must support any deformity in such a way that any further deterioration is minimised. They also describe seat belts and/or harnesses, in combination with a head rest, as being important additions in combatting the effects of spasms and poor trunk control.

From experience of using FES in this population, Smith et al. [70] explain that the presence of contractures, deformities and poor bone mineral density can compromise the safety of a subject while using a rehabilitation system, therefore careful evaluation must take place. Where older children, particularly adolescents, are concerned, appearance is a high priority so any equipment or system used as part of the rehabilitation process should take this into account.

3.3 FES in the Paediatric Spinal Cord Injured Population

Research dedicated solely to the rehabilitation of spinal cord injured children, particularly that which includes FES, is comparatively rare. As discussed, this population makes up a small portion of people who have what is already a relatively uncommon condition. This, coupled with the unique medical issues and associated complications within this group, means that the vast majority of resources are channelled into fully developed children and adults [71].

To date, almost all FES-orientated studies in this population have focussed on returning function, rather than on exercise. As a result, development and use of devices for activities such as hand grasping, standing or ambulating has been most prominent. Several investigations have reported successful implementation of such FES systems (using surface, percutaneous and implanted simulation technology) for children [72, 63, 73, 70, 74, 75], though mostly in older age groups. In a study which describes an approach to stimulate, directly, the denervated muscles of children who suffer from flaccid paralysis (caused by a range of diseases), Eichhorn et al. [40] demonstrated FES-cycling in one child, who had a lesion of the spinal cord.

Data on health benefits, although scarce, appears to follow the trends seen in the adult population. In a two-year study where the quadriceps of four subjects (aged between three and twelve) were stimulated initially for training and ultimately standing, Popovic et al. [72] found an increase in trabecular bone density of the tibia of 6.6% (although were not able to conclude if stimulation was soley responsible), along with gains in mass, strength and fatigue resistance of the quadriceps. Betz et al. [63] found that subjects who participated in 6-month FES standing or walking programmes, which included monitoring of bone densities around the hip and femur, showed a site-specific increase in bone density of the distal femur.

Robinson et al. [76] investigated and compared maximal physiological responses of arm cranking exercise. FES of the lower limbs and a combination of the two. Participants were aged fifteen to seventeen years with injury levels between T5 and T7. In this study, stimulation of the quadriceps and gluteal muscle groups provided a large cardiopulmonary stress, when compared to rest, but less than arm cranking alone. The hybrid system which involved both types of exercise showed the highest physiological responses.

3.4 Discussion

FES-cycling has given rise to a succession of systems that encompass a range of approaches to design and stimulation control. Although, clearly, there is still a requirement to improve aspects such as efficiency, there is also scope for the inclusion of more modern sensor and control technology in an effort to reduce bulk and increase accuracy. In addition, the health and recreational benefits that cycling offers are, arguably, even more pertinent to the spinal cord injured child. Thus, it would seem logical to investigate the transfer of this technology to the younger population.

3.4.1 FES-cycling: Moving out of the Laboratory

Broadly speaking, FES-cycle systems tend to be designed for either research development, or training/recreation. In the case of the latter, design goals shift towards practicality and ease of use, therefore with a view to moving this technique out of the laboratory and into both the clinical and home setting, those issues should take priority.

When considering the layout of FES-cycle systems, those capable of being both stationary and mobile devices appear to offer the most benefits. Although commercial systems such as the ERGYS II seem to be fairly reliable and easy to use, they do not offer the attraction of outdoor cycling, are rather bulky and are still very expensive. Those capable of locomotion highlight separate issues, of course. Stability must be ensured at all times and although approaches that maintain an upright rider position have been successful [42], the necessary mechanical adjustments made a significant weight increase. A more supine, and lower to the ground, position for the rider also offers increased stability, therefore modification of standard recumbent tricycles [46, 14, 13] provides a low-cost option in achieving this. Utilising standard devices in an FES system has other advantages, too. The final device will look more akin to one which an able-bodied person would use, possibly making it more appealing. A wider range of replacement parts, standard cycle trainers and sensor equipment can also be easily connected to it.

Assistance in some form is clearly needed during the early stages of training and to allow recreational FES-cycling to be practical. The inclusion of an auxiliary motor and its required control is the logical option, and most popular, but necessitates further instrumentation and increased weight. Inclusion of arm cranking, such as in hybrids, is an attractive alternative but does not offer the same accuracy as a motor and relies on the subject having sufficient energy to propel the device with their upper limbs (something that is not an option for those with tetraplegia).

Control of stimulation has evolved from using desktop computers [39] to devices that contain both stimulator and control software [14]. Intensity modulation is governed automatically in some systems. Although this approach is suitable for stationary ergometry (and does simplify operation for the user), on a mobile device, control over what will ultimately be forward velocity must remain with the rider. Moreover, it may be desirable to always (with the exception of exercise testing, where a higher precision is needed) give control of stimulation intensity to the rider. It is, perhaps, arguable that in relinquishing this to software, the rider could become decreasingly motivated as they become a less active participant in what should, at least partly, be a recreational activity.

In the short term at least, surface stimulation appears to be the best way to apply stimulation for this modality. Although it requires time-consuming donning/doffing of electrodes and cables, it still allows an effective and non-invasive route. Cycling using implanted electrodes has been successfully demonstrated, and does allow for a "neater", potentially more efficient system. However, it also requires surgery and thus may be an unattractive option for many potential users.

Optical shaft encoders have traditionally been used for pedal position measurement because of their accuracy and durability. However, as limb motion is restricted by the pedals during cycling, any angle within the lower-limb/pedal geometry may be used as the reference position data required for stimulation control. Measurement, and use, of limb position could offer an alternative source that would allow for a reduction in tricycle instrumentation and thus be a step closer to a self-contained system which could be transferred to any cycle device. Moveover, analysis of the literature indicates that such an approach has not been attempted thus far in FES-cycling control. In addition, the inclusion of modern and small computational devices, like palm-tops, could further miniaturise equipment needed and increase ease of use through improved user interfaces.

In an effort to research these possibilities, we propose an investigation into using both a limb-mounted sensor and new multi-functional, PDA-based FES system to implement FES-cycling. This work will be described in chapter 4.

3.4.2 Child Proof?

Paediatric spinal cord injury is a relatively rare event. A lowered motivation for research in light of the size and variation of this population, along with difficulties in seeking ethical approval, mean that both the condition itself, and rehabilitation of those affected, has received comparatively little attention. Although it is unfortunate (bearing in mind the circumstances of this population) that the impetus for more focused research in this area should be, in part, financially driven, modern life expectancy of an injured child is near-normal and thus the cost of care and rehabilitation during this time comes into question. Thus, with the advent of new exercise and assistive techniques (such as FES) which have been shown to improve the health of adults, a concerted effort is now being placed on transferring these technologies to children.

Until now, FES in this population has been used almost exclusively for standing, ambulation and hand-grasping. There is one reported exception to this [40], however little information is presented on the subject or subsequent effects. Also, a new paediatric FES-cycling ergometer has recently become available (Restorative Therapies' RT300-S), but as yet there are no published data concerning its use. Given that the health-promoting and recreational attributes of cycling, in addition to its smooth dynamic nature, appear to suit the particular needs of spinal cord injured children very well, this application may, potentially, have the most to offer them.

The health gains to be had from taking part in an exercise programme are clear. However, persuading children (especially the youngest) to commit, both initially and in the long term, is not straightforward, as long-term welfare and health are not in the forefront of their minds. Instead, play and engaging in social activities are often a much higher priority. Indeed, some adults who sustained their injury while children have expressed dissatisfaction with the lack of opportunities for social activity when growing up [77]. Thus, the recreational aspects of cycling may encourage increased participation.

Cycling could also offer promise to those with substantially weak bones (and who therefore are at the highest risk of fracture), who, as a result, may have been precluded from other FES research programmes. With the smooth, repetitive motion (and comparatively low force generation) involved, motor assisted systems might offer a lower-risk technique for building bone mineral density.

When choosing the design criteria for a child-orientated FES-cycling system, the previously discussed specific needs of the child who has a spinal cord injury must be taken into account. It should be safe, flexible, simple to use, allow for anatomical deformations such as contractures and scoliosis, while still being aesthetically attractive. The equipment involved in many systems originally designed for adults are bulky and not cosmetically pleasing from the child's perspective (something that has been speculated on, by those who have enrolled children in FES-research programmes [58], as being a major factor in the reluctance to participate). Moreover, it is particularly desirable for the system to resemble, more closely, those used for exercise and activity by able-bodied peers, thus enhancing the psychological benefits.

Although extra challenges must be faced in order to address the unique issues presented by this population, the range and success of FES-cycling approaches in adults suggest that this technology can, and should, be applied to children. To this end, we propose the development of FES-cycle systems which can be used within the paediatric spinal cord injured population for both stationary and mobile cycling. This work will be described in chapters 5 and 6.

4 Implementation of FES-cycling Using a Multi-functional FES System and Limb-mounted Sensors

In this chapter, we describe the development of FES-cycling stimulation control strategies which employ new approaches for obtaining crank position data (used as a stimulation activation reference) using a limb-mounted sensor. These strategies, in addition to a "traditional" approach which employs a shaft encoder, have been implemented into a new PDA-based, multi-functional, FES-system which can be used for either surface or implanted stimulation. The work is divided into three main stages:

(i) Testing and validation of the limb mounted sensor pack (section 4.2).

(ii) The creation and testing of an angle-conversion algorithm (section 4.3).

(iii) Incorporation of this algorithm and an FES-cycling strategy within the PDA-controller (section 4.4).

Before this, a description of the new equipment that will be utilised is given in section 4.1 in order to explain its layout and capabilities. Conclusions drawn from this chapter's findings are given in section 4.5.

4.1 The Neopraxis Multi-functional FES System

The implementation of a new multi-functional FES system into an existing FES-cycle setup has been investigated. For background purposes, the following section will describe the layout, capabilities and use of this system in international research up to this point.

4.1.1 Overview

A small, portable FES system has been developed by Neopraxis Pty Ltd[1]. It contains a palm top controller called the navigator, which can implement FES strategies through either an eight channel surface stimulator, called the Exostim, or a 22 channel implanted stimulator. The system also contains small limb-mounted sensor packs, which can measure orientation and acceleration data.

(a) Navigator

(b) Sensor pack

Figure 4.1: The Neopraxis Navigator and sensor pack.

The Navigator (155mm x 85mm x 40mm), shown in figure 4.1(a), is a small, portable device which consists of a hand-held PC that has been modified with a custom-designed compact flash (CF) card to provide a serial peripheral interface (SPI) to the remaining components of the entire system. Internal software, called "Clinix", allows user-friendly access through the Navigator's touch screen to a range of pre-designed stimulation strategies (muscle strengthening, standing etc.) that may be implemented using either of the stimulators. In addition, a clinician or researcher may assign different stimulation parameters (frequency, pulsewidth and amplitude limits) to individual muscles groups or nerves and create simple strategies. More complicated sequences can be incorporated through use of a Matlab/Simulink[2] interface, which allows Simulink models to be compiled and downloaded into Clinix.

[1]Formerly a subsidiary of Cochlear Ltd, Lane Cove, Australia. http://www.cochlear.com/. Neopraxis Pty Ltd ceased operation in 2003.
[2]The MathWorks Inc., http//www.mathworks.com/

Orientation and acceleration data for use in closed-loop control strategies are obtained from small limb-mounted sensor packs (65mm x 34mm x 12mm). These devices (Figure 4.1(b)), which consist of two two-dimensional accelerometers, a miniature rate gyroscope and a micro controller, are powered from, and communicate with, the navigator through its CF card [78]. Multiple sensor packs may be used concurrently, with information from each (and therefore feedback from several different limbs) being monitored in realtime by the Navigator. An additional feature is the inclusion of three analogue inputs that allow acquisition of data from external hardware, such as switches.

4.1.2 Surface Stimulation

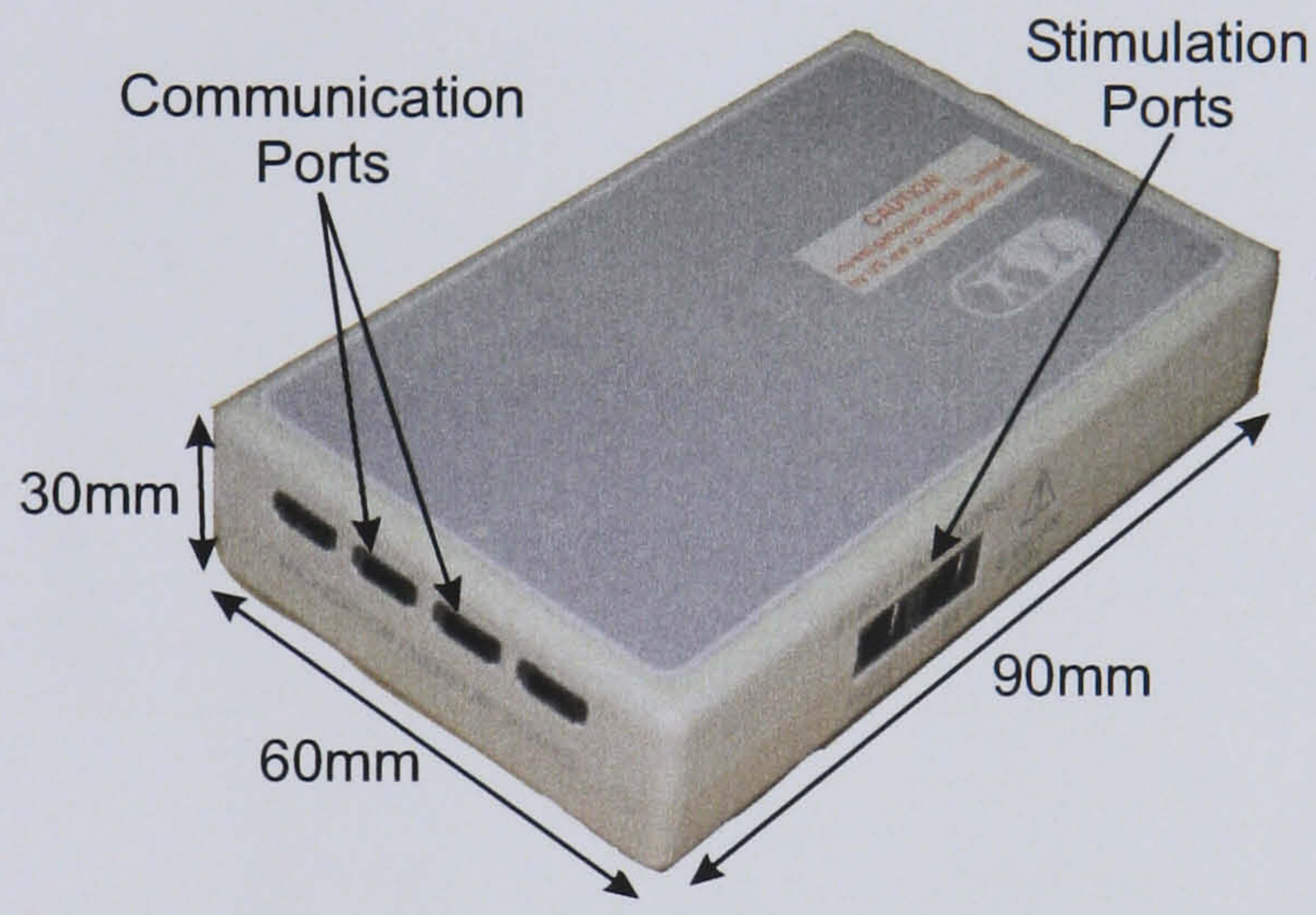

Figure 4.2: The Exostim surface stimulator.

Surface stimulation is carried out using an eight channel, belt-worn device (weighing approximately 500g) called the Exostim (Figure 4.2). Like the sensor packs, communication with the navigator is carried out via the CF card. However, as the card has only three SPI ports, the Exostim also acts as a thoroughfare for sensor pack data (using additional ports located on its side) when feedback from multiple limbs is required [79]. Stimulation parameter ranges are shown in table 4.1. When using this device, frequency and charge pulsewidth remain constant while intensity is governed by modulation of the amplitude between threshold (the minimum level that produces a visible or palpable response) and saturation (the level above which no increase in force is achieved) current levels. All values are set for individual channels using the navigator.

Stimulator	*Amplitude*	*Frequency*	*Pulsewidth*
Exostim	0 - 216mA	17 - 100Hz	25 - 500μs
FES-24B	250μA - 8mA	0 - 14400Hz	25 - 600μs

Table 4.1: Stimulation parameter ranges for the Exostim and FES-24B stimulators.

4.1.3 Implanted Stimulation

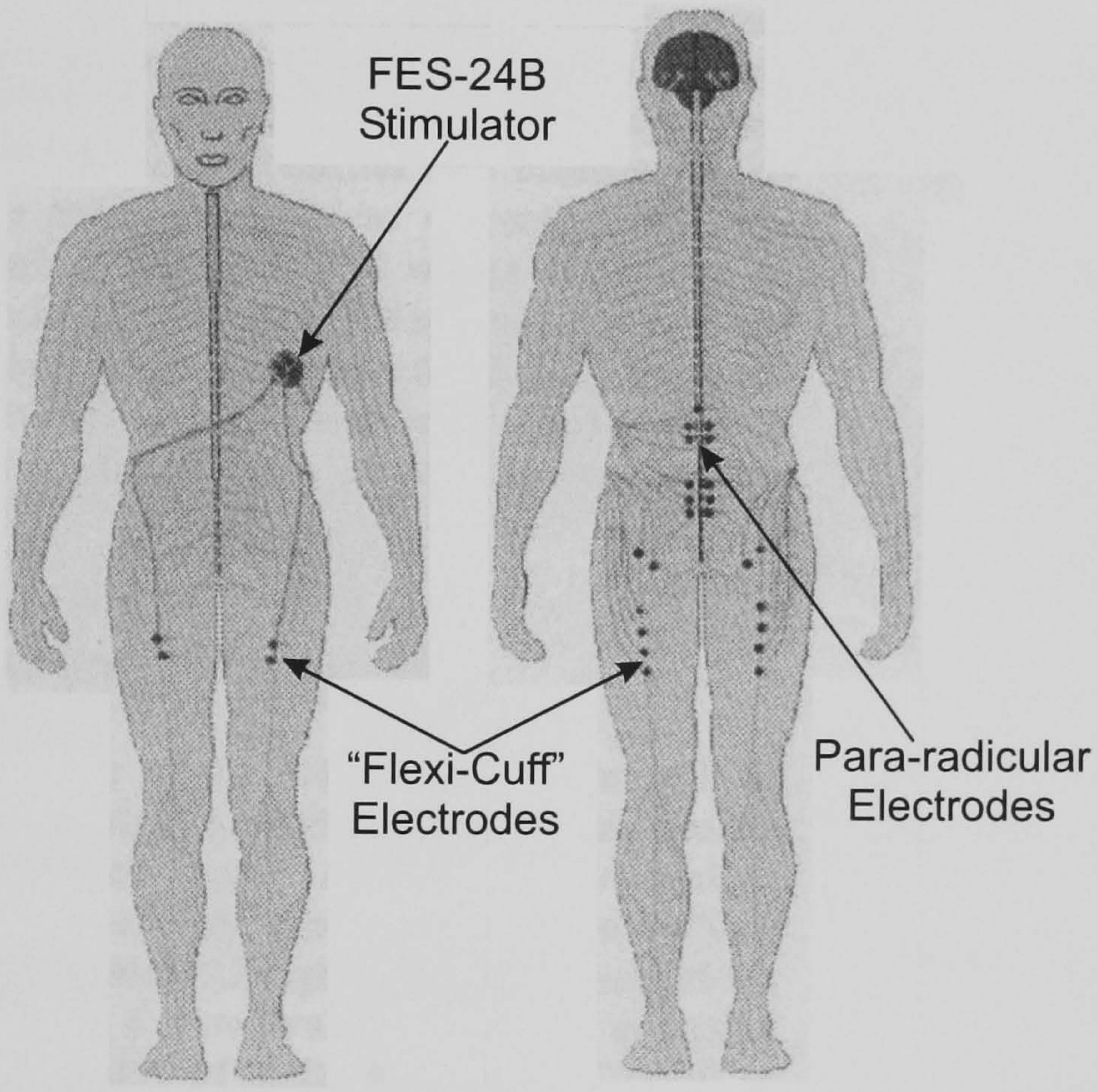

Figure 4.3: Location of the FES-24B stimulator and its electrodes. (Adapted from http://www.ifess.org/cdrom_target/Vienna01/Posters/Davis.htm)

The navigator and sensor packs can also be connected to a 22-channel implanted stimulator, called the FES-24B, forming the "Praxis" system. The stimulator, which is based on the Nucleus 22 cochlear implant [80], is placed in the lower right intercostal margin and connected to electrodes via subcutaneous, stretchable, conducting leads (figure 4.3). Communication between the navigator and the stimulator is achieved by an RF-linked antenna which holds on to the skin because of a magnet in the stimulator. Two techniques for implanted stimulation are demonstrated with this system: peripheral nerve stimulation and direct nerve root stimulation.

18 channels are designated for lower-limb muscle contraction. The individual nerves or branches (and the corresponding muscle contracted) to which each channel is assigned are shown in Table 4.2. The electrodes themselves are either "Flexi-Cuff" electrodes, which encircle the nerve, or platinum button electrodes, which are sutured to adjacent connective tissue [81].

Channel/ Electrode	*Nerve*	*Innervation Level*	*Muscle Contracted*	*Action*
1,10	Obturator Sciatic	L2,L3,L4,L5,S1	Adductor magnus	Adducts and extends thigh at hip
2,11	Sciatic	L5,S1,S2,S3	Biceps femoris	Extends thigh at hip
3,12	Inferior Gluteal	L4,L5,S1,S2	Gluteus maximus	Extends and laterally rotates thigh at hip
4,13	Lumbar Plexus	L2,L3,L4	Psoas	Flexes thigh at hip
5,14	Femoral	L2,L3,L4	Vastus lateralis	Extends leg at knee
6,15	Femoral	L2,L3,L4	Vastus medialis	Extends leg knee
7,16	Super Gluteal	L4,L5,S1	Gluteus medius	Abducts thigh at hip
8,17	Peroneal	L4,L5,S1	Tibialis anterior	Dorsiflexes foot
9,18	Tibial	L5,S1	Gastrocnemius	Plantarflexes foot and flexes leg at knee

Table 4.2: Position of implanted electrodes for lower limb movement.

Three further channels are connected to linear para-radicular electrodes, which are inserted into the external sacral foramina for bladder control, and sexual function in males. This eliminates the need for a posterior sacral rhizotomy, which was one of the goals of the Praxis system. A posterior sacral rhizotomy (which involves a sacral laminectomy) is carried out when fitting cuff electrodes to the anterior sacral roots for use with existing bladder stimulation systems. The drawback to this procedure is that it prevents future reflex erections in males. The final channel (connected to an epidural, spinal-cord-stimulating electrode) is assigned for modulation of spastic bladder and bowel reflexes. In addition to the 22 stimulation channels. the front and back of the stimulator case act as two return channels. Like the Exostim, charge pulse amplitude is modulated to control stimulation intensity and individual parameters are set using the navigator. Ranges for these parameters are shown in table 4.1.

4.2 Sensor Pack Testing and Validation

Initial experience with the sensor pack indicated the existence of a drift in orientation data. Therefore, before using it within an FES-cycle setup, experiments were carried out to test and validate the signals. The following details this work.

4.2.1 Methods

Aims and Objectives

The aim is to investigate further a possible drift in orientation data, recorded by the sensor pack, that was found previously. To achieve this, orientation, velocity and raw voltage signals would be recorded under both static and dynamic conditions. similar to those found in cycling, while any observed drift in the data would be quantified.

Static

Experiments were set up as as shown in figure 4.4. The sensor pack was attached to a wooden rod which can be held in position by a clutch system. A potentiometer was placed on a second pole and directly coupled to the rod so that an equivalent voltage could be used for position comparison. The rod was placed at five different angles: 0°. 45°, 90°. 135° and 180° (an inclinometer was used to confirm both these and the equivalent potentiometer voltage).

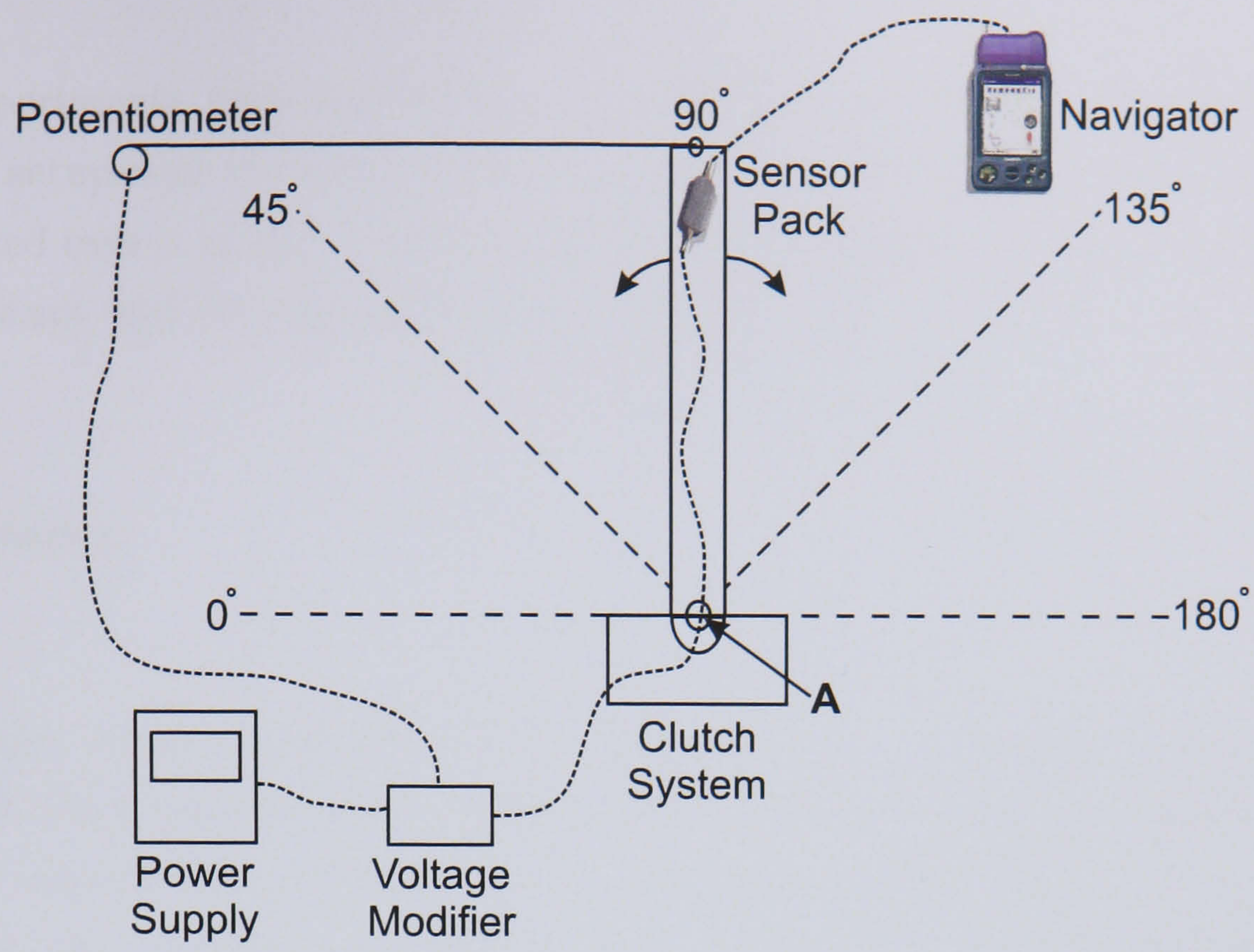

Figure 4.4: Experimental setup. Rod is rotated around point A and held in place with the clutch system.

At each position, three experiments were conducted in which the purpose was for the rod and sensor pack to remain static over a period of four minutes. A Matlab sequence which samples (at a rate of 20Hz) and logs information from the sensor pack during this period was created, compiled and downloaded for use on the navigator. Four variables were recorded directly from the sensor pack (Table 4.3). The potentiometer output voltage was converted to be within the limits of the sensor pack's analogue input by a custom voltage modifier, supplied to the sensor pack and recorded as "Analogue input 1 voltage". All data were uploaded from the navigator and analysed offline.

Variable	*Source*
Time (s)	Sensor pack
Sagittal angle (deg)	Sensor pack
Sagittal velocity (deg/s)	Sensor pack
Gyroscope voltage (V)	Sensor pack
Analogue input 1 voltage (V)	Potentiometer

Table 4.3: Variables recorded for sensor pack validation experiments.

Dynamic

Further experiments were carried out to investigate the drift under dynamic conditions. The setup was the same as for the static experiments. However, here the rod was oscillated over a range of approximately 12°. Experiments were carried out using both a constant and varying oscillation frequency.

4.2.2 Results

Static

Sagittal angle, velocity and the raw voltage output from the sensor pack are plotted in figure 4.5. Each subplot shows data logged over a period of four minutes from three consecutive experiments carried out at a rod position of 45°. In each case, there is a clear drift in the measured variable during the first 50 to 100 seconds, corresponding to approximately 0.9 - 2°, 2 - 6.6°/s and 8 - 24mV respectively. This behaviour was displayed at every measured rod position, in all experiments, and with drift ranges consistent with those shown above found in each case. The average drift, found over all 15 experiments, is shown in table 4.4.

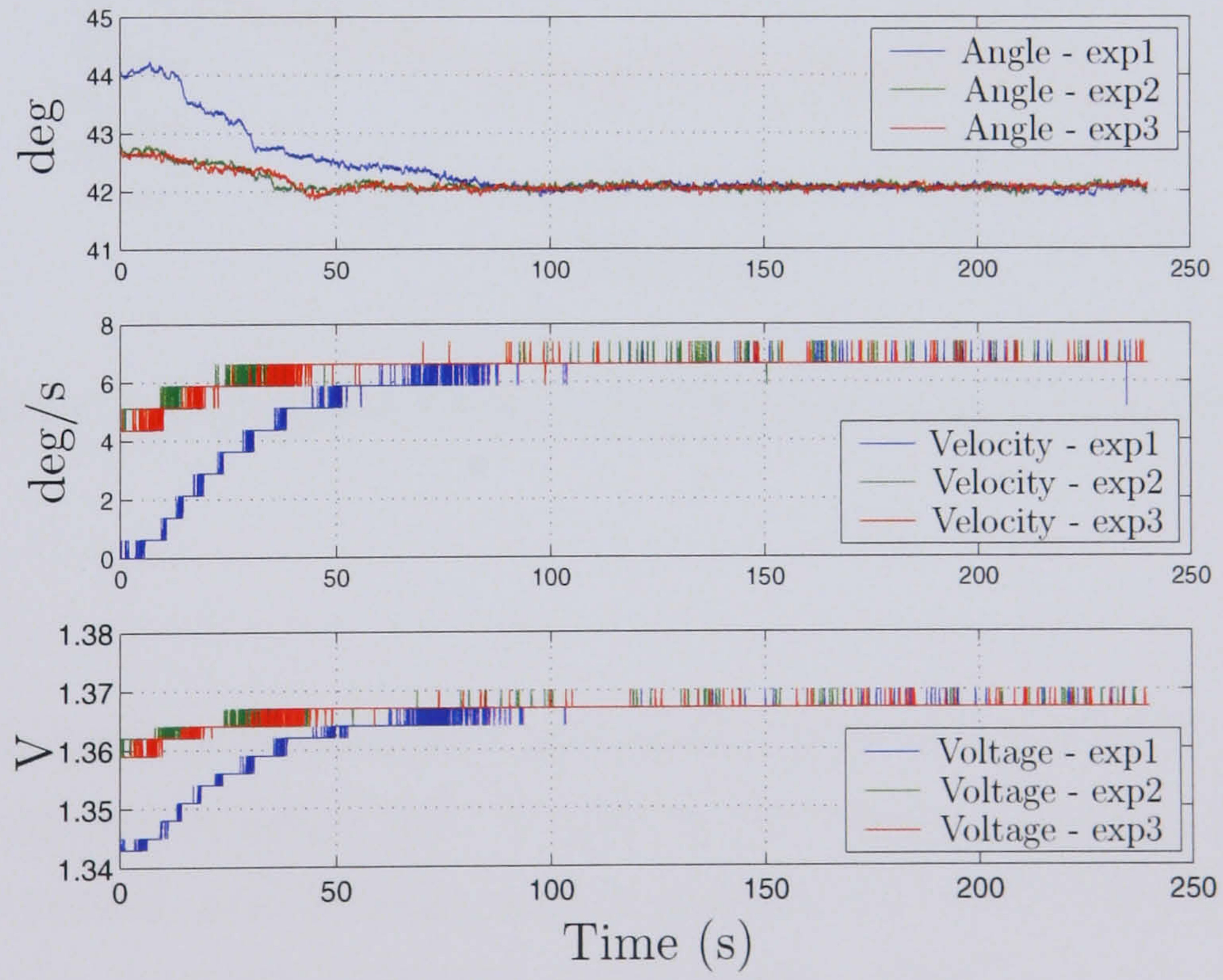

Figure 4.5: Sagittal angle, sagittal velocity and gyroscope voltage during three experiments at a rod position of 45°.

Variable	*Average Drift*
Sagittal angle (deg)	1.281 ± 0.57
Sagittal velocity (deg/s)	4.408 ± 2.58
Gyroscope voltage (V)	0.02 ± 0.024

Table 4.4: Average drift ($\pm$ standard deviation) in recorded data over 15 static experiments.

For comparison, sagittal angle data from the sensor pack are plotted against the equivalent potentiometer angle (obtained from its output voltage) at a rod position of 89° (figure 4.6). A similar drift to that displayed in figure 4.5 can be seen in the sensor pack data whilst the potentiometer angle remains almost constant throughout.

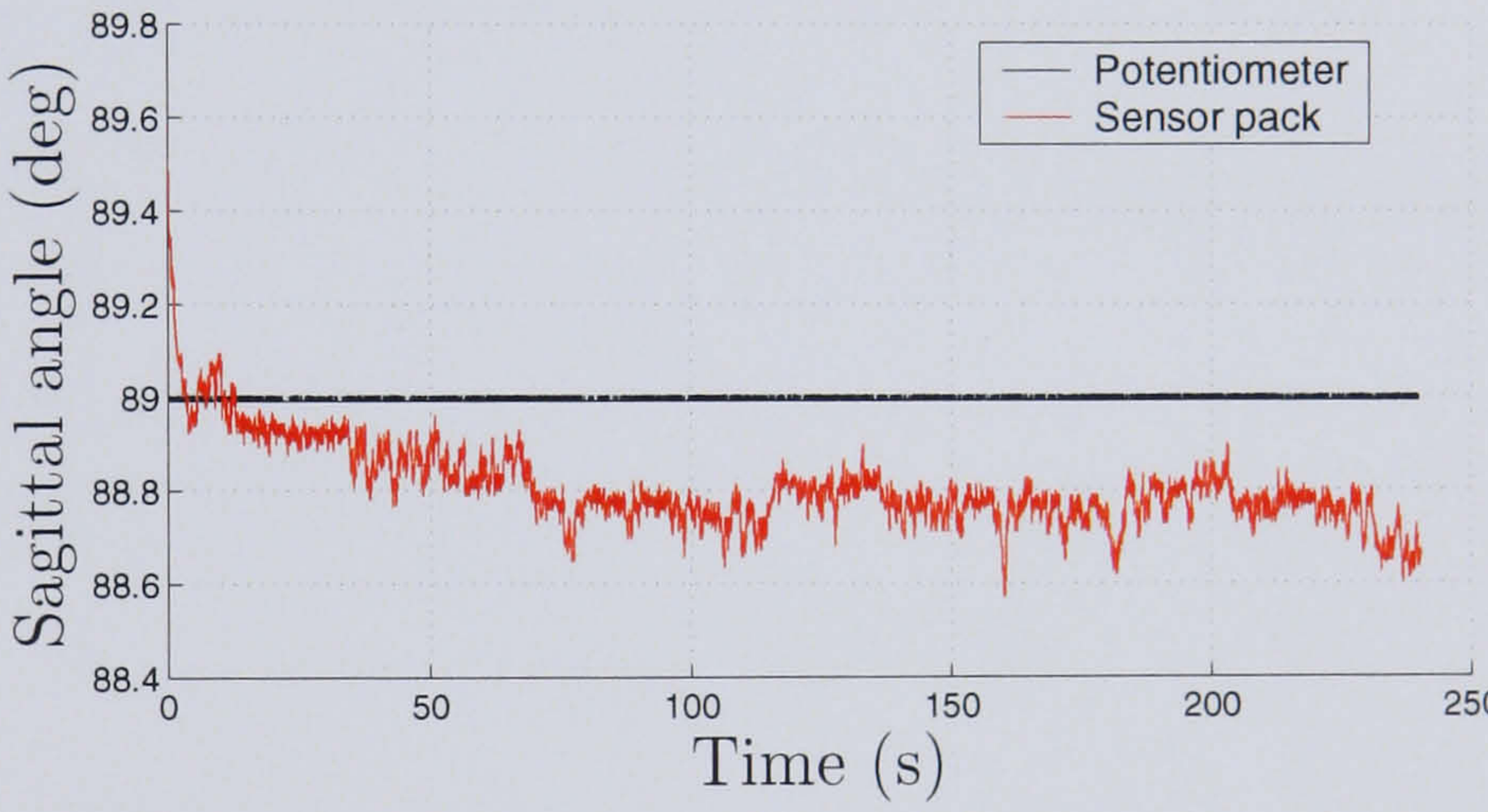

Figure 4.6: Sensor pack sagittal angle versus equivalent potentiometer angle at 89°.

Dynamic

Angle data from both potentiometer and sensor pack during the variable oscillation experiment are shown in figure 4.7. A drift in the sensor pack data is apparent over both the whole period, and sections with a constant oscillation frequency. The latter was verified in the constant frequency experiments. Moreover, the amplitude of the sensor pack angle data appears to vary with the oscillation frequency. This is highlighted in figure 4.8, where the sensor pack error (with respect to the potentiometer angle) appears to closely follow the frequency behaviour.

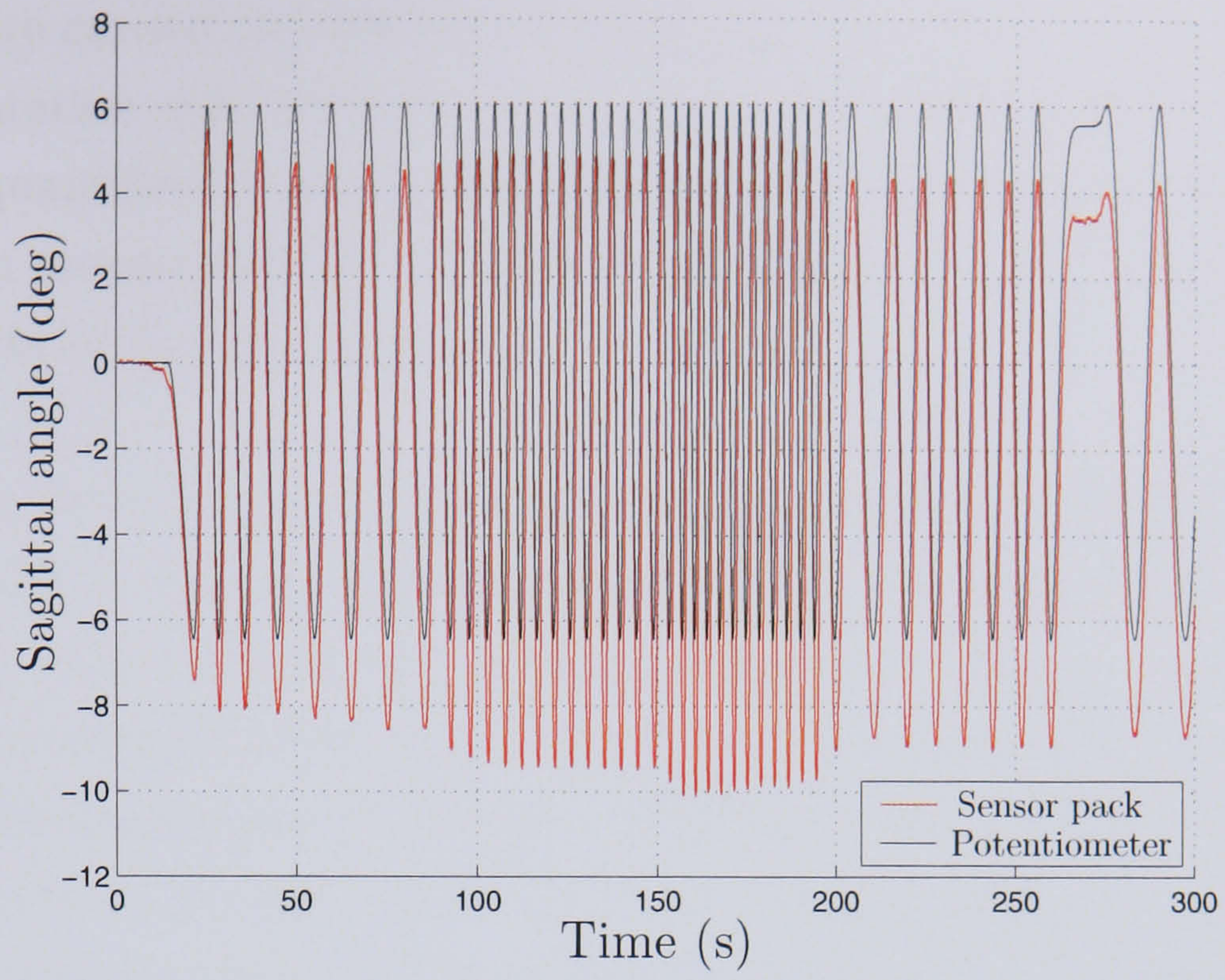

Figure 4.7: Sensor pack sagittal angle versus equivalent potentiometer angle during variable oscillation frequency experiment.

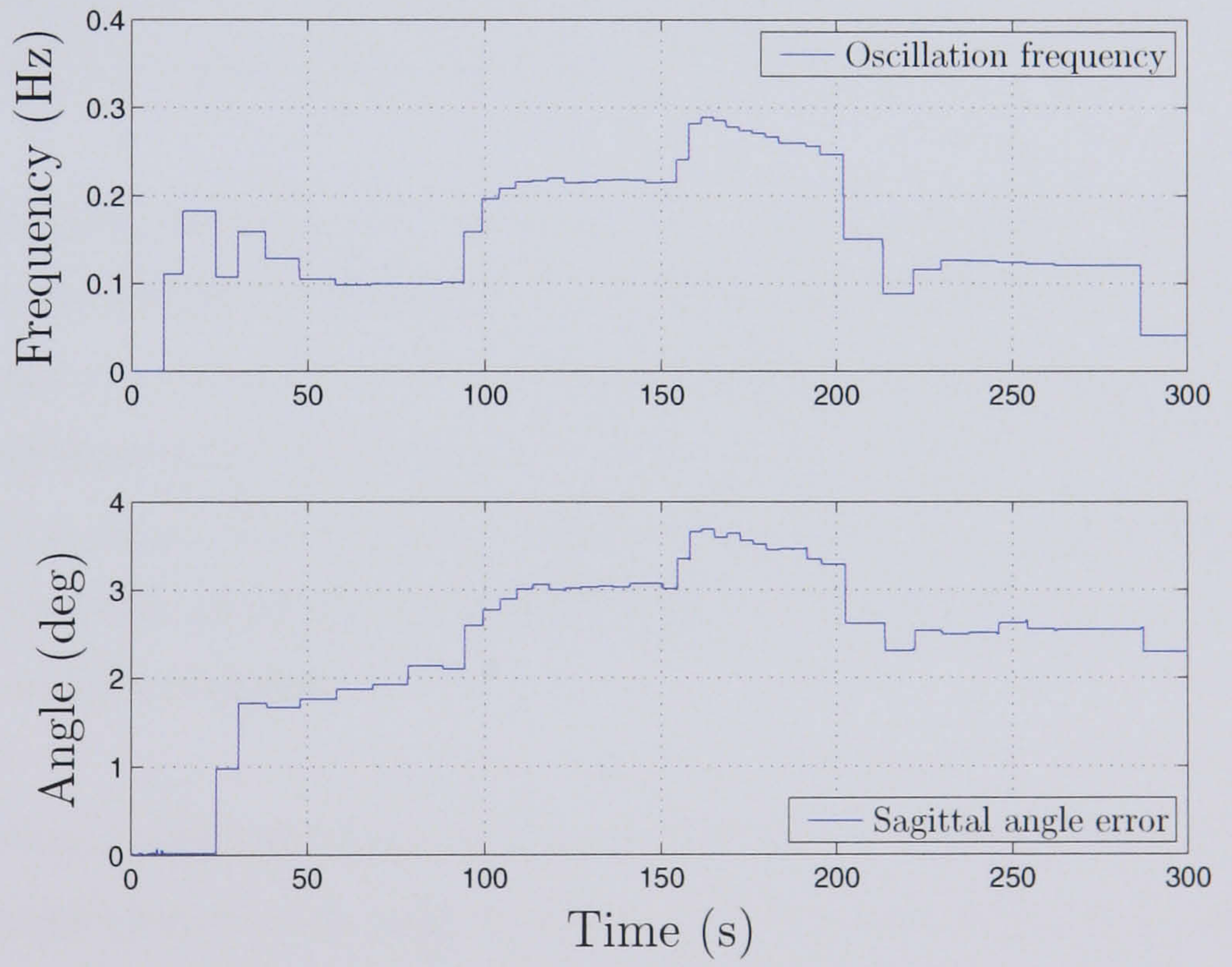

Figure 4.8: Rod oscillation frequency and sensor pack sagittal angle error during variable oscillation frequency experiment.

4.2.3 Discussion

Experiments were carried out which were designed to test the performance of the sensor pack. Orientation data were observed under both static and dynamic conditions with any error quantified. It should be noted that the manufacturer of the sensor pack ceased operation around the time of these experiments so it was not possible to obtain replacement parts or further assistance.

In a recent study, carried out by those who designed the device, Simcox et al. [78] detail the control algorithm used to estimate orientation by the sensor pack and investigate its performance using a 3D motion analysis system. To estimate sagittal angle, the sagittal velocity (obtained from the gyroscope) is integrated, then compared with the accelerometer signals and passed through a nonlinear filter in order to remove any drift (caused by integration of small errors and noise in the gyroscope). Our static experiments showed a drift in orientation data over the first 50 to 100 seconds in all data sets. After this time period, however, the estimated angle does remain relatively constant with a reasonably small offset. Moreover, the magnitude of the error ($1.281 \pm 0.57°$) appears to be within acceptable limits illustrated by similar sensors. Luinge et al. [82], who adopt a similar sensor fusion approach in their device, showed a maximum error of approximately 1.5° over a period of 140s.

During the dynamic experiments, however, this error not only increased significantly (up to 3.69°, at an oscillation frequency of 0.289Hz) but did so in conjunction with the oscillation frequency of the rod. Orientation data shown by Simcox et al. [78] during sit to stand and walking experiments show a fairly close correlation between a sensor pack and 3D analysis system. However, our findings may not be comparable as the dynamic behaviour of the their experiments is different to ours and data are only shown over the first three to four seconds.

Although the static performance of the sensor pack, shown in these experiments, is impressive (considering its size and weight), the dynamic behaviour observed has consequences for its planned use as a source of orientation data for cycling. The sinusoidal behaviour of the oscillating rod resembles that of the thigh during recumbent cycling, therefore the fact that the sensor pack's estimated angle moves outwith the geometrical constraints, displayed by the potentiometer (figure 4.7), means control which incorporates this device must somehow compensate.

4.3 Angle Conversion

Following testing of the sensor pack, an approach was decided upon which would make use of the orientation data in such a way that crank position could be calculated directly from limb position, therefore allowing existing stimulation timing patterns to be used. For this, a conversion algorithm would be created that converted a measured hip angle to an estimated crank angle whilst taking into consideration the drift issues found in section 4.2.

4.3.1 Methods

Aims and Objectives

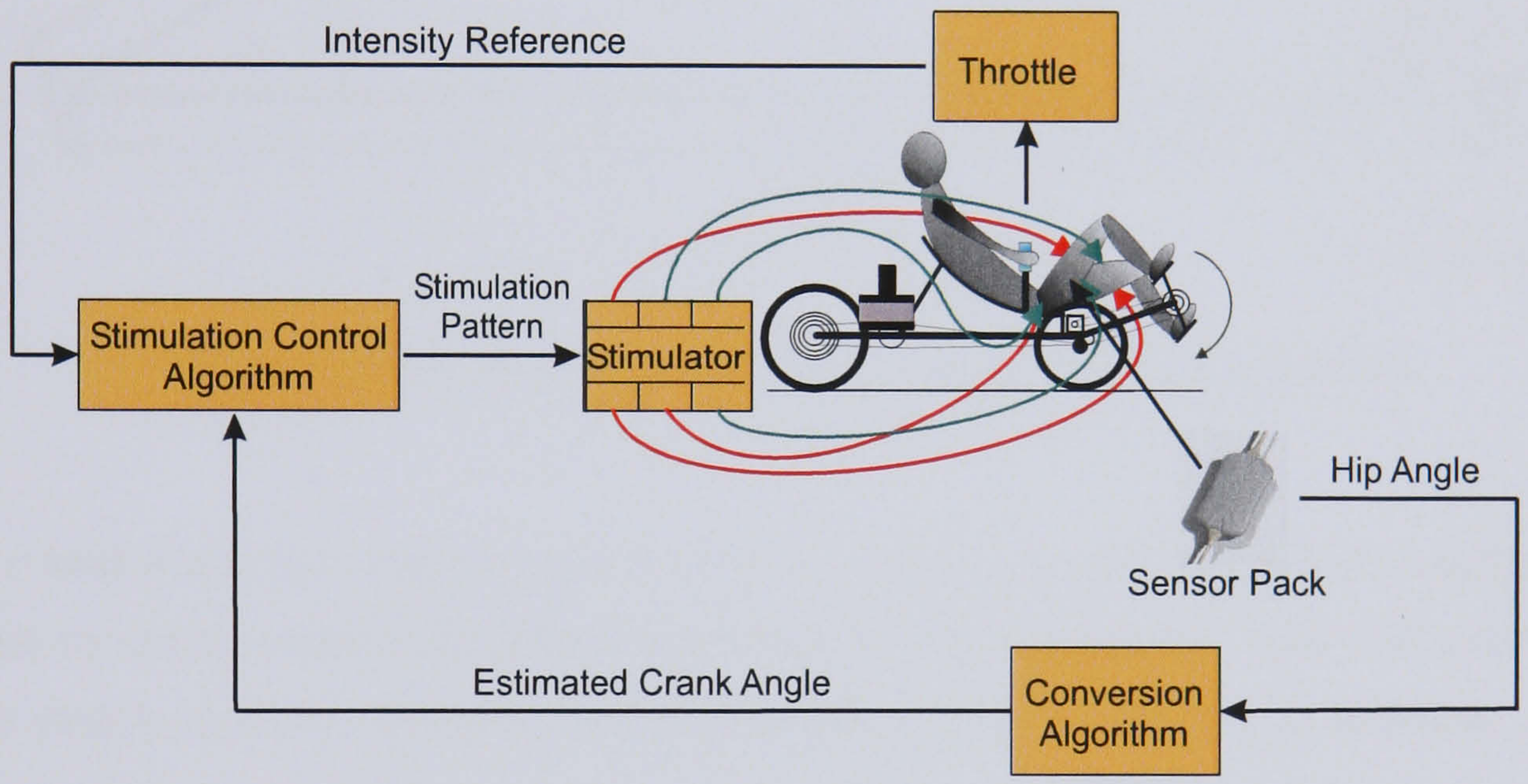

Figure 4.9: Schematic showing incorporation of sensor pack into FES-cycling system.

The aim is to incorporate the limb-mounted sensor pack into an existing FES-cycling strategy (as shown in figure 4.9) by using a measured hip orientation to calculate an estimated crank angle. There are three stages involved in this.

(i) Creation of an algorithm which converts a hip angle to corresponding crank angle.

(ii) Validation of the algorithm through simulation.

(iii) Validation of the algorithm using real data.

Geometric Approach

Two approaches were used to estimate crank position based on the angle of a subject's hip to the horizontal. The first is carried out using the geometric relationship shown below [51].

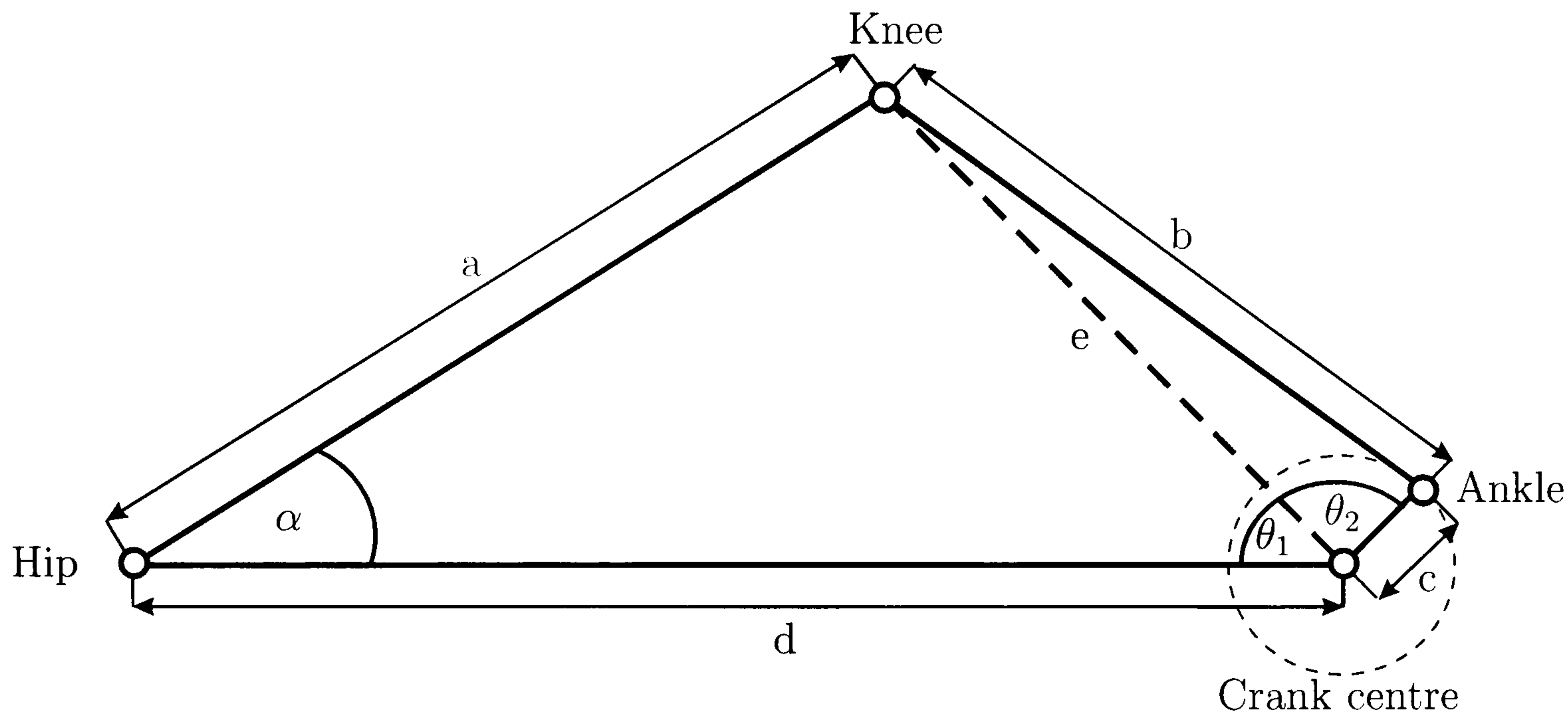

Figure 4.10: Hip to crank centre geometric relationship.

If a, b, c and d are the thigh length, lower leg length, crank arm length and length from hip joint to crank centre (baseline) respectively (figure 4.10), e (the distance from knee joint to crank centre) can be calculated from the hip angle (α) as follows:

$$e = \sqrt{a^2 + d^2 - 2ad\cos\alpha} \tag{4.1}$$

Using e and assuming the feet are fixed to the pedals, θ_1 and θ_2 can then be calculated and added together to obtain a crank angle (θ_C) via the following relationships:

$$\theta_1 = \cos^{-1}\left(\frac{d^2 + e^2 - a^2}{2de}\right) \tag{4.2}$$

$$\theta_2 = \cos^{-1}\left(\frac{e^2 + c^2 - b^2}{2be}\right) \tag{4.3}$$

$$\theta_C = \theta_1 + \theta_2 \tag{4.4}$$

An algorithm, which incorporates this relationship, was created using Matlab. Bio-mechanical measurements, a, b, c and d (which will vary with different subjects and trikes) are measured beforehand and defined as constants within the algorithm. The sampled hip angle (α) is the input variable and estimated crank angle (θ_C) the output.

Conversion Issues

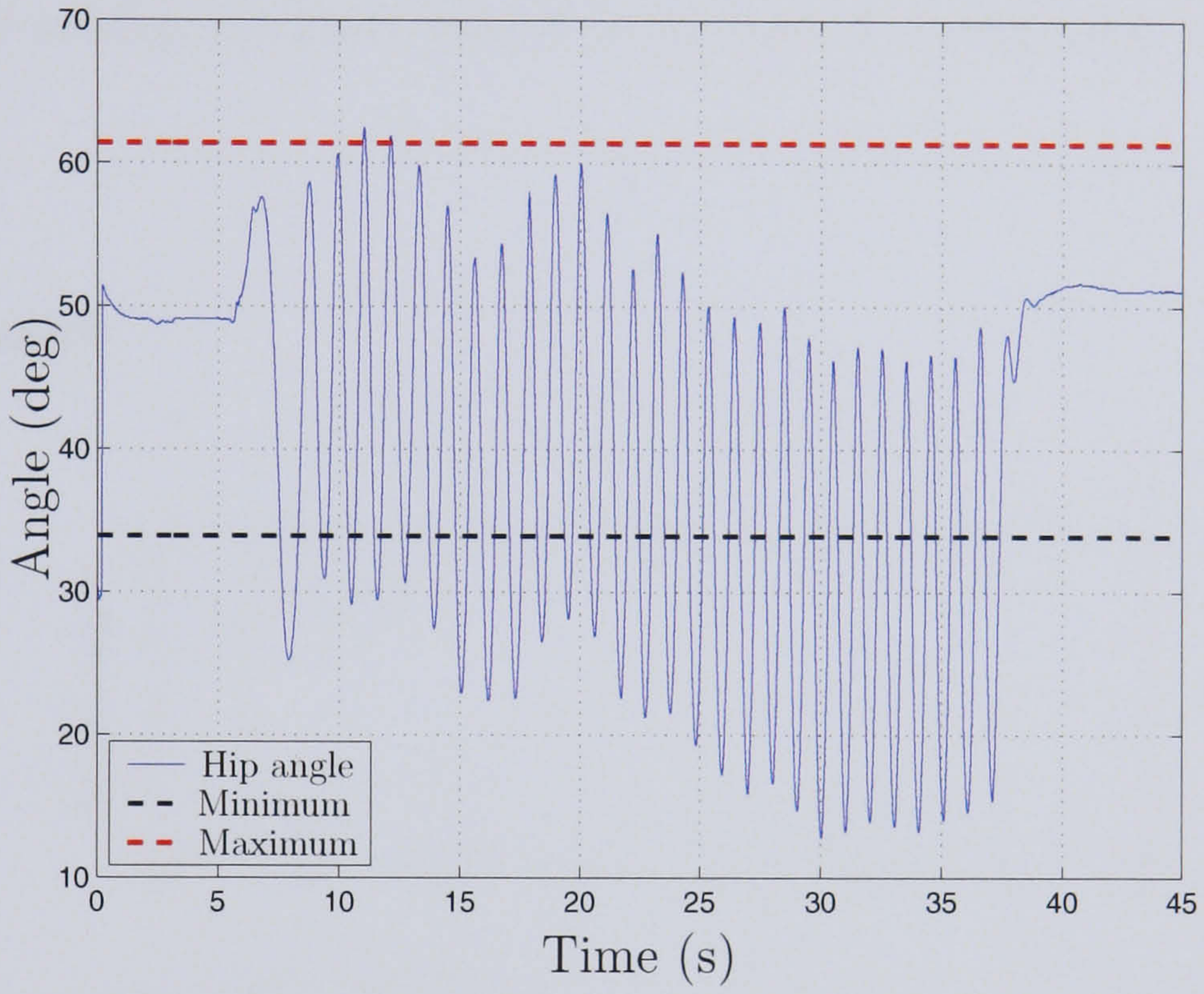

Figure 4.11: Comparison of measured hip angle over time versus theoretical maximum and minimum hip angles.

As the experiments described in section 4.2 showed, orientation data calculated by the sensor pack are subject to significant drift during oscillatory conditions. Also, in reality, the distance between hip joint and crank centre may not be constant during a period of cycling, as the rider moves in the seat. The effect of these issues is illustrated in figure 4.11, which shows a hip angle over time, as recorded by the sensor pack, for an individual cycling on a recumbent tricycle. The two horizontal lines correspond to the maximum and minimum hip angles based on the individual's initial bio-mechanical measurements (a = 0.57m, b = 0.57m, c = 0.135m and d = 0.77m), and calculated using the following equations:

$$\alpha_{max} = \cos^{-1}\left(\frac{a^2 + d^2 - (b+c)^2}{2ad}\right) \tag{4.5}$$

$$\alpha_{min} = \cos^{-1}\left(\frac{a^2 + d^2 - (b-c)^2}{2ad}\right) \tag{4.6}$$

As can be seen, the measured hip angle moves significantly outwith the initial theoretical constraints. To combat this behaviour, the geometric conversion algorithm limits a measured hip angle signal within the initial, calculated, maximum and minimum values (possible because of the repetitive and constrained nature of cycling). This operation is carried out by scaling the data (based on the initial constraints) on a cycle-to-cycle basis.

Heuristic Approach

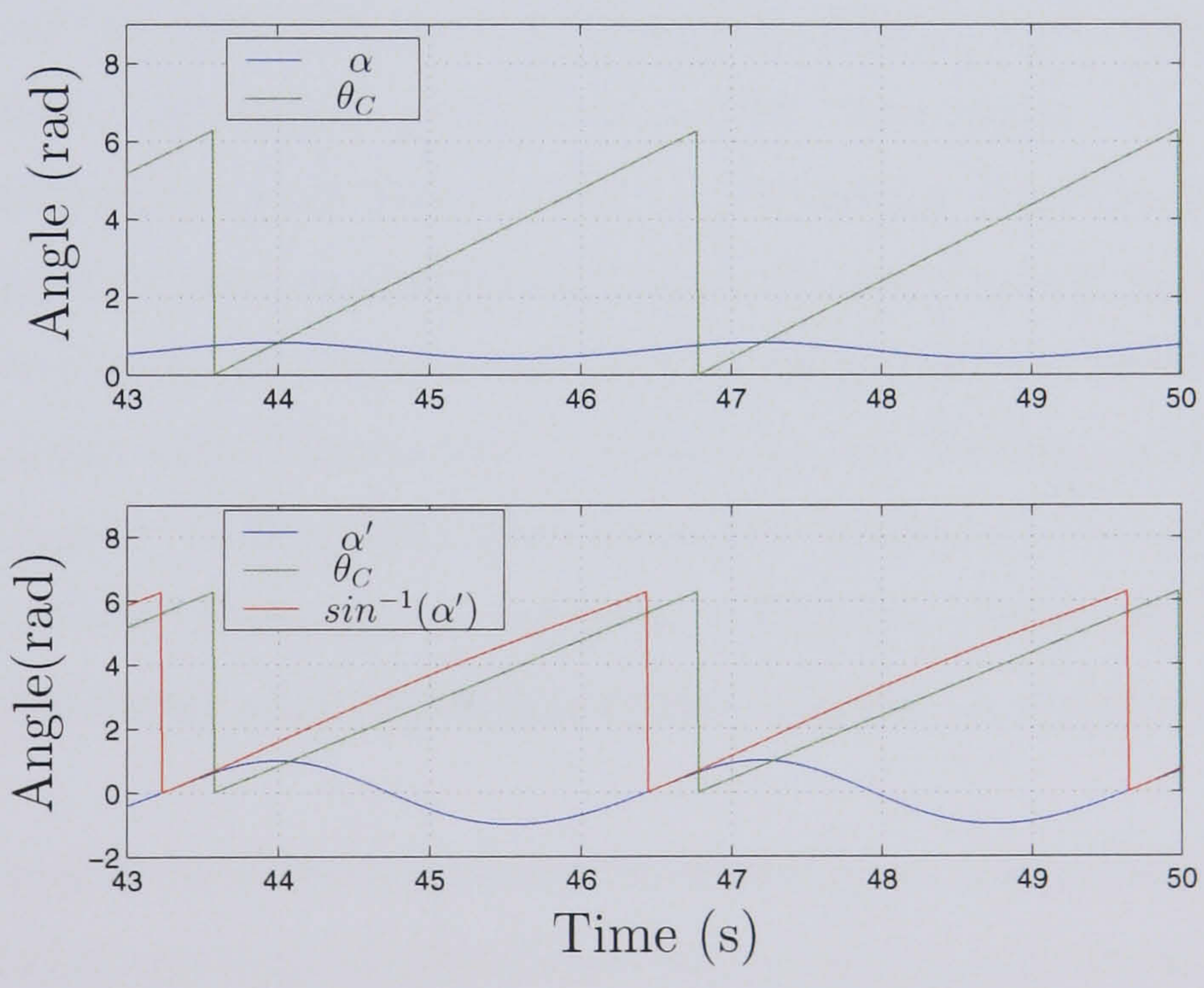

Figure 4.12: Crank angle, θ_C, versus the corresponding hip angle, α (upper plot). Scaled hip angle, α', and inverse sine versus crank angle (lower plot). ψ is the phase shift between θ_C and $sin^{-1}(\alpha')$.

The second approach involves manipulation of the hip angle in its sinusoidal form to obtain a crank position using the following relationships (represented graphically in figure 4.12):

$$\alpha' = \left(\frac{\alpha - \alpha_{av}}{\alpha_{max} - \alpha_{av}} \right) \tag{4.7}$$

$$\theta_C = \sin^{-1}(\alpha') + \psi \tag{4.8}$$

Here, α is a measured hip angle over a period of time (α_{av} and α_{max} are the mean and maximum values respectively), and α' is this value scaled between one and minus one, then the corresponding crank angle (θ_C) may be expressed as the inverse sine of α' plus an undetermined phase shift (ψ).

Equations (4.7) and (4.8) were implemented in a second algorithm. One notable factor when using this approach is that it purely involves manipulation of the output hip angle and no bio-mechanical measurements are required.

Procedure

As a first step, both algorithms were validated through simulation. A single degree of freedom model of the rider/tricycle system [83], which gives a hip and corresponding crank angle for a simulated period of cycling was used. By correlating initial bio-mechanical parameters with those used to determine the behaviour of the model, simulated hip angle data were converted into an estimated crank angle using both algorithms and compared with that produced by the rider/tricycle model. Simulations and subsequent crank angle calculations were carried out for cycling cadences of 10 − 80rpm, with intervals of 5rpm. Additional data were also gathered at cadences used during collection of real data for comparison purposes. The time step used for all simulations was 0.05s, thus correlating with the sample rate utilised in obtaining real data.

The second stage was to test both conversion algorithms using real data recorded from the sensor pack during cycling. Experiments were carried out using a standard recumbent tricycle[3], modified for FES-cycling as described in [43]. The rider was seated as shown in figure 4.13, with the sensor pack attached to their right thigh. To measure crank position, the tricycle's shaft encoder output voltage was recorded using one of the sensor pack's analogue inputs.

[3]Inspired Cycle Engineering Ltd., Falmouth, UK. http://www.ice.hpv.co.uk/

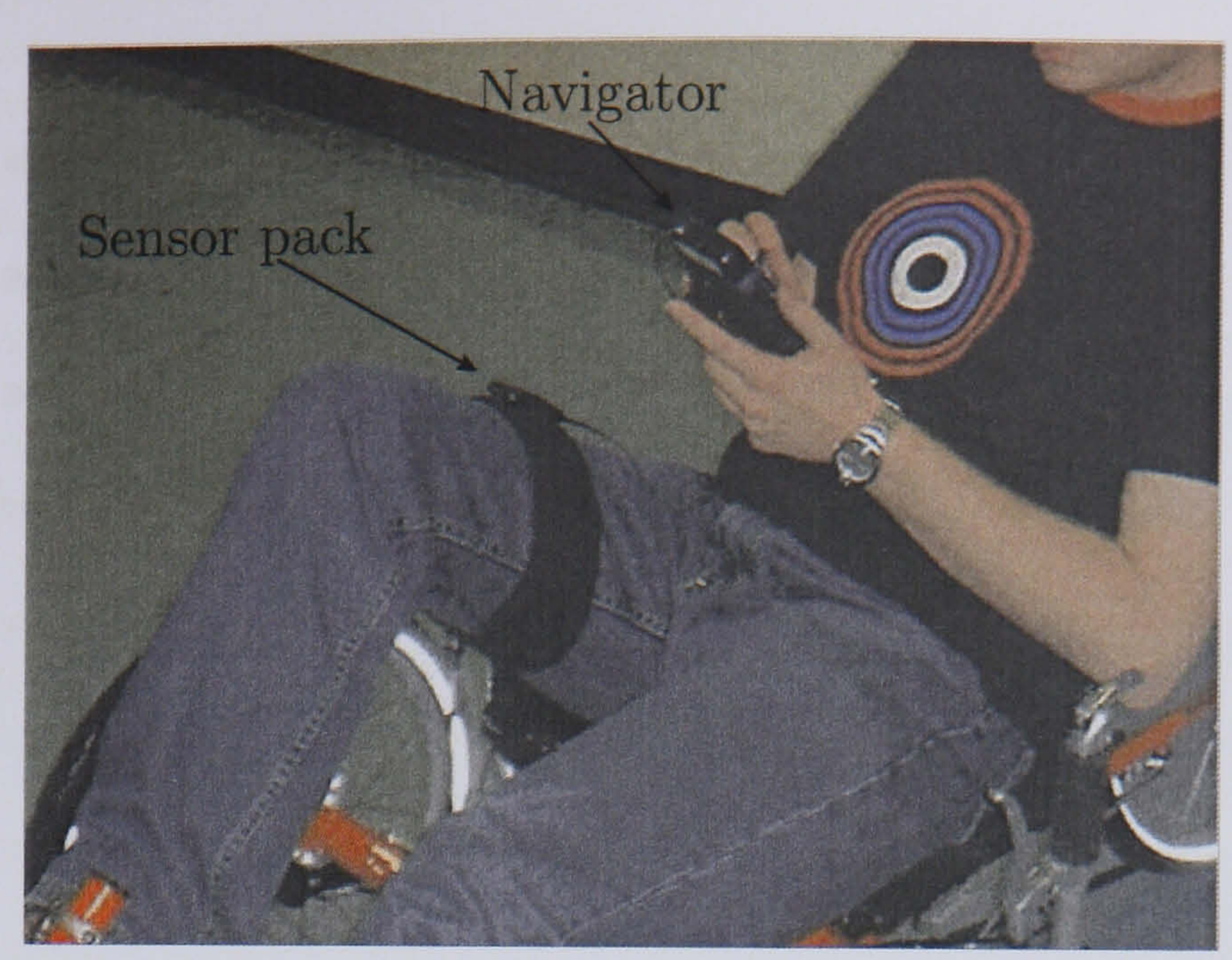

Figure 4.13: Angle conversion algorithm validation - experimental setup.

A matlab sequence was created and downloaded onto the Navigator which would record sagittal (hip) angle and convert the shaft encoder's output voltage into crank position. Data were recorded at a sample rate of 20Hz over three sessions. During each, and following a static period to allow any initial orientation drift to settle, the rider cycled for up to a minute at selected cadences of approximately 24rpm, 31rpm, 43rpm, 55rpm and 70rpm. Data were subsequently analysed offline, using both algorithms to compare the measured and estimated crank angles.

4.3.2 Results

Simulated Data

A comparison of estimated crank angle (θc_{est}), using the geometric approach, versus actual (θc_{act}) crank angle at a simulated cycling cadence of 50rpm is shown in figure 4.14. Here the estimated angle is calculated based on a simulated hip angle and the corresponding initial bio-mechanical parameters the rider/tricycle model uses to calculate it ($a = 0.43$m, $b = 0.53$m, $c = 0.1$m and $d = 0.76$m). A delay of exactly 0.05s between θc_{est} and θc_{act} was found during all simulation experiments. This is equivalent to one sample at 20Hz and occurs because the algorithm uses a data point one sample previous to the current during its calculations.

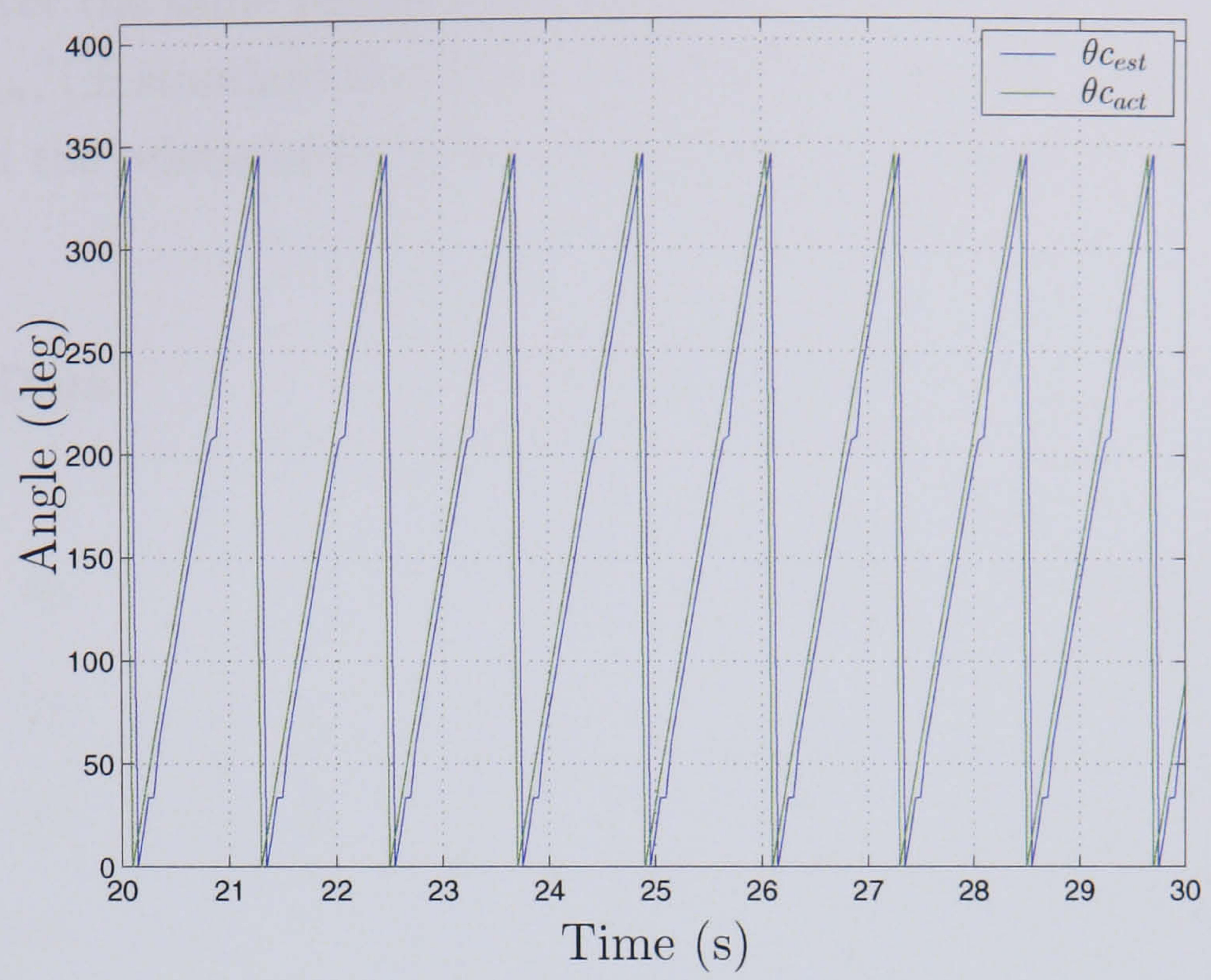

Figure 4.14: Simulated crank angle, θc_{act}, produced by rider/tricycle model [83] at a cadence of 50rpm, versus estimated crank angle, θc_{est}, as calculated using the geometric algorithm.

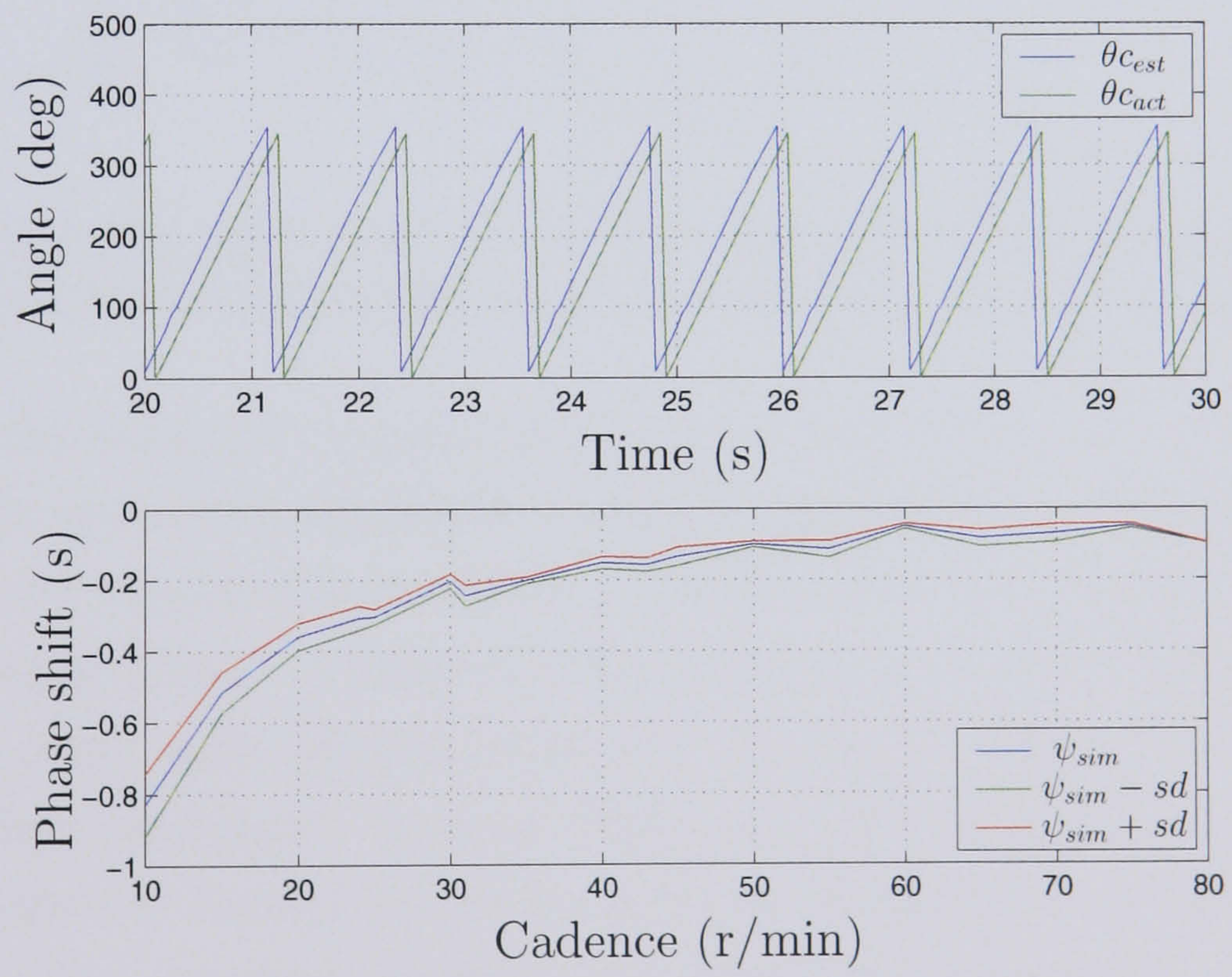

Figure 4.15: Simulated crank angle versus estimated crank angle, as calculated using the heuristic algorithm at 50rpm (upper plot). Relationship between average phase shift (ψ_{sim}) and cycling cadence across all simulations and using heuristic algorithm (lower plot). sd - standard deviation.

In the upper plot, figure 4.15 shows the estimated crank angle calculated by the heuristic algorithm over the same period and using the same data set as in figure 4.14. The phase shift, ψ_{sim}, ($\pm$ standard deviation) between θc_{act} and θc_{est} was calculated for all simulations and the relationship with cycling cadence is shown in the bottom plot.

Experimental Data

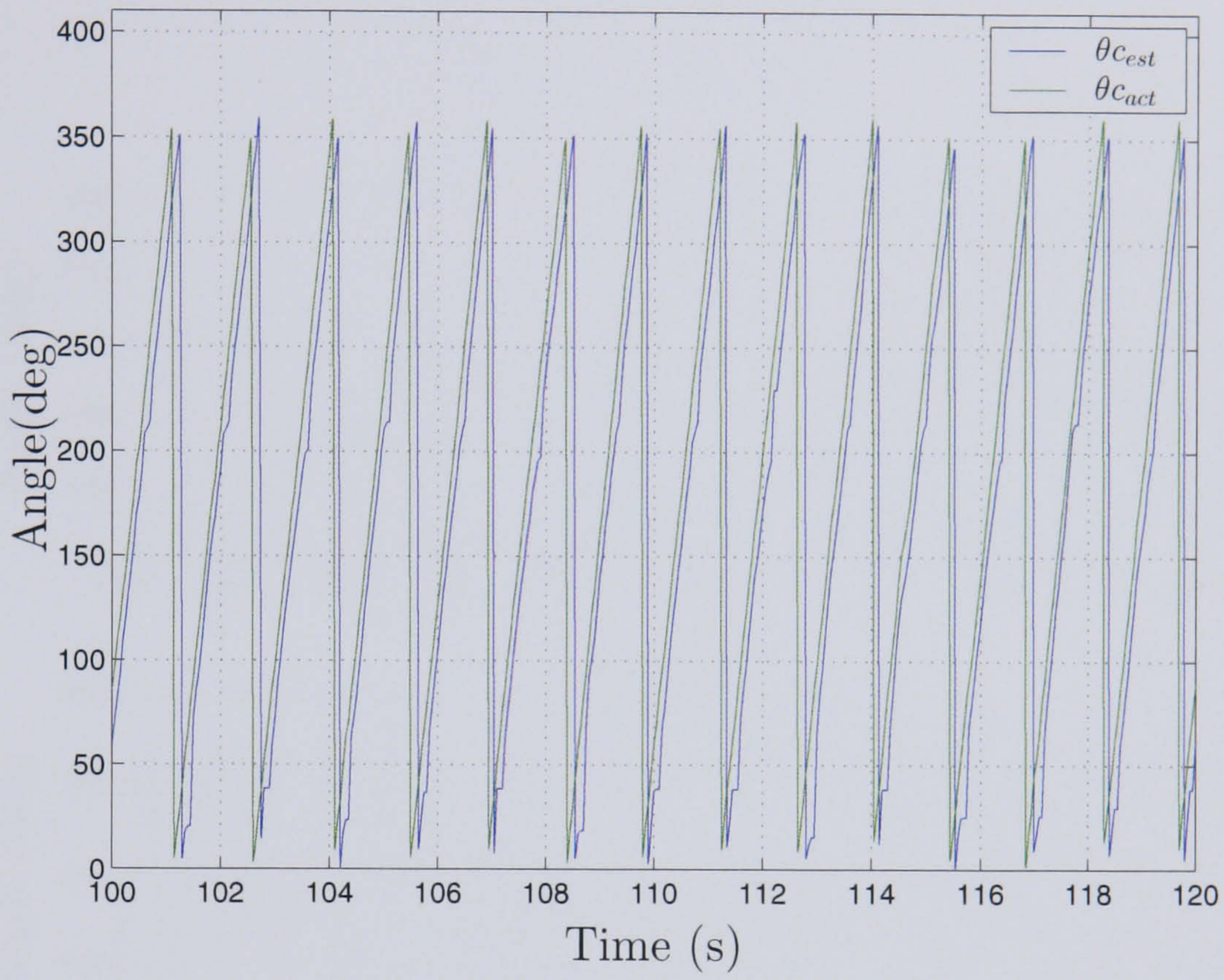

Figure 4.16: Measured crank angle, θc_{act}, at a cadence of approximately 43rpm, versus estimated crank angle, θc_{est}, as calculated using the geometric algorithm.

In figure 4.16, the estimated crank angle (θc_{est}), calculated from a sensor-pack-measured hip angle by the geometric algorithm, is plotted against the corresponding crank angle obtained from the tricycle's shaft encoder. The cycling cadence during this experiment was approximately 43rpm. A delay of 0.121 ± 0.031s is evident between the measured and estimated crank angle. Similar behaviour was found in data sets acquired and calculated from each experiment. Average delays ($\pm$ standard deviation) for each cadence are given in table 4.5. Figure 4.17 shows portions of estimated crank angle data, with the respective delay removed, against their measured counterparts at approximately 43 and 55rpm.

Cadence (rpm)	D_{mean} (s)
~ 24	0.095 ± 0.028
~ 31	0.09 ± 0.032
~ 43	0.121 ± 0.031
~ 55	0.102 ± 0.078
~ 70	0.043 ± 0.118

Table 4.5: Average delay ($\pm$ standard deviation) between estimated (θc_{est}) and actual (θc_{act}) crank angles using geometric algorithm during selected cadences.

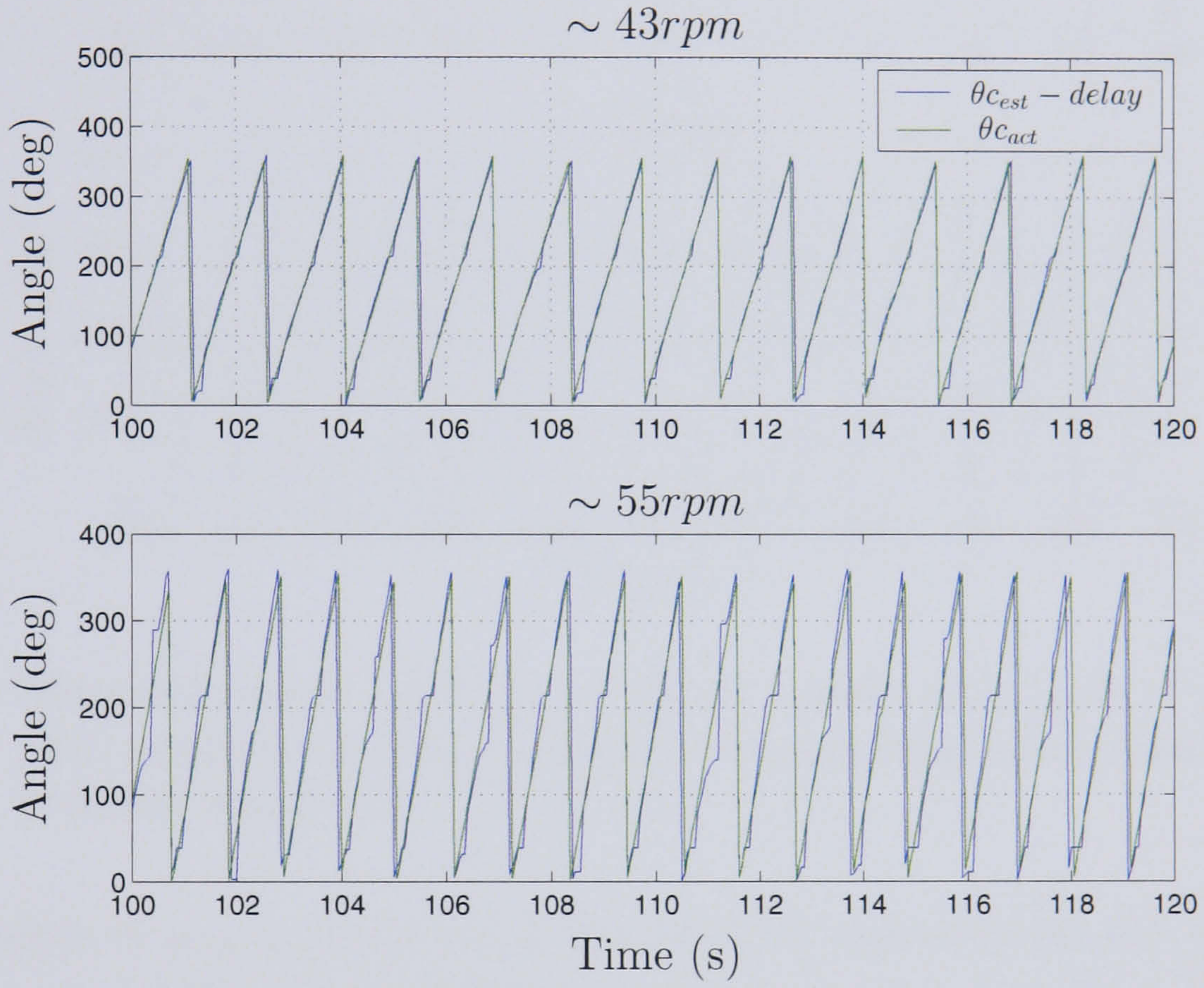

Figure 4.17: Measured crank angle at $\sim$ 43rpm (upper plot) and $\sim$ 55rpm (lower plot) versus estimated crank, following delay correction and using geometric algorithm.

Cadence (rpm)	ψ_{mean} (s)
~ 24	-0.195 ± 0.028
~ 31	-0.126 ± 0.025
~ 43	-0.064 ± 0.029
~ 55	-0.068 ± 0.027
~ 70	-0.095 ± 0.058

Table 4.6: Average values ($\pm$ standard deviation) of θc_{est} phase shift, ψ, using heuristic algorithm during selected cadences.

Applying the heuristic algorithm to data recorded during each experiment yielded the average phase shifts (ψ_{mean}) shown in table 4.6. Phase shift corrected crank angles, plotted against the corresponding measured crank position, are shown in figure 4.18.

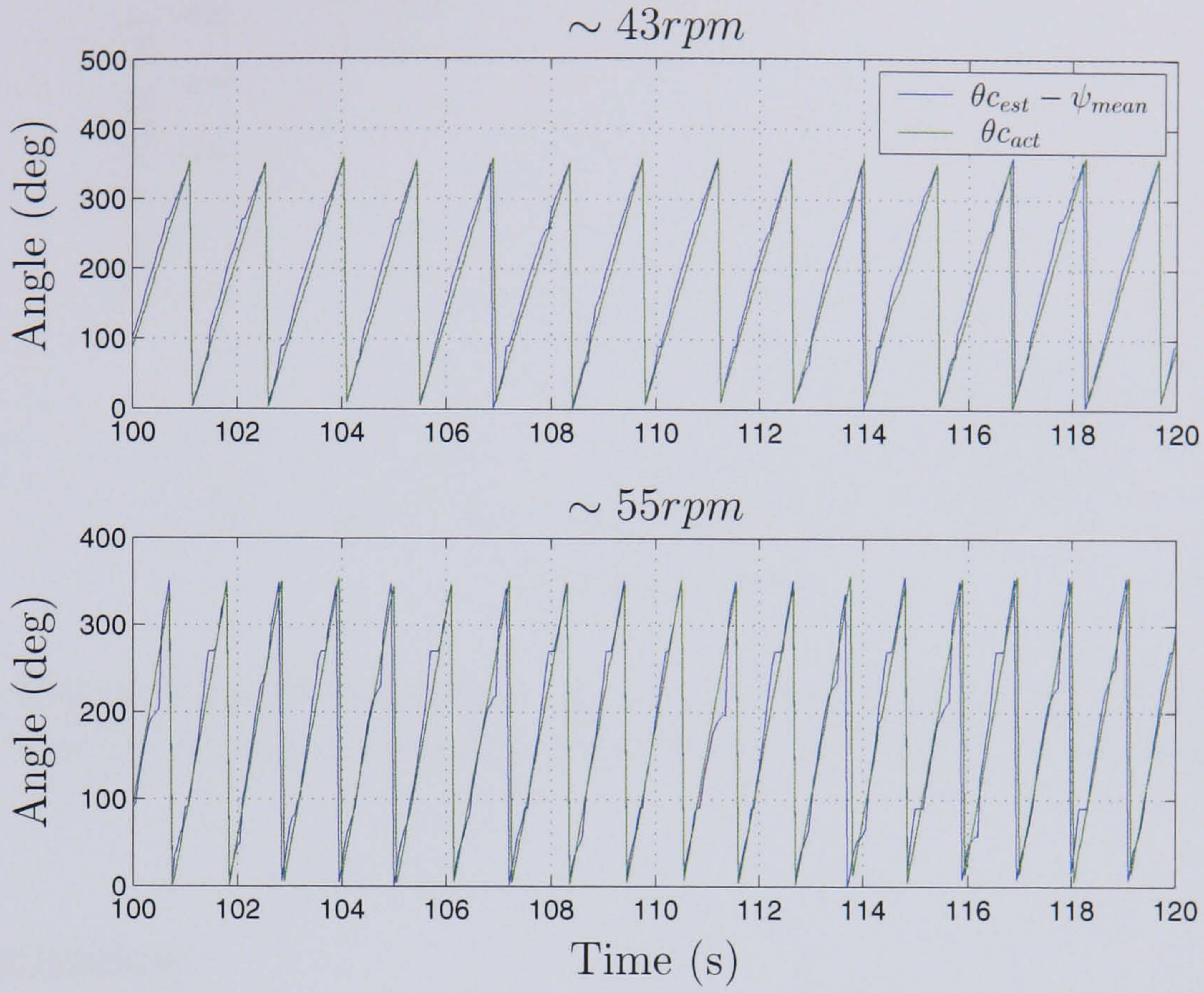

Figure 4.18: Measured crank angle at $\sim$ 43rpm (upper plot) and $\sim$ 55rpm (lower plot) versus estimated crank angle minus average phase shift (ψ_{mean}) using heuristic algorithm.

Although values of ψ_{mean} found using the heuristic approach do not quite fit those shown during simulation (figure 4.15), if it is assumed that the delay found between θc_{act} and θc_{est} in data calculated using the geometric algorithm is caused by some form of measurement error, in combination with the delay found during simulation, then:

$$\psi = \psi_{real} - (D_{real} - Ts) \tag{4.9}$$

Where ψ_{real} is the calculated phase shift using the heuristic approach and D_{real} is the estimated crank angle delay using the geometric approach. Ts is one time step.

To compare experimental values of ψ against those simulated, mean values of ψ_{real} and D_{real}, as shown in tables 4.6 and 4.5 respectively, were used in equation (4.9) to calculate the true phase shift calculated from experimental data. This value, ψ_{exp}, is plotted for all experiments against cadence in figure 4.19. Ts is 0.05s (to correlate with the 20Hz sample rate used during experiments).

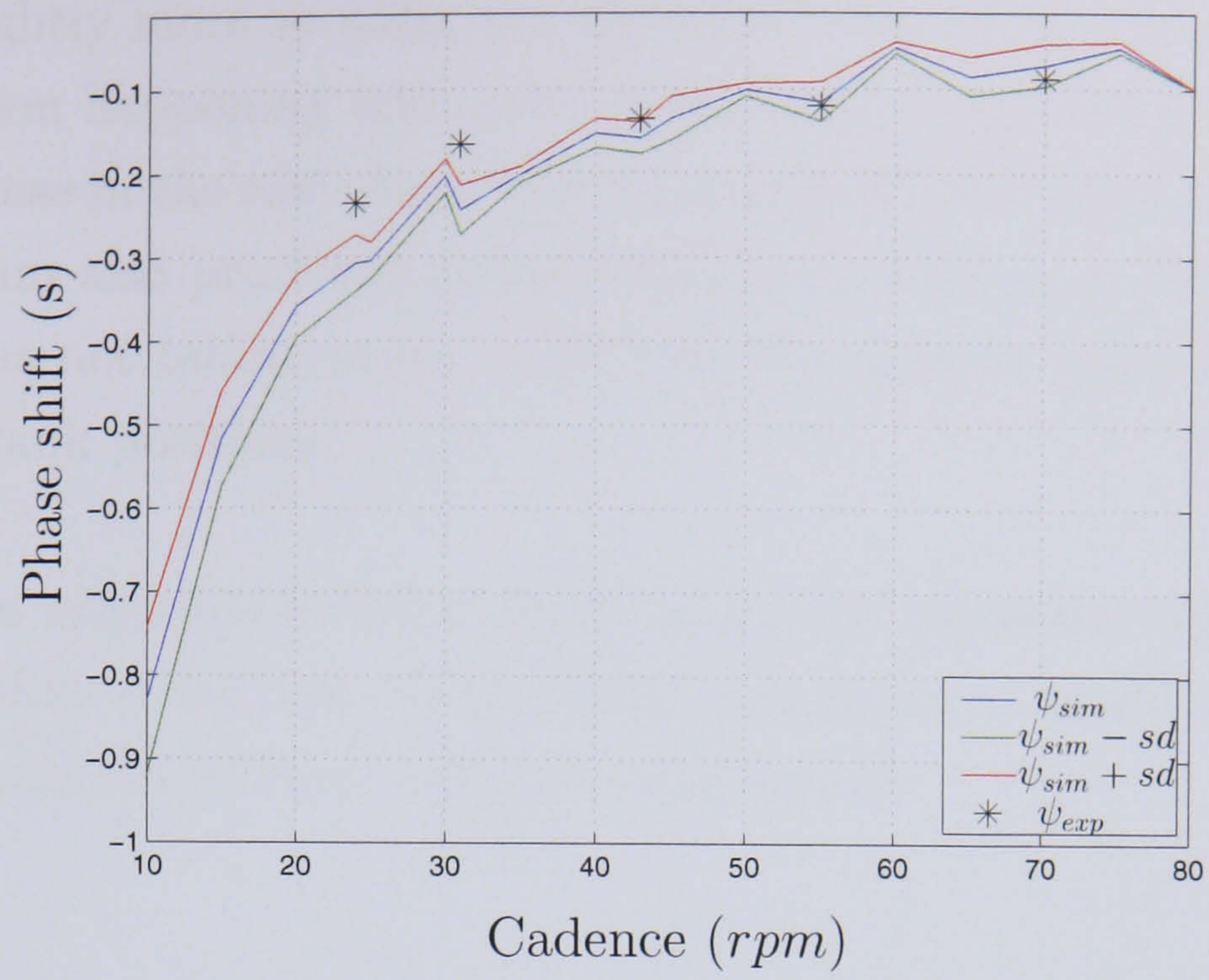

Figure 4.19: Comparison of measured (ψ_{exp}) and simulated (ψ_{sim}) phase shift found using heuristic approach over selected cadences. sd - standard deviation.

4.3.3 Discussion

For incorporation of a limb mounted sensor into an FES-cycle strategy, two algorithms which convert a hip angle into crank position, using different approaches, have been created. Each has been tested using both simulated and experimental data.

The estimated crank angle obtained using the geometric algorithm appeared to be very accurate throughout all simulated cycling cadences. An expected delay of one time step, that remained constant throughout, was found when comparing relevant data sets. When using measured data, the length of delay between actual and estimated crank angles increased beyond one sample and varied with each experiment. When the expected delay is removed in each data set, the final estimated angle is always within two samples of the actual.

The phase shift between actual and estimated crank angle using the heuristic approach demonstrated a non-linear relationship with cadence during simulation. When using real data, the calculated phase shift (following removal of the unpredicted delay that was found using the geometric algorithm) correlates quite closely with this relationship (figure 4.19), more so at higher cadences.

Using real data, the behaviour of the estimated crank angle in both approaches is quite smooth at low cadences. However, as the speed increased, it appeared to be more erratic (slightly more so using the geometric algorithm), with occasional lags in position estimation happening mid cycle. Upon inspection, this behaviour appears to originate from noise in the raw sensor data at maximum and minimum hip angles. The heuristic algorithm also produced rather undesirable behaviour during static periods. When cycling was not taking place, noise from the sagittal angle data was converted into erroneous crank positions.

The origin of the unpredicted delay found using the geometric algorithm is unclear. However, given that it did not occur during simulation it would appear to be from some form of measurement error using the sensor pack.

4.4 Integration Into an Existing FES-cycle System

With two possible approaches which utilise a limb mounted sensor within an FES-cycling stimulation strategy now available, the final stage of this investigation was to incorporate stimulation control strategies within the navigator which could use either a traditional position reference (such as a sampled crank angle), or limb position.

4.4.1 Methods

Aims and Objectives

The aim is to integrate FES-cycling stimulation control strategies within the Neopraxis FES system which incorporate a new hip-to-crank angle conversion algorithm (to employ the limb mounted sensor pack), are capable of utilising existing control interface hardware and may be implemented using both surface and implanted stimulation on a tricycle-based system. As a first step, the conversion algorithms (described in section 4.3 and thus far used offline) had to be converted into matlab sequences which could run on the navigator and calculate an estimated crank angle in realtime.

Next, an existing FES-cycling control strategy, which usually runs from a laptop, would be modified to run on the navigator and implement one of the two approaches illustrated in figure 4.20. The first, depicted by the outer loop, involves using the tricycle system's shaft encoder and throttle as control references while the second, shown in the inner loop, incorporates one of the new conversion algorithms to replace the shaft encoder with the sensor pack as a source of position information.

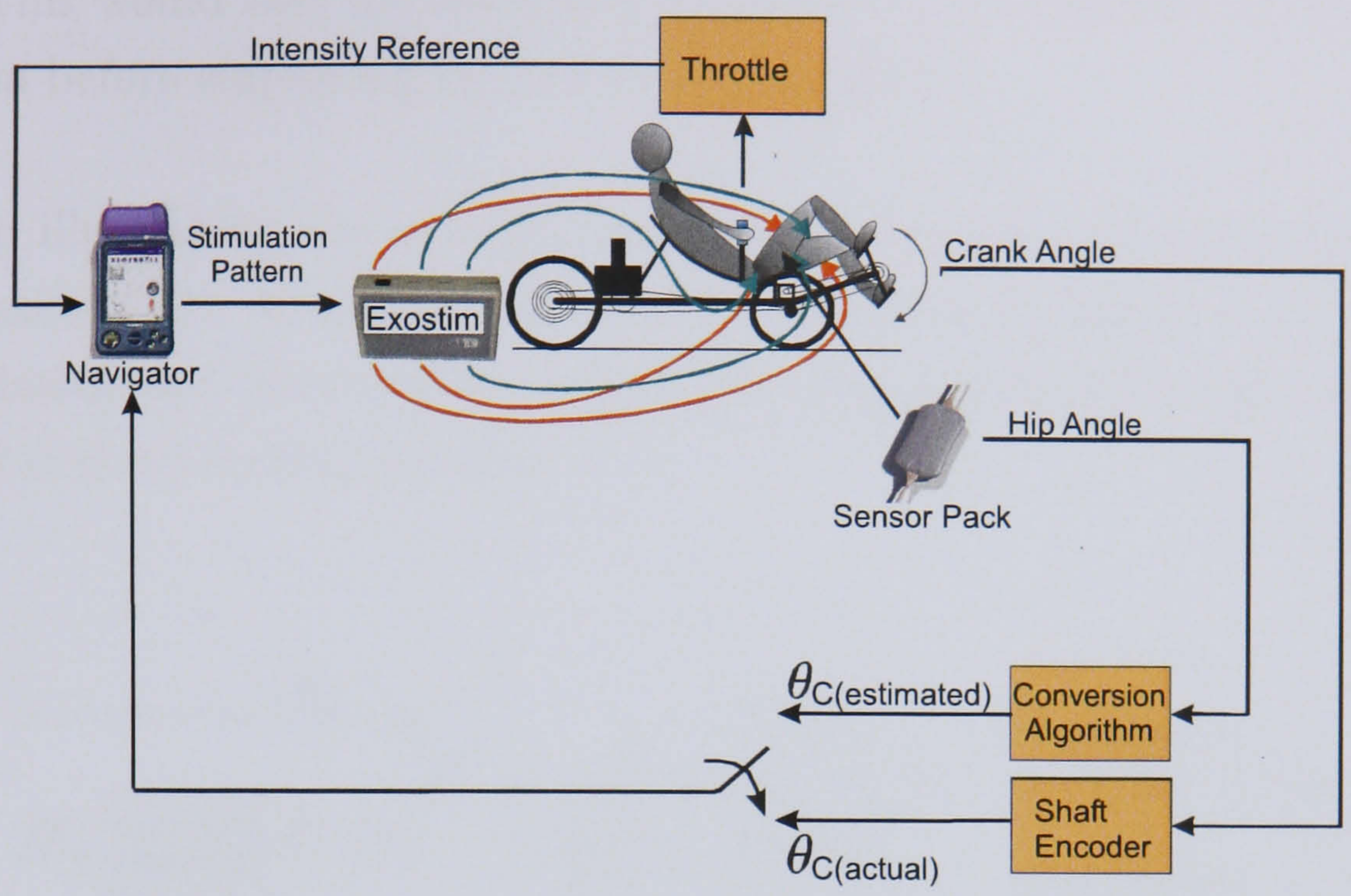

Figure 4.20: Schematic showing approaches for incorporation of Neopraxis surface FES-system into an FES-cycling setup. θc - sampled crank angle.

Realtime Conversion Models

Although both the geometric and heuristic conversion approaches had been shown to work relatively well offline, to work as part of a stimulation control strategy they must be capable of running in realtime. To investigate the feasibility of this, both algorithms were converted into simulink models whose inputs were sagittal angle and shaft encoder voltage that are converted into estimated and actual crank angle outputs. Both models were tested initially on a PC using simulated data at 30, 50 and 70rpm to validate the estimated crank angle and confirm expected delays/phase shifts incurred during iteration ($D_{expected}$ = 0.1s and $\psi_{expected}$ = 0.05s for the geometric and heuristic models respectively).

Next, the models were compiled, downloaded to the Navigator and experiments running the models in realtime were carried out at approximately the three cadences mentioned above. An exception to this was the third geometric model experiment which was carried out at approximately 79rpm due to difficulties in maintaining a desired cadence. All data were analysed offline with average values of D and ψ calculated.

Cycling Strategy Using Shaft Encoder

The first strategy to be adapted for use on the navigator was one that would follow existing FES-cycling approaches and use a directly measured crank position as its timing reference. This would test the feasibility of running such software on the new PDA-based system before employing the conversion algorithm.

A schematic illustrating the operation of the stimulation control strategies used is shown in figure 4.21. Based on the method described by Hunt et al. [43], muscle activation timing and intensity are calculated using a sampled crank angle, throttle position and derived cycling cadence.

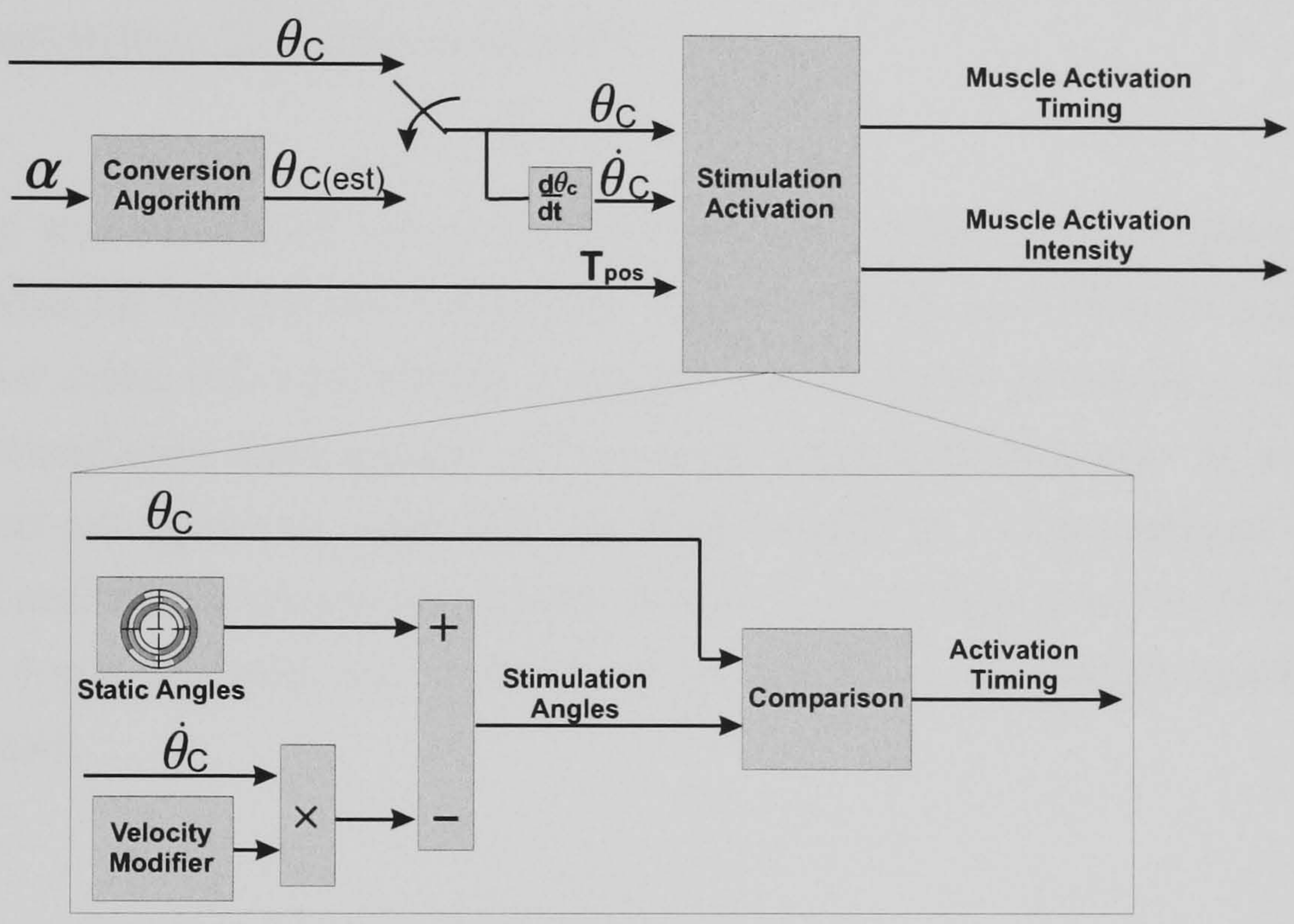

Figure 4.21: Schematic illustrating operation of stimulation control strategies used on Navigator. θc - crank angle, θc_{est} - estimated crank angle, $\dot{\theta} c$ - crank angular velocity, α - hip angle, T_{pos} - throttle position.

The highlighted portion of the activation sequence shows how timing is calculated. As discussed in the previous chapter, to determine which muscle requires to be stimulated at any given point, the position of the crank is monitored and compared with a static stimulation pattern. As the dynamics of the muscle contraction involve a delay between stimulation onset and production of maximum force, an additional velocity modifying term must be included. If the delay is assumed to be constant (approximately 150ms), then this term may be multiplied by the cadence to calculate a compensatory angle range. A new stimulation timing arc can then be produced by removing this range from the static values. Throttle position (between closed and fully open) is directly proportional to the level of stimulation intensity. On the Navigator, this is taken as a percentage between threshold and saturation current.

Input Variables	*Output Variables*
Shaft encoder voltage (V)	Stimulation level (%) - Q,H,G
Throttle voltage (V)	Stimulation timing (s) - Q,H,G
	Activation arc (deg) - Q,H,G
	Sampled crank angle (deg)
	Cadence (*rpm*)
	Throttle level(%)

Table 4.7: Variables logged in shaft-encoder-sourced strategy. Q - quadriceps, H - hamstrings, G - gluteal muscles.

The strategy was converted into a Simulink model which could be compiled as a sequence suitable for use on the Navigator. Shaft encoder and throttle position signals were obtained using the sensor pack analogue inputs while all outputs, that would be sent to the stimulator, were logged. All variables logged during tests at approximately 28 and 40rpm are shown in table 4.7. As there would be no stimulation during these experiments and the focus was on correct muscle activation times, the stimulation output channel (only one was was included in the model) and velocity modifier variable were set to zero.

Cycling Strategy Using Conversion Algorithm

The second strategy incorporated into the Navigator utilised the two conversion models described in section 4.4.1. This would test the feasibility of producing accurate stimulation patterns based on a hip angle source. Two models were created with the same stimulation control approach described above, but which also employed either the geometic or heuristic angle conversion model to produce an estimated crank angle as an input.

To ensure that delays and phase shifts found using the conversion algorithms would not result in incorrect muscle activation timing, the resulting error would have to be compensated for within the models. As mentioned, a velocity modifier variable is introduced to compensate for muscle contraction latency. Thus, adding the expected delay or phase shift caused though using the conversion algorithm to this variable should result in correct muscle activation timing. Tests were carried out at approximately 30 and 50rpm where all variables shown in table 4.7 were logged and, additionally, the measured sagittal angle and calculated estimated crank angle were also recorded. As no stimulation was carried out, the output stimulation channel was set to zero and the velocity modifier variable consisted solely of the values of D or υ found during the conversion model experiments.

Procedure

Experiments were run in the same way as described in section 4.3, with a rider cycling on a modified recumbent trike. All sequences were tested with the rider cycling at a desired cadence and the sensor pack attached to their right thigh. Shaft encoder and throttle voltages were recorded from a 10-bit optical encoder (located on the crank shaft) and throttle potentiometer (located on the handlebars), respectively. A supply voltage of approximately 2.5V was chosen for both to adhere to the sensor pack's analogue input limit of 2.8V.

During testing of the stimulation strategies, all stimulation channels included in the model were set to zero (with the Exostim still connected to ensure the sequences performed correctly whilst the Navigator was communicating with it). However, the throttle was still turned during each cycling period, to simulate stimulation, and all output variables were recorded. In all models, the sampling rate was set at 20Hz.

4.4.2 Results

Realtime Conversion Models

Figure 4.22 shows estimated (θc_{est}), versus actual (θc_{act}) crank angle when running both conversion models on a PC at a cycling cadence of 50rpm and using simulated data created by the rider/tricycle model [83] employed in section 4.3. In all results using the geometric model and simulated data, a constant delay of 0.1s was found between actual and estimated crank position. The heuristic model showed phase shifts that followed the cadence/phase shift relationship found in section 4.3.2 exactly, plus 0.05s throughout all experiments using simulated data.

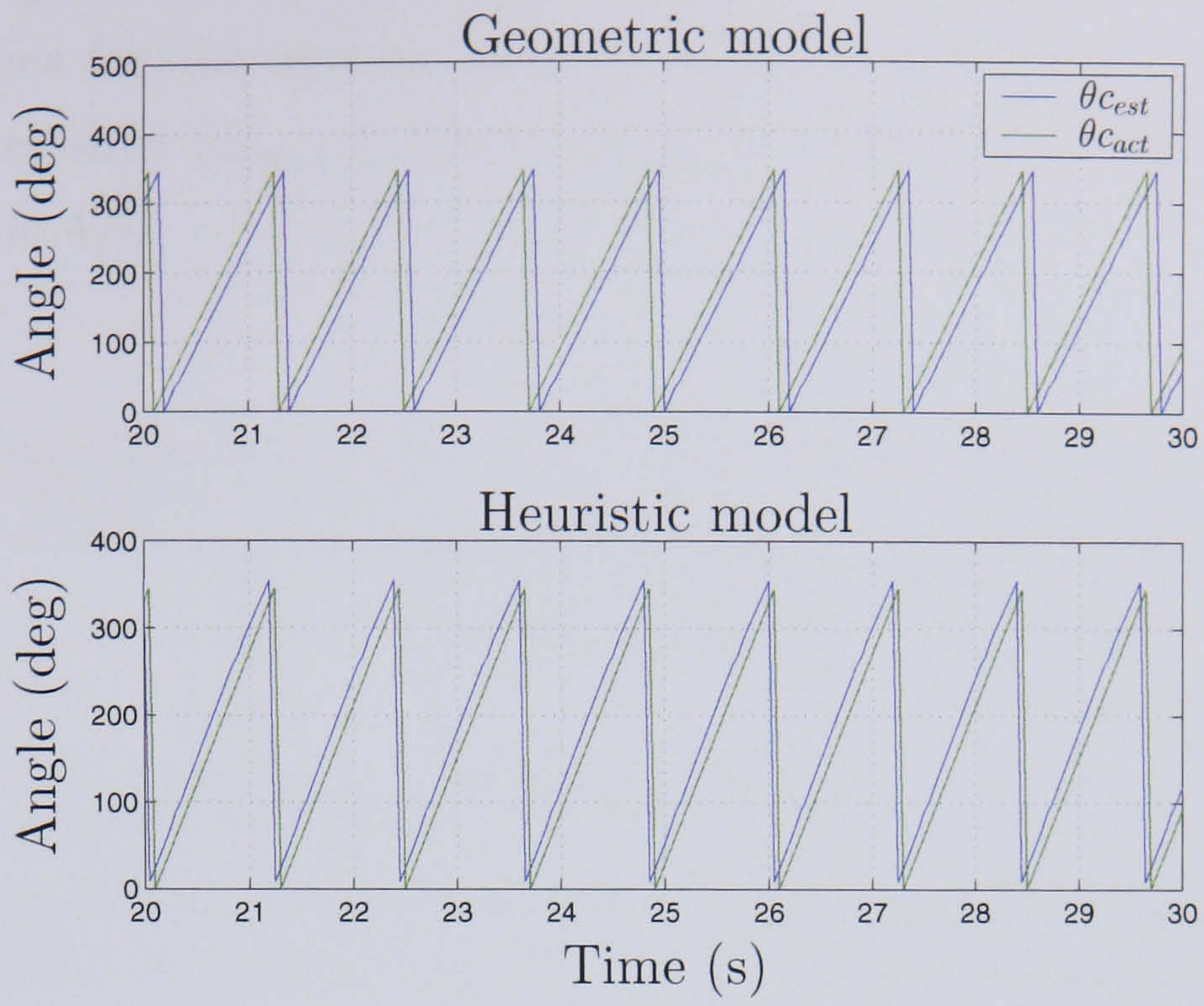

Figure 4.22: Estimated versus simulated actual crank angle at 50rpm using geometric (upper plot), and heuristic model (lower plot). Calculated on PC using simulated data.

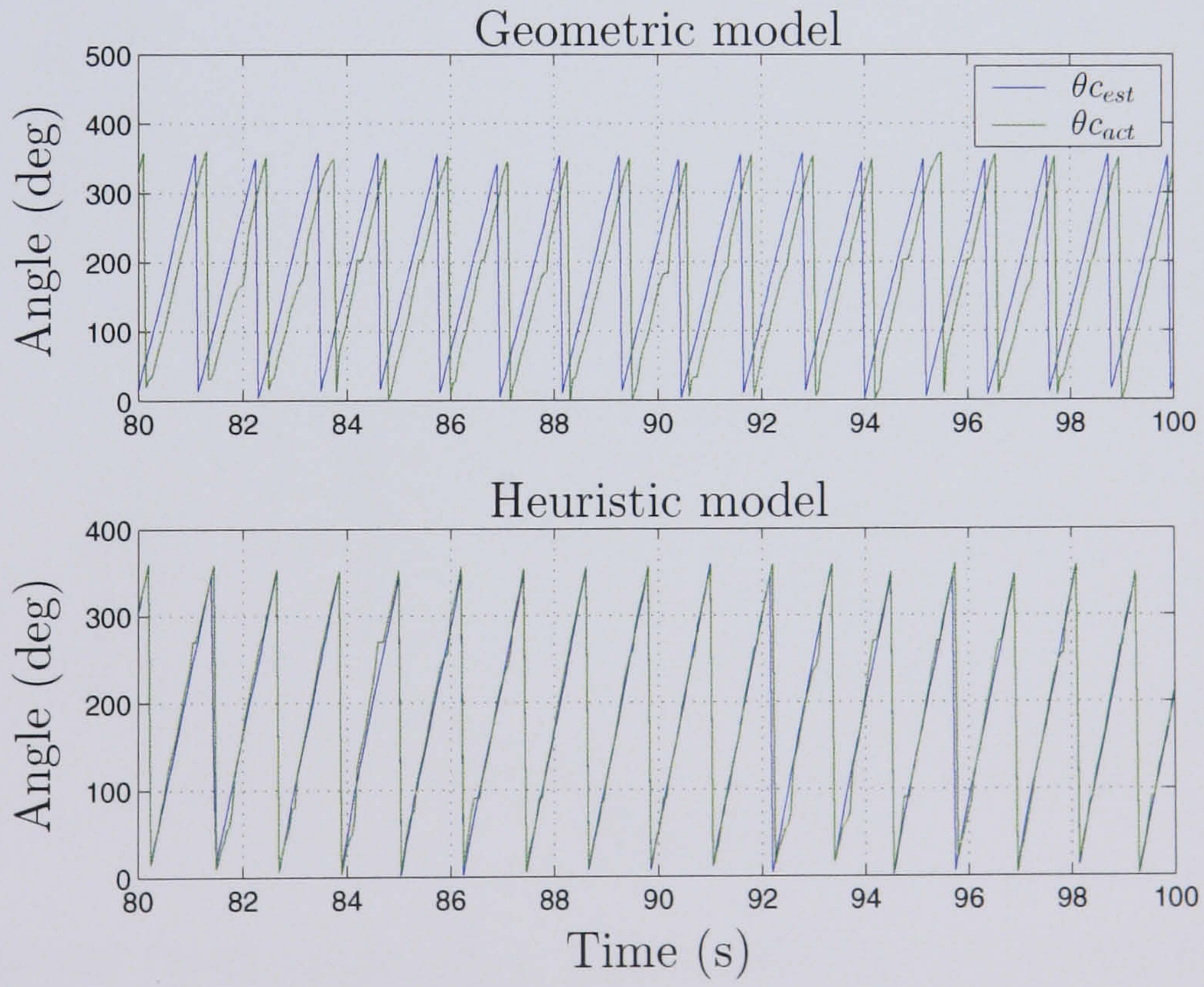

Figure 4.23: Estimated versus measured actual crank angle at $\sim$ 50rpm using geometric (upper plot), and heuristic model (lower plot). Calculated in realtime on the Navigator using measured data.

Estimated and measured crank position data collected at approximately 50rpm in real time on the Navigator and using both the geometric and heuristic models is shown in figure 4.23. Values for the average delay (D_{mean}), found using the geometric model, and average phase shift (ψ_{mean}), found using the heuristic model, for all experiments are shown in table 4.8.

Cadence (rpm)	D_{mean} (s)	ψ_{mean} (s)
~ 33	0.202 ± 0.017	-0.023 ± 0.0253
~ 50	0.208 ± 0.051	0 ± 0.024
~ 70	–	-0.01 ± 0.026
~ 79	0.099 ± 0.052	–

Table 4.8: Average values ($\pm$ standard deviation) of θc_{est} delay (D_{mean}) using geometric model and θc_{est} phase shift (ψ) using heuristic model during experiments.

Cycling Strategy Using Shaft Encoder

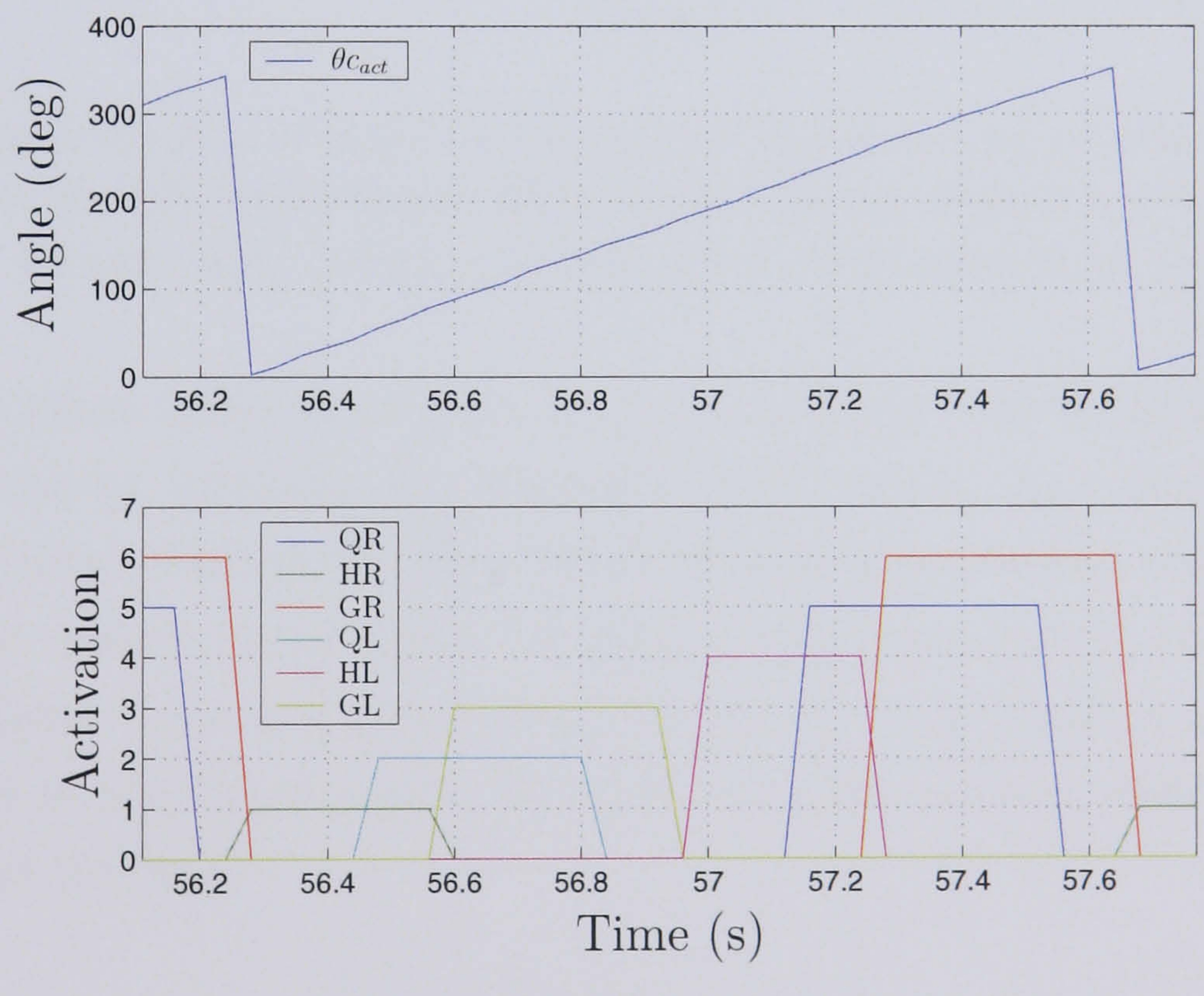

Figure 4.24: Actual crank angle, θc_{act}, (upper plot) versus activation times for each muscle group (lower plot) at $\sim$ 40rpm using cycling strategy with shaft encoder as position source (zero point - right leg forward). QR - quadriceps right, HR - hamstrings right, GR - gluteal right, QL - quadriceps left, HL - hamstrings left, GL - gluteal left.

Stimulation activation timing for six muscle groups over the course of one crank revolution at approximately 40rpm is shown in figure 4.24. Throttle input voltages and resulting stimulation intensity (in terms of maximum current) for the left quadriceps at the same cadence, over a period of 155s are shown in figure 4.25.

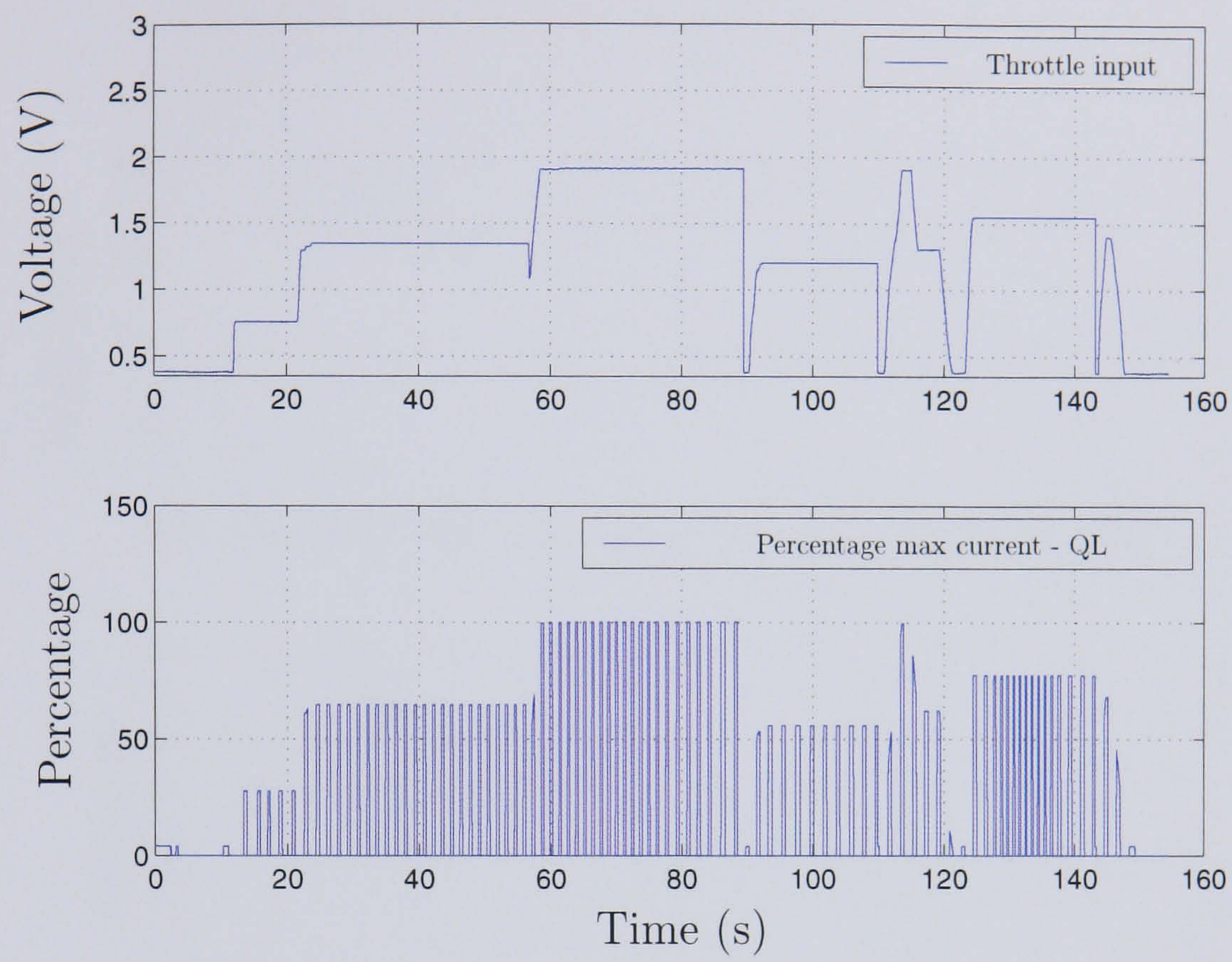

Figure 4.25: Input throttle voltage versus percentage of maximum stimulation intensity for the left quadriceps (QL) muscle group during a period of cycling at $\sim 40rpm$ using cycling strategy with shaft encoder as position source.

These data are taken from information logged in realtime, on the Navigator, using the first cycling strategy (utilising the tricycle's shaft encoder as a position source and throttle as intensity reference). The values of activation timing and stimulation intensity for each muscle group define the final stimulation pattern that is sent to the Exostim stimulator. The zero point (that where the crank angle is zero) of the shaft encoder used is at a position where the crank arms are parallel with the ground with the right foot to the front.

Cycling Strategy Using Conversion Algorithm

Stimulation activation timing for six muscle groups over the course of one crank revolution at approximately 30rpm and using the cycling model which incorporates the geometric algorithm is shown in figure 4.26. The same variables recored when using the heuristic approach model are plotted in figure 4.27. The crank angle plotted in both figures is a measured value, recorded for comparison, and the zero point of the shaft encoder is where the crank arms are parallel with the ground with the left foot to the front. Values for the average delay (D_{mean}), found using the geometric-algorithm-based model and average phase shift (ψ_{mean}), found using the heuristic-algorithm-based model, for all experiments are shown in table 4.9.

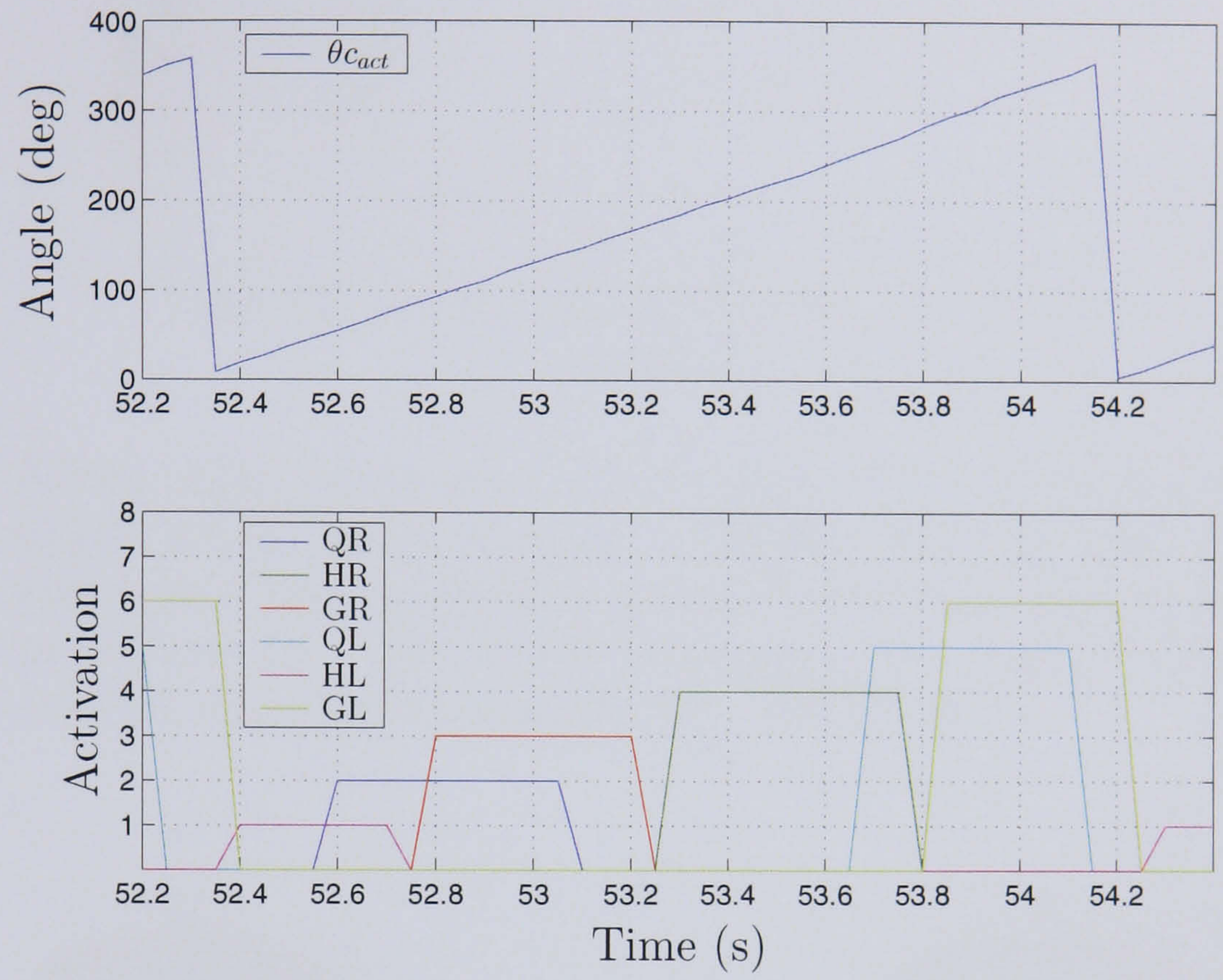

Figure 4.26: Actual crank angle, θc_{act}, (upper plot) versus activation times for each muscle group (lower plot) at $\sim$ 30rpm using geometric cycling strategy with sensor pack as position source (zero point - left leg forward). QR - quadriceps right, HR - hamstrings right, GR - gluteal right, QL - quadriceps left, HL - hamstrings left, GL - gluteal left.

Cadence (rpm)	D_{mean} (s)	ψ_{mean} (s)
~ 30	0.212 ± 0.049	-0.026 ± 0.025
~ 50	0.208 ± 0.019	-0.004 ± 0.02

Table 4.9: Average values ($\pm$ standard deviation) of θc_{est} delay, D_{mean}, using geometric cycling strategy and θc_{est} phase shift, ψ, using heuristic cycling strategy during experiments.

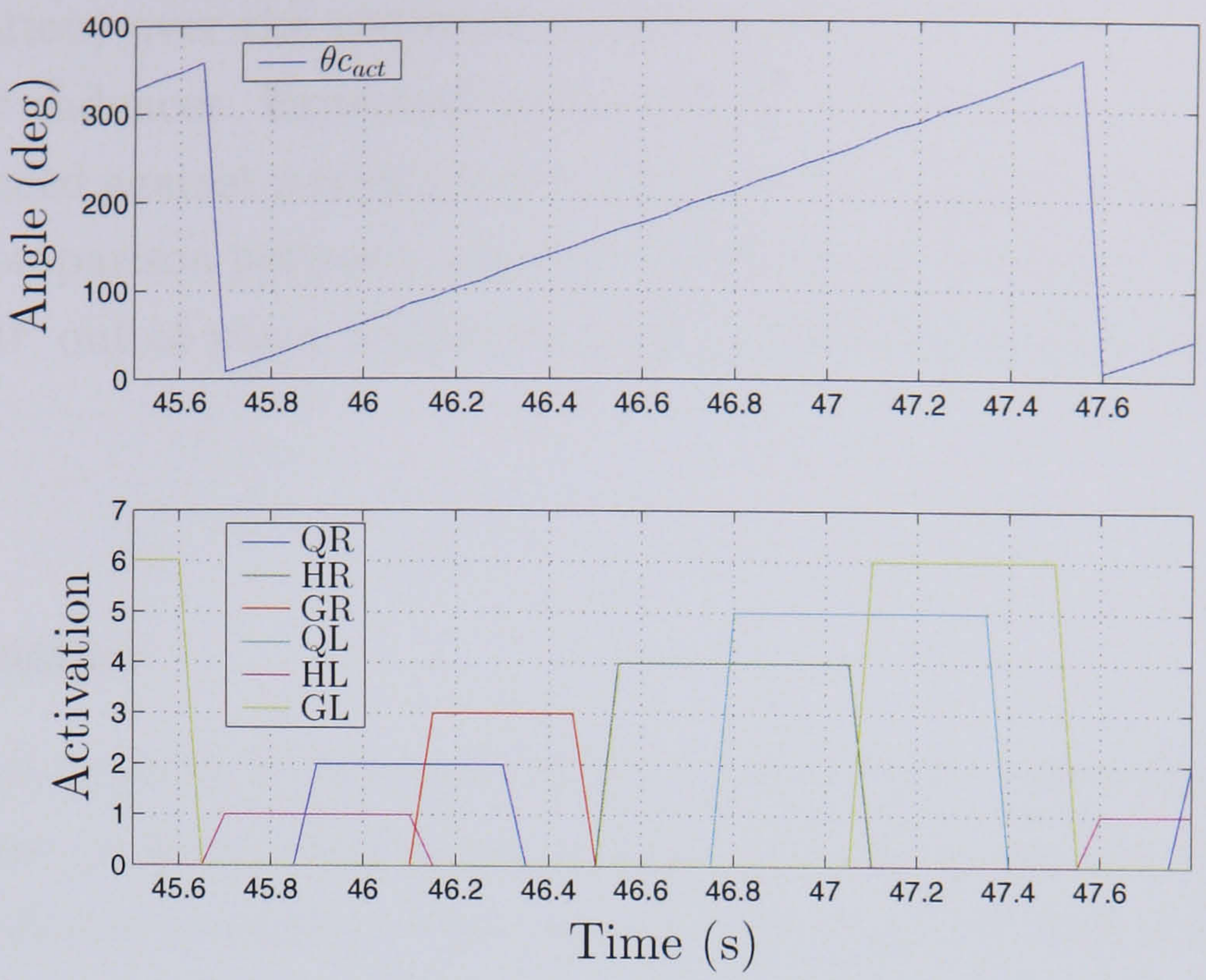

Figure 4.27: Actual crank angle, θc_{act}, (upper plot) versus activation times for each muscle group (lower plot) at $\sim$ 30rpm using heuristic cycling strategy with sensor pack as position source (zero point - left leg forward). QR - quadriceps right, HR - hamstrings right, GR - gluteal right, QL - quadriceps left, HL - hamstrings left, GL - gluteal left.

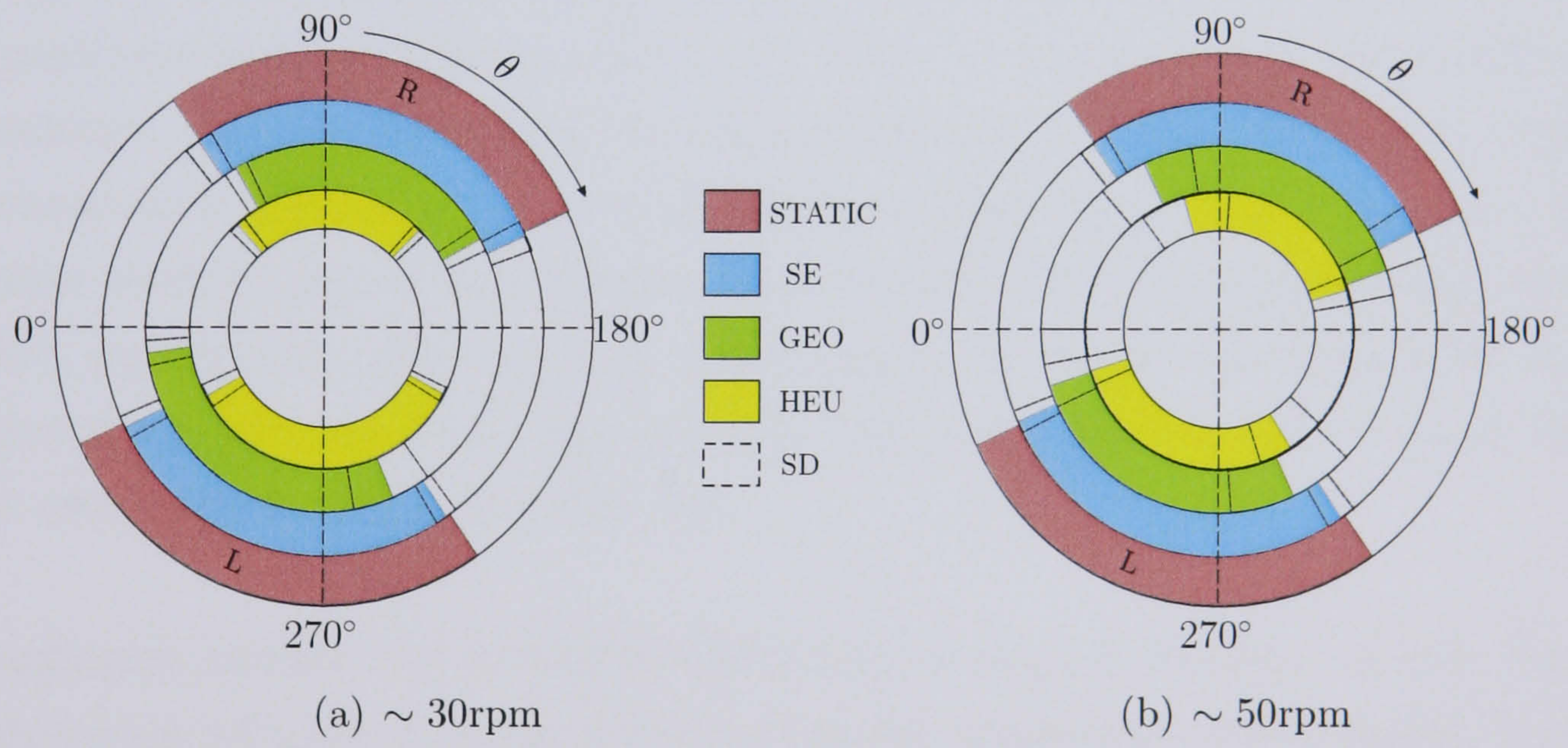

Figure 4.28: Phase angle diagram showing average stimulation activation arcs ($\pm$ standard deviation) for left and right quadriceps over one cycling session, at 30rpm and 50rpm, using each approach (zero point - left leg forward). θ - crank position, R - right, L - left, STATIC - static/reference, SE - shaft-encoder-sourced approach (+ 180°), GEO - geometric sensor-pack-sourced approach, HEU - heuristic sensor-pack-sourced approach, SD - standard deviation.

Figure 4.28 shows average left and right quadriceps stimulation activation arcs (with standard deviation) over the course of a cycling session for all three approaches and at two different cadences. Expected/static arcs are shown in purple and all measured data are referenced against a crank position which was obtained using the tricycle shaft encoder. For comparison purposes, arcs for the shaft encoder sourced approach (shown in blue) are 180° out of phase because data were gathered using a "right leg forward" zero point.

4.4.3 Discussion

Implementing an existing PDA-based FES-cycling strategy which employs a shaft encoder to measure position information yielded encouraging results. Muscle activation times and stimulation intensities, that together constitute the final stimulation pattern to be sent to the stimulator, activated correctly. As illustrated in figure 4.28, the activation arcs for the quadriceps coincided closely with static ranges during the course of a cycling session and showed this approach to be the most accurate of the three investigated. All other muscle groups displayed similar results. Standard distribution did increase slightly with higher cadence (figure 4.28(b)), but from a practical point of view probably not enough to be detrimental to a smooth cycling motion. A constant sampling rate means that as pedalling speed increases there are less instantaneous crank positions measured during one cycle. Thus, activation timing error will increase with cadence, and the effect will be more significant at lower frequencies. However, this behaviour is also present in established systems where a sampling rate of 20Hz (the value used during all our experiments) has been used successfully and, therefore, shouldn't significantly affect cycling performance. A higher accuracy could of course be achieved by increasing the sampling rate. However, there are some issues with the current setup which might preclude this.

The maximum sample rate available when using a matlab sequence on the Navigator in combination with the Exostim is limited by the complexity of the model, number of inputs and stimulator channels used. During experiments, only one stimulation output channel was activated. When more were added, it was found that the maximum number that could be utilised with this model and still have both a sampling rate and stimulation frequency of 20Hz was four. Supporting documentation reports an upper limit of 200Hz divided by the number inputs plus the number of Exostim channels employed and this would suggest that model complexity was the limiting factor. However, further investigation showed that use of analogue input signals as opposed to only sensor signal inputs also had a detrimental effect, therefore using the shaft encoder and throttle voltages in this model probably also contributed.

The two angle conversion models that were created to function in realtime appear to work correctly. Estimated crank angles produced (on a PC) using simulated data in the geometric model showed the expected delay of 0.1s during all cadences. Processing the same data with the heuristic model produced an estimated crank angle delay which was almost exactly 0.05s (the value of the expected delay produced by the model) plus the expected phase shift, obtained from the cadence/phase shift relationship found in section 4.3, at each cadence. When both models were downloaded onto the Navigator and used, as seen previously when using real data, an unexpected delay (in addition to values of D and ψ found through simulation) was seen between estimated and measured data.

This measurement error appeared to vary across cadences and interestingly the values of D_{mean} and ψ_{mean} at $\sim$ 33 and $\sim$ 50rpm in table 4.8 are almost identical to those found during testing of the cycling strategies which incorporated angle conversion. However, all those data sets were obtained on the same day. Experiments carried out on different days (at similar cadences using the same equipment), as well as those described in section 4.3 yielded different values. Although there did appear to be a trend for the error to reduce at higher cadences on all occasions, and one suggestion for a difference in values might be the influence of environmental factors such as temperature on the sensors, the volume of data is not sufficient to draw a significant conclusion as to its origin.

Both cycling strategy models using a leg-mounted sensor and conversion algorithm showed practical (although not ideal) stimulation activation times when using velocity modifying variables which were based on values of D and ψ shown in table 4.8. Position errors can be seen when the two approaches are compared with the static pattern at 30rpm (figure 4.28(a)). However, it may be possible to reduce these by fine tuning the velocity modifier. Although the average activation position was more accurate at 50rpm, standard deviation did increase. Rather than being caused by delays in estimated crank angle (which were reasonably constant - table 4.9), this behaviour is more likely related to sensor pack measurement noise which, in turn, results in an erroneous crank position at that particular time. Thus, even though our results did not show any significant deviation from the static pattern (one that might be detrimental to cycling motion) when using either of the angle conversion approaches, should there be one, the resulting individual activation time error will not be carried through to subsequent muscles. Moveover, although a particular estimated crank position may be incorrect when compared with the actual pedal position, stimulation activation depends on the estimated angle only and, therefore, no antagonistic muscle co-contraction will take place.

As with the shaft encoder based strategy, experiments were carried out with only one stimulation output channel included. Upon further testing though, and unlike the other model, those incorporating a conversion algorithm operated successfully with six output channels at a sampling rate and stimulation frequency of 20Hz. This was only achieved, however, using sagittal angle as the only input and setting stimulation intensities to a constant value, therefore it would seem that use of the analogue inputs is the main limiting factor and not model complexity.

4.5 Conclusions

Investigations into using a new PDA-based FES-system, capable of both surface and implanted stimulation, for FES-cycling and the feasibility of using a limb mounted sensor as a position information source in this modality have been performed. We have shown that, in principle, a limb-mounted sensor may be used in an approach where the crank position required by a stimulation control algorithm is estimated relatively accurately based on a measured hip angle. Moreover, this approach, assuming there is accurate sensor measurement, can be built into an FES-cycling stimulation control strategy and produces a practical stimulation pattern. In addition, a "traditional" stimulation control approach, where the shaft encoder is used as a position source, can also be implemented using the PDA-based system and yield accurate output patterns.

Even though testing of the sensor pack signals showed a significant drift and amplitude error under oscillatory conditions, results from the angle conversion algorithms using simulated data show that, given the repetitive and predictable motion involved in cycling, this can be compensated for effectively. Although the approach of scaling the data within predefined constraints does incur a delay (through using preceding data points to find new maximum and minimum values), because it is constant, it may be compensated for during stimulation activation control. The unexpected delay found when using the sensor pack is a different matter, however. This measurement error varied between 0.04s and 0.11s across all experiments. Put in perspective, at 50rpm, this would result in a significant delay of approximately 30° and, consequently, probable antagonistic muscle contraction. Although the exact origin is unclear, the presence of the error has significant implications in achieving accurate muscle activation timing when using this setup. Thus, further investigation is required to ensure higher accuracy. The fact that the error changed when using the same setup on different days might suggest the influence of environmental factors (such as temperature or pressure) on sensor pack measurement. As the error appeared to always be at least one sample in length (at 20Hz), it may be possible to reduce its effect by increasing the velocity modifying variable to compensate. Furthermore, as it would seem to be originating during measurement, further tests should be carried out using a different sensor, such as the Xsens MT9-B[4].

Both angle conversion approaches appeared to work both offline and on the Navigator, using data in realtime. The geometric approach requires knowledge of anthropometric measurements beforehand and displayed lags in estimated crank angle at higher cadences. Conversely, the heuristic approach does not require prior knowledge of anthropometric variables, involves less iteration and did appear to produce a smoother estimated angle. In addition, although the phase shift varied non-linearly with cadence, it would seem that the resulting relationship found through simulation can be used to predict a fairly accurate phase shift when using real data. Performance of the heuristic approach when the sensor pack is stationary, however, is potentially problematic. During these periods, noise from the sagittal angle data is converted into erroneous crank positions (behaviour that is not replicated using the geometric approach) and ultimately significantly incorrect muscle activation timing. While this does not happen under dynamic conditions, the implications for muscle activation testing (where each muscle is stimulated during their respective static timing arc while the legs are stationary) prior to a typical FES-cycling session could be severe. To combat this, options for practical use of the heuristic approach could include filtering of the hip angle signal or using the velocity and acceleration data, available from the sensor pack, to indicate when the legs are stationary.

Implementation of a cycling strategy within the navigator that uses a shaft encoder and throttle potentiometer voltage as inputs was successful when using a maximum of four stimulation channel outputs and sampling rate/stimulation frequency of 20Hz. Although this obviously limits the number of employable muscle groups to two per leg, FES-cycling under these conditions has been demonstrated by several authors [12, 41, 44]. Moreover, according to support documentation, the influence of the number of Exostim channels used by the model on correct operation is not replicated when using

[4]Xsens Technologies BV, Enschede, The Netherlands. http://www.xsens.com/

the FES-24B stimulator. Thus, application of this strategy using more channels may be possible when using the implanted stimulator.

The strategies which include angle conversion algorithms showed practical stimulation activation timing. However, for the reasons discussed above, this is dependent on accurate prediction of measurement error. Successful operation was carried out with six output stimulation channels. However, this involved omitting the use of analogue inputs. To include the required throttle input, the strategy could either be implemented using four channels, to employ an external potentiometer voltage, or a simple slider bar on the PDA display can be used to set stimulation intensity.

As discussed in the literature review, making FES-cycling and its benefits available to as many potential users as possible will require a concerted effort to adapt the technology for practical home use. In our opinion, the work reported in this chapter is a significant contribution to this effort. The two new angle conversion strategies for stimulation control eliminate the need for a fixed angle encoder and, therefore, have the potential for implementation on non-modified cycles. Moreover, when embedded in a convenient PDA device which can be used for a range of additional FES-applications, the strategies could make FES-cycling more accessible.

5 FES-cycling for the Child with a Spinal Cord injury - Development of a Tricycle-Based System

We describe the development of methods and equipment for FES-cycling that are suitable for use within the paediatric spinal cord population for both stationary and mobile cycling. A further contribution is the demonstration of stationary FES-cycling with a motor complete, paraplegic child on this device. Section 5.1 outlines aims and objectives involved, while an overview of the methods used for all testing involving spinal cord injured subjects is given in section 5.2. A description of the new tricycle-based system and design evaluation is given in section 5.3. Testing of this device (at a US-based paediatric spinal cord injury research hospital and involving 10 subjects) to investigate the feasibility of FES-cycling within its target population is described in section 5.4. Finally, conclusions drawn are given in section 5.5.

5.1 Aims and Objectives

With respect to the arguments formed in the literature review, we propose the development of an FES-cycle system which is suitable for use within the paediatric spinal cord injured population for both exercise and recreation. The development, which will consider the specific needs of this group, can be defined through the following objectives:

(i) Modify a standard child's tricycle to be suitable for use by both paraplegic and tetraplegic paediatric SCI subjects.

(ii) Modify a standard child's tricycle with equipment necessary for both stationary and mobile FES-cycling.

(iii) Evaluate the suitability of the system for spinal cord injured subjects through seating sessions.

(iv) Assess the feasibility of both stationary and mobile paediatric FES-cycling through testing within the target population.

5.2 Experimental Methods - Overview

To carry out objectives (iii) and (iv), experiments involving spinal cord injured subjects were split into two stages. Each will be described in more detail later but, broadly, an initial seating session was undertaken with all subjects (n=10) to assess their comfort, safety and capacity to attempt FES-cycling using the system. Following this, if all of these outcomes were deemed satisfactory, then an electrical stimulation induced cycling session was attempted.

All experiments were undertaken at Shriners Hospital for Children in Philadelphia, USA. This centre specialises in paediatric spinal cord injuries and carries out leading research in the investigation and development of applications for functional electrical stimulation in the upper and lower extremities within this population. Thus, their experience in these areas, in addition to having access to a large number of potential subjects, meant this was the ideal location to test the new system. Testing was undertaken over a period of eight months at times when subjects were based in-house, at the hospital. In addition to the system operator, a physiotherapist (familiar with the subject's medical history) and family members were present during all experiments.

In all, ten subjects were recruited initially, three of which went on to attempt FES-cycling. The work reported here was a collaboration between the University of Glasgow and Shriners Hospital for Children, Philadelphia. It also formed part of a separate FES-cycling study being carried out at this hospital (Shriners Hospitals for Children, grant #8540). All relevant ethical approval for this work was reviewed and granted by a university affiliated institutional review board (Temple University, Philadelphia).

5.3 System Design

The following section describes the development of a new FES-cycle system suitable for use by the spinal cord injured child, including a description of the initial design and its evolution, based on consultation with experts from appropriate disciplines and testing within the target population.

5.3.1 Device Description

Tricycle

Following on from the arguments presented in chapter 3, a tricycle-based system has been developed in an attempt to provide a practical, while still aesthetically pleasing, solution which is capable of both stationary and mobile use.

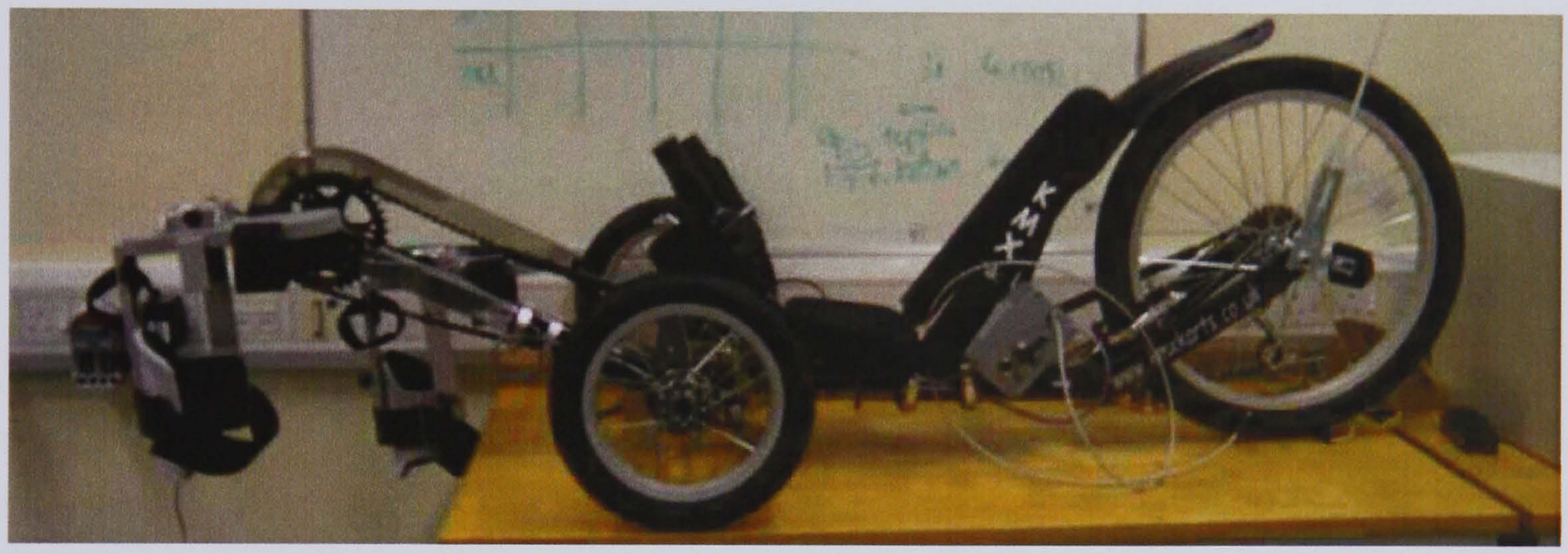

Figure 5.1: Modified child's tricycle.

Dimensions (cm)	*Weight* (kg)	*Ground clearance* (cm)	*Wheel diameters* (cm)
146 x 68 x 55	16	7.6	Rear - 50, Front - 28

Table 5.1: Unmodified tricycle specifications.

The device consists, primarily, of a child's tricycle[1] which is modified with the necessary instrumentation and safety equipment (figure 5.1) [84]. The standard tricycle (specifications are given in table 5.1) is a small, light-weight design with a low centre of gravity,

[1] KMX Karts, UK. http://www.kmxkarts.co.uk

making it extremely stable. Originally designed for ages $8-14$ years, there is 10cm and 15cm of longitudinal adjustment available (via quick-release clamps) on the seat and boom respectively. Gears are adjusted through a seven-speed indexed twist grip on the handle bars. Hand guards located between these and the wheels, in addition to a chain guard which encompasses the front sprocket, protect the rider from moving parts.

Orthotic and safety equipment

Figure 5.2: Ankle orthoses.

To ensure the system is suitable for spinal cord injured subjects, several additional adaptations have been made. A set of ankle orthoses (figure 5.2), which allow the subject's feet to be secured to the pedals and restrict movement to one plane, are attached to 12.5cm crank arms (both made to specification by Hasomed GmbH[2]). Each weighs approximately 1.6kg and has dimensions of 22.5cm x 7.5cm x 25cm. The padded calf support can be adjusted vertically, raising the overall height a further 7.5cm, and may be rotated to fit the natural position of the rider's leg (particularly useful if contractures are present). The foot, calf and ankle are secured in place by adjustable straps and foam padding.

Although the tricycle is extremely stable, potential subjects may have poor trunk control and therefore require additional security (especially for mobile cycling). To ensure this, a waistcoat/harness system[3] which wraps round the rider's waist can be fixed to the seat back.

[2]Hasomed GmbH, Magdeburg, Germany. http://www.hasomed.de/
[3]James Leckey Design, Dunmurry, Northern Ireland. http://www.leckey.com/

Instrumentation and Stimulation equipment

To adapt the tricycle for FES, it is instrumented with a 10-bit optical shaft encoder, throttle-potentiometer and interface box (all provided to specification by Hasomed GmbH).

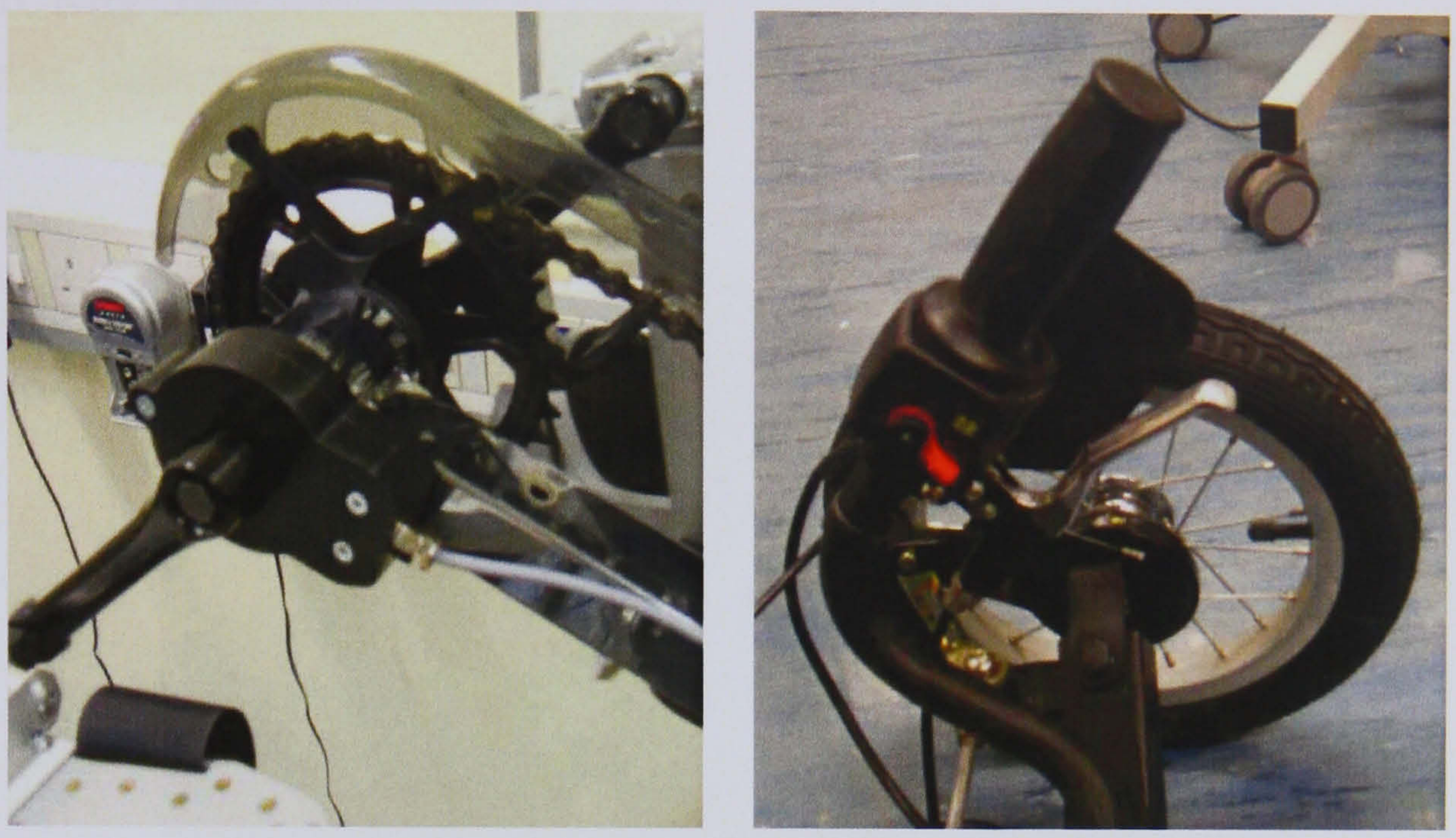

(a) Shaft encoder (b) Throttle

Figure 5.3: Throttle potentiometer and shaft encoder.

The shaft encoder (figure 5.3(a)) is attached to the axle of a standard square-taper bottom bracket for position measurement. The unmodified tricycle contains a one-piece BMX crank. Prior to fitting the encoder, this was removed and replaced with a bottom bracket of suitable length using a BMX cup adaptor. The throttle, attached to the right hand grip (figure 5.3(b)), is equipped with a spring system which returns it to the zero position when not being held, and an LED which indicates the presence of a supply voltage. A switch on the side sets the throttle output to the last value measured before activation, and thus allows the user to maintain a desired stimulation intensity without continually twisting the hand grip.

The supply voltage for both throttle and shaft encoder (as well as digital to analogue conversions for the latter) is provided by a rechargeable battery within the interface box. This box, located to the rear of the tricycle (figure 5.4) and attached to the frame with adjustable brackets, provides the stimulator with shaft encoder and throttle signals through an eight-pin connector.

Stimulation is carried out using one of two eight-channel devices (the Hasomed RehaStim, figure 5.4, or Stanmore stimulator [85]) which can either be controlled externally, by a laptop/PC, or implement an internal cycling algorithm. Approaches to stimulation control (similar to those described in the previous chapter and [43]) which include velocity modification and adjustment of intensity through pulsewidth modulation are adopted by both devices. For placement on the tricycle, either device can be attached via a KLICKfix[4] mounting system, located on the frame. This setup of FES hardware allows for an independent system which is ready for mobile cycling.

Figure 5.4: The RehaStim stimulator and interface box.

Training apparatus

For indoor/stationary cycling, the tricycle may be mounted on a standard cycle trainer[5] which can provide a load (specified by the user) to the rear wheel using an electronically controlled brake. As this device is designed for a minimum wheel diameter of 61cm, a custom height adaptor (figure 5.5) was constructed to raise the brake device to a level where it could come in contact with the rear wheel. To level the tricycle, the front tyres are placed in raised wheel guides.

In addition, the cycle trainer can be connected to a laptop/PC with virtual reality software (also provided by Tacx) which controls the load in such a way as to emulate terrain produced by an on-screen animation.

[4] Rixen and Kaul GmbH, Solingen, Germany. http://www.klickfix.de/

[5] Tacx, Wassenaar, Netherlands. http://www.tacx.com/

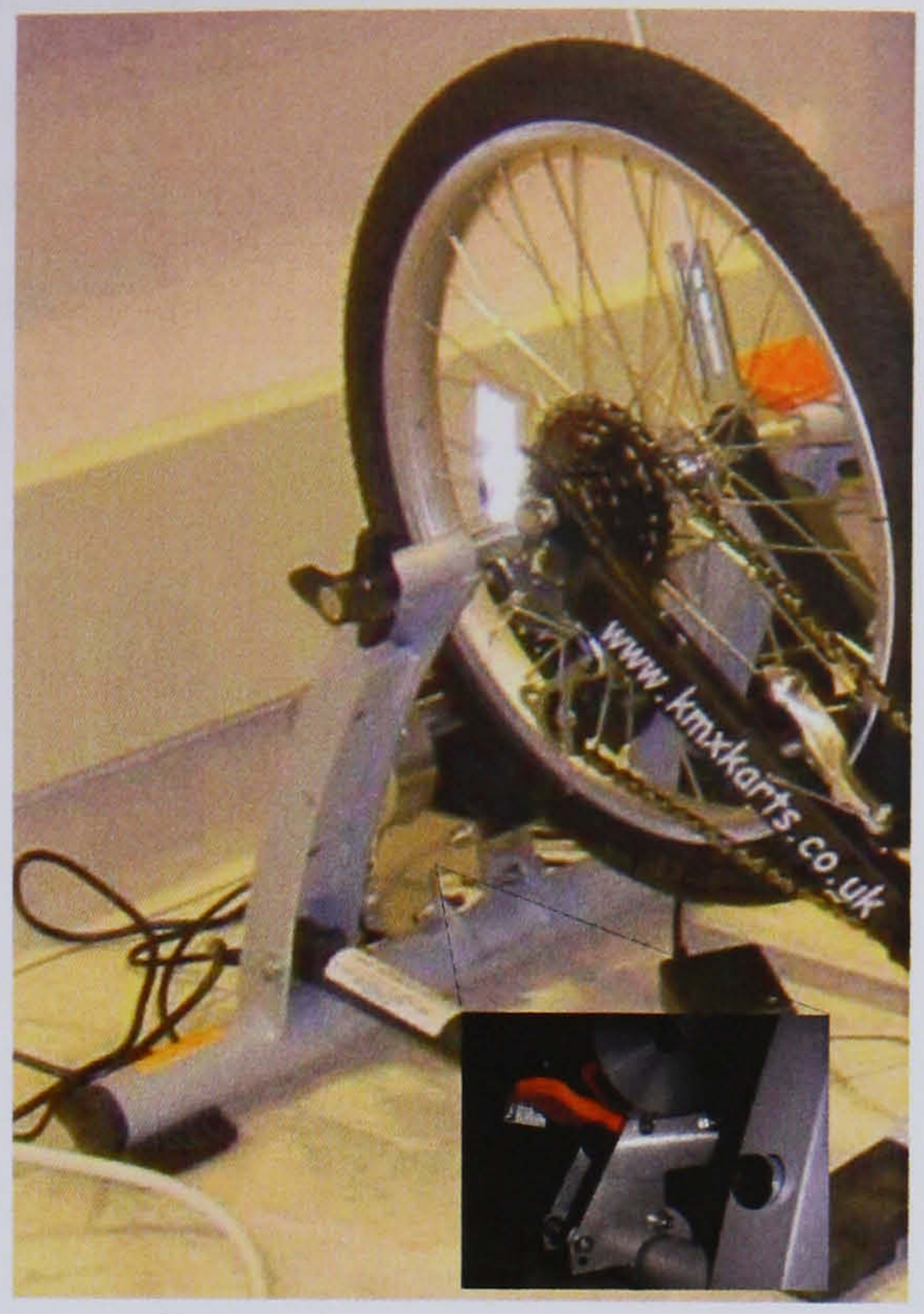

Figure 5.5: Cycle trainer with custom height adapter.

5.3.2 Design Evaluation and Evolution

Figure 5.6: Paediatric FES-cycle system following new design adaptations.

Following initial development, the new system was subjected to a series of experiments involving its target population. In addition to investigating the feasibility of FES-cycling (which will be described in section 5.3), they also involved seating sessions to assess the system's suitability for spinal cord injured children. Through consultation with subjects, their parents and physiotherapists (who specialise in paediatric spinal cord injury) during the tests, several issues concerning the system were identified. resulting in the adaptations shown in figure 5.6. The points raised and a description of the necessary modifications are given here.

Seating Session Methods

A total of ten spinal cord injured subjects (anthropometric data for all are shown in table 5.2) undertook seating sessions, where they could sit on the tricycle without stimulation, to evaluate their comfort, safety and capacity for performing FES-cycling. Essentially this involved transferring the subject on to the tricycle (an operation performed by family members and physiotherapist) and then examining different arrangements of seat, orthoses and padding in order to find the best layout that would guarantee a free, safe cycling motion while also ensuring their comfort and security.

Subject	Age	*Height* (cm)	*Weight* (kg)	*Leg length - R/L* (cm)	*Thigh circumference - R/L* (cm)
A	7	119	27.5	56.5/57	38.2/37.3
B	12	144.5	29.1	72/70.7	32.8/32
C*	8	122.5	26.8	58.8/58.6	36.4/37.1
-	-	-	-	-	-
D	13	171.4	70.2	87.6/88.2	56.2/56.1
E	8	134.7	37	68.6/68.3	43/42.1
F	12	161.3	72.6	79.7/80.1	56.7/55.5
G	11	146	45	71.8/72.1	49.4/49.9
H	12	161.5	54.8	84.6/85.4	54.8/53.4
I	11	156	49.1	77/77.1	48.5/49
J	12	167	75.4	89.4/89.6	60.3/57

Table 5.2: Anthropometric data for all subjects who attempted a seating session on the new system. * Subject C was the only participant who undertook testing with the new seat and handlebars. R - right, L - left.

Of those recruited initially, seven (subjects D-J) were excluded from further testing because they were deemed too large to use the system safely in its initial configuration. The remaining three completed seating sessions and went on to attempt FES-cycling.

Experimental Issues

Throughout testing, an aspect of the initial design that affected riders the most was the position and orientation of the hand grips. Part of a one-piece steering arm/handle bar, they sit low down and at a slight angle towards the front of the tricycle. Although the rider's feet and ankles are secured at the pedals, their thighs may still point very slightly away from the centre (owing to the paralysed nature and/or deformation of the lower limb) and in the case of some subjects, this was sufficient to raise the danger of potential contact with the handgrips during cycling. The nature of this problem, in combination with the width of the original seat, meant that the trunk and thigh diameters of subjects D-J were too large for safe positioning on the tricycle. Thus, even though their leg lengths were satisfactory, these subjects were excluded from further testing.

For smaller subjects, who required the shortest distance between seat and pedals, the orientation of the handlebar caused further difficulties as the ankle orthoses' calf supports came into contact with the brake levers (although this particular issue could be resolved easily by rotating the levers outward).

For those that could be seated safely on the tricycle, the original seat worked satisfactorily. However, one issue arose with subjects who had higher level injuries (and therefore poor trunk control) where the seat-base length (15cm) proved to be too small, affecting their ability to remain upright. Although the harness could provide adequate security, the setup was still not ideal from the point of view of rider comfort. The seat back consists of a padded arch attached to the base, and whilst initial observations did not suggest any problems from using this, it was felt that the because the rider's back is supported at the edges only, the localised pressure could be detrimental to long-term skin health.

Although the ankle orthoses offered good versatility in positioning the subjects' legs for maximum comfort and, in most cases, the calf support could be rotated inward to prevent significant thigh abduction, difficulties were found with those who had particularly thin lower legs. The depth of the calf support, and position of the strap insert holes (figure 5.7(a)) is such that securing the lower leg became difficult. With those subjects who needed the shortest seat-to-pedal distance, this problem was confounded. In order to avoid contact with the seat, the calf support had to be lowered further towards the ankle (and thus to an area where the leg has a smaller circumference), as shown in figure 5.7(b).

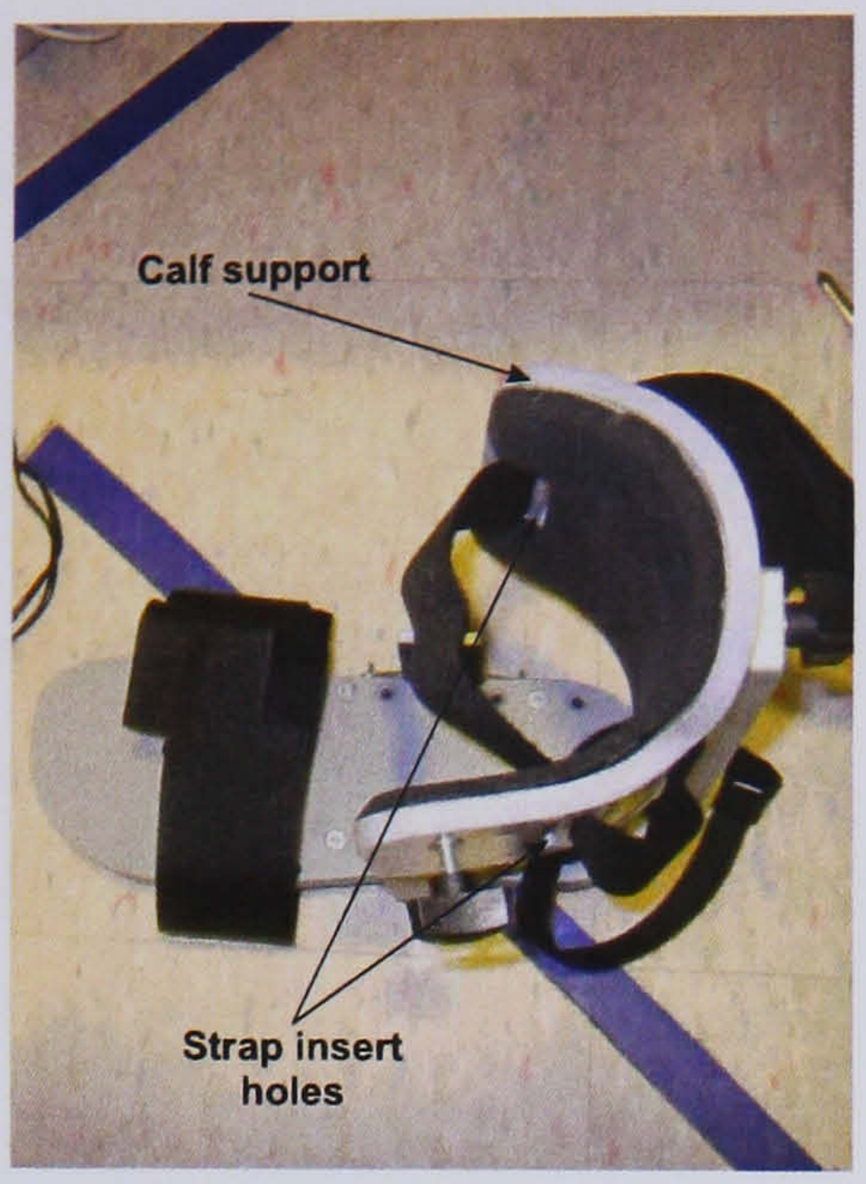

(a)

(b)

Figure 5.7: Plan view of ankle orthoses with calf support (a), and subject demonstrating security issues (b).

New Modifications

As suspected from analysis of the literature, the biggest influence on successful operation of the new system was the large variance in anthropometric measurements and orientations shown by subjects. This further highlights the need for maximum adjustability of the tricycle's component parts. In addition, initial experience suggested the system may benefit from a more modular approach, where a range of easily interchangeable parts are employed for those components that the rider is in direct contact with (such as the seat or ankle orthoses).

Although the original design of the tricycle contributed to some of the issues (i.e. because it is low cost and simple with a minimum of adjustable components), its compatibility with standard bicycle parts made further adaptation easier.

To address concerns about the original seat, a new, larger version was introduced. A standard seat from an adult tricycle (provided by the same company which manufacture the child's version) was adapted for use on the new paediatric FES-cycle system (figure 5.6). In addition to having a larger base and back area, this seat (dimensions, 35cm x 20cm x 45cm) allows a more supine position for the rider with a seat-back angle 15° lower than the original. Moreover, the back has a nylon mesh cover across it (thus pressure is distributed evenly) and a padded head restraint. To attach the new seat to the tricycle frame, a custom nylon spacer was inserted into the existing front quick-release bracket, while the rear is stabilised with a custom strut (which has adjustable brackets at both ends to ensure longitudinal seat movement, and quick removal is still possible) linking the head restraint and central frame. Other adaptations for comfort include additional foam padding inserted in the base and head restraint arch.

As described previously, the tricycle's original steering arm/handlebar arrangement caused difficulties, and in addition, the wider base of the new seat meant steering would be compromised. To address these issues, a new custom-made one-piece steering arm/handle bar, shown in figure 5.8(a), was manufactured with hand grips that sit higher than on the original and are not angled forward. In addition, the whole arm (which is held in position with an adjustable clamp) may be pivoted forward or back to best suit rider position, while during transfer they can be laid completely flat.

(a) Pivoting steering arm.

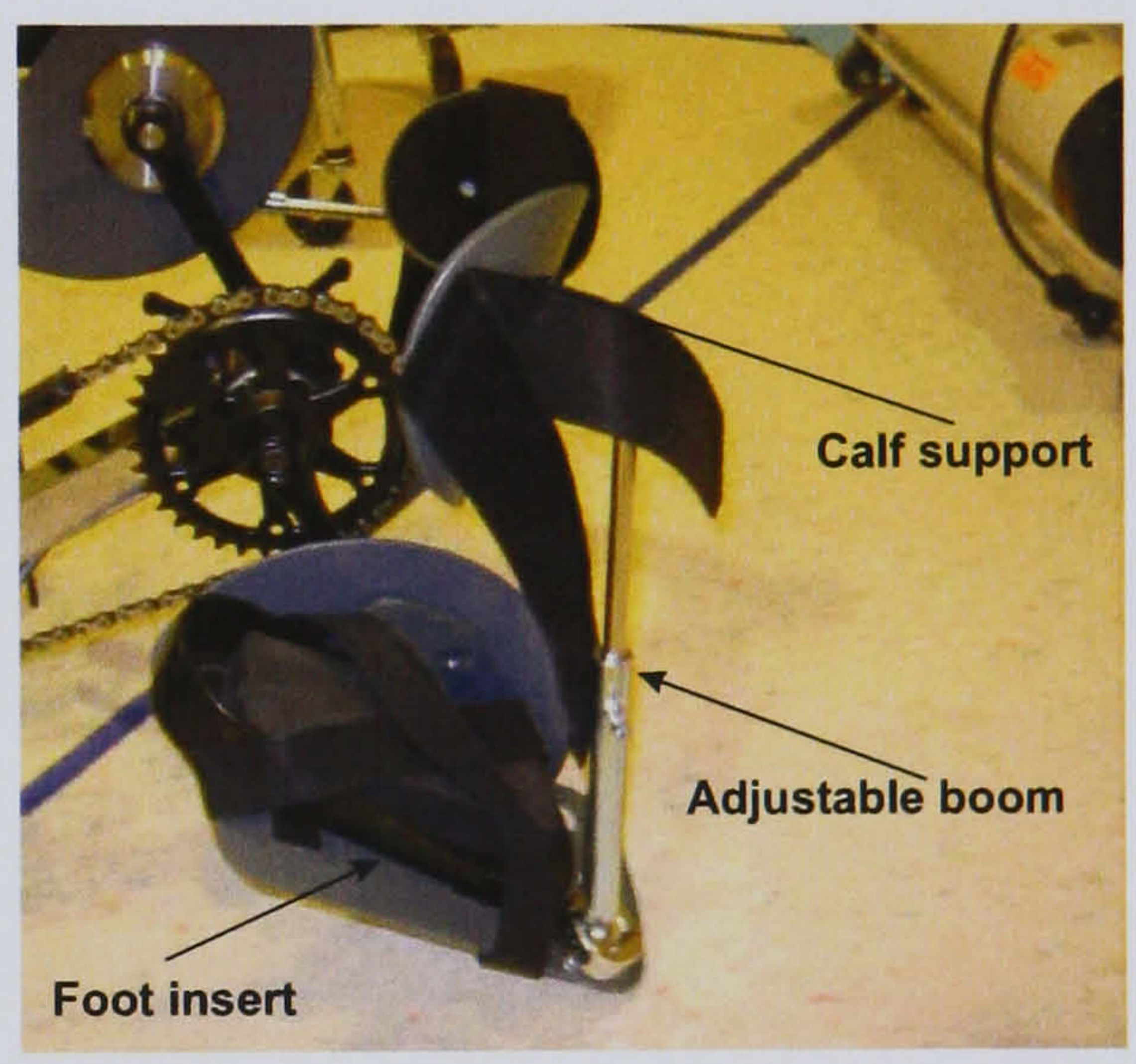

(b) Medica orthoses.

Figure 5.8: New, pivoting, steering arm (a), and alternative orthoses (b).

To increase the range of options available for securing the rider's lower limbs, a second pair of ankle orthoses[6] can be attached to the system. The alternative design (figure 5.8(b)) includes different sized foot inserts, which can be rotated to locate the foot in its normal resting position. The calf support is connected via an adjustable boom with ball joints at either end and can be applied to either the front or the back of the leg, allowing for substantial flexibility in adjustments. In addition, a common crank arm connecting bolt means these orthoses can be easily interchanged with the original

[6]Medica Medizintechnik GmbH, Hochdorf, Germany. http://www.medica-medizin.de/

ones. It should be noted, however, that they are slightly heavier than the Hasomed versions, designed for an ergometer with which the user cycles from their wheelchair, and are weighted for this position.

5.4 Proof of Concept

To assess the new systems's feasibility for FES-cycling, those subjects who successfully completed a seating session undertook further experiments. The methods involved, results found and discussion of the findings are presented in this section.

5.4.1 Methods

Subjects

Subject	*Age*	*Sex*	*Level of injury*
A	7	Female	$T4/T6$ (Complete)
B	12	Male	$C7$ (Complete)
C	8	Male	$C8/T1$ (Complete)

Table 5.3: Details for recruited subjects, who undertook FES-cycling experiments, at time of testing.

Three subjects participated in the experiments. Selected data concerning them are given in table 5.3. All subjects were untrained at time of testing, but had prior, limited experience of lower-limb electrical stimulation through familiarisation sessions and using a separate, stationary, FES-cycle device (the Restorative Therapies RT-300-S[7]). A description of this system is given in the review of FES-cycling design and technology presented in chapter 3.

Stimulation Parameters and Control

The Stanmore stimulator was used during experiments. Initial stimulation parameters, which were chosen to agree with the values each participant used when cycling on the RT-300-S device, are shown in table 5.4. Stimulation control was performed

[7]Restorative Therapies Inc, Baltimore, USA, http://www.restorative-therapies.com/

using either a laptop or the stimulator's stand-alone cycling algorithm. Intensity level (set using the throttle and controlled by the system operator at all times) and cycling cadence were monitored through an on-screen display while all data concerning stimulation activation and tricycle instrumentation were recorded for offline analysis.

Subject	*Current - Q* (mA)	*Current - H* (mA)	*Current - G* (mA)	*Max PW* (μs)	*Frequency* (Hz)
A	120	120	100	150	33
B	80	80	60	150	33
C	90	90	0	150	33

Table 5.4: Initial stimulation parameters used during experiments for all subjects. Q - quadriceps, H - hamstrings, G - gluteal muscles.

Static stimulation angles (i.e., the pedal position arcs which result in a positive driving torque at rest) used for each muscle group during all experiments are shown in table 5.5. The zero-point is taken as left leg forward with the crank arms horizontal.

Muscle group	*Start*	*Stop*
Quadriceps - right	55°	155°
Quadriceps - left	234°	335°
Hamstrings - right	188°	265°
Hamstrings - left	8°	85°
Gluteal - right	90°	180°
Gluteal - left	270°	360°

Table 5.5: Static stimulation angles used during experiments for all subjects.

Procedure

Initially, a seating session was undertaken (as described in section 5.3) to find the optimum system configuration for safe and free cycling motion. Final apparatus arrangements used for each subject during experiments are shown in table 5.6. For all experiments involving electrical stimulation, blood pressure and heart rate were monitored throughout so that any dysreflexic behaviour (upon which stimulation would be terminated) exhibited by the subject might be indicated.

Subject	*Seat*	*Orthoses*	*Safety belt*
A	Original	Hasomed (with 25mm foam insert)	No
B	Original	Medica	No
C	New/larger	Medica	Yes

Table 5.6: Final seating/orthoses arrangements for each subject who undertook FES-cycling experiments.

Upon finding an appropriate system layout, sessions were carried out in which FES-cycling was attempted. Prior to transfer, surface electrodes (two for each muscle group/channel) were placed on appropriate skin locations for stimulation of the quadriceps, hamstrings and gluteal muscles then connected to colour-coded wires, which link to the stimulator. Once seated on the tricycle, a brief passive cycling test was carried out (turning the cranks by hand) to ensure a good range of motion, following which suitable muscle contraction and timing was assessed by initiating stimulation (while the legs were static) at pedal positions corresponding to the relevant static angle arcs shown in table 5.5.

With the tricycle placed on a trainer and no load applied, pedals were turned by hand initially while stimulation intensity was gradually ramped up to a point where the torque produced by the subject's muscles was sufficient to cycle independently at a target cadence (approximately 50rpm). Stimulation was increased to compensate for fatigue until the predefined maximum pulsewidth (table 5.4) was reached and the target cadence could not be maintained. At this point the cycling attempt was terminated. Following a period of rest, subsequent attempts were made observing the same protocol each time.

5.4.2 Results

Full seating sessions were completed by three of the initial ten recruited subjects who went on to attempt FES-cycling following the procedure described above. The final seating arrangement and results from each subject's cycling attempts are as follows:

Subject A

During the seating session, the front boom and seat had to be placed as close together as possible. In addition, a 25mm foam insert was placed in the bottom of the orthoses to reduce pedal-to-seat distance further, and ensure no hyper-extension of the knee joint was possible whilst pedalling. Also, a pillow was placed behind the subject to evenly distribute pressure on the back and allow them to sit further forward on the seat.

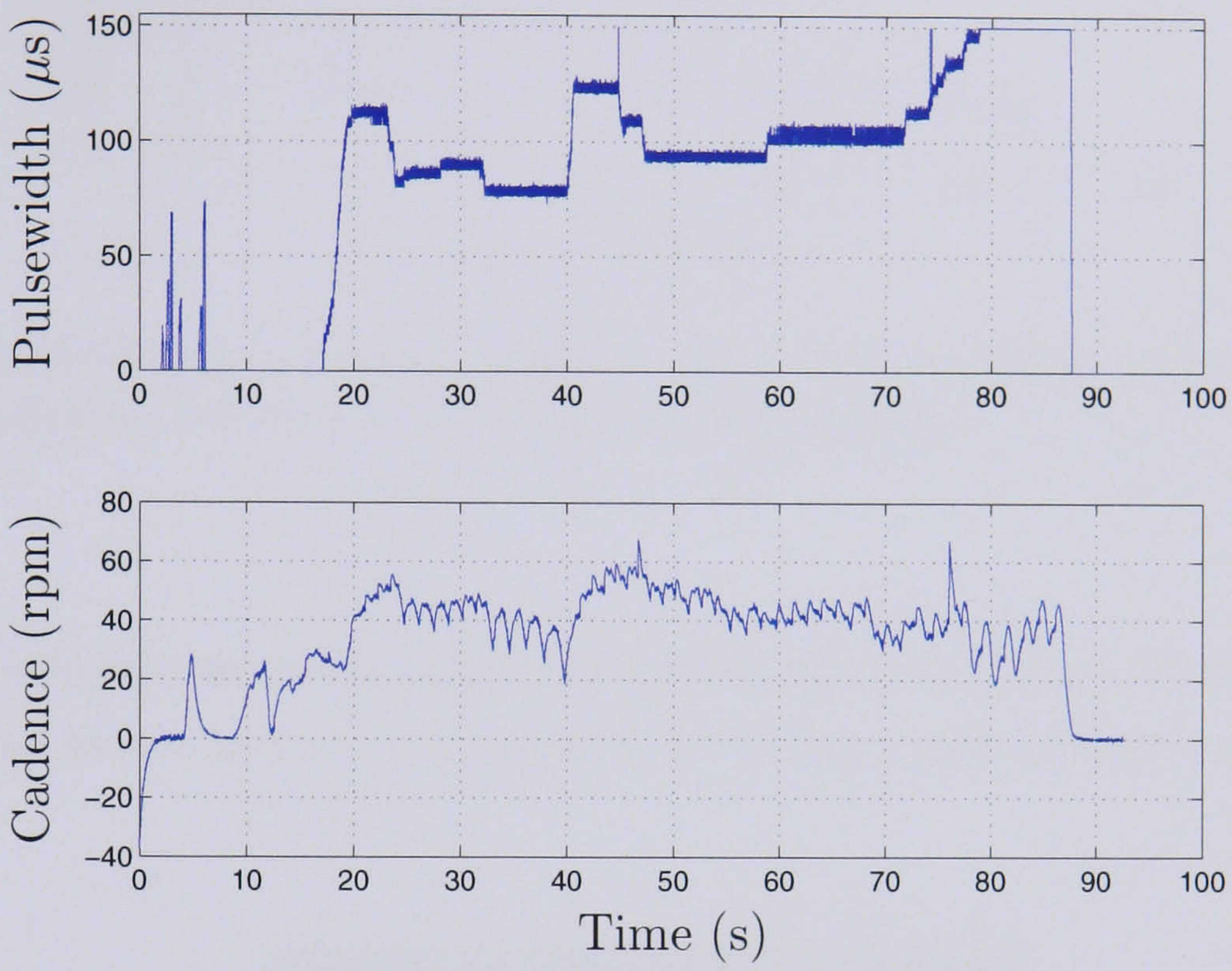

Figure 5.9: Stimulation intensity (upper plot) and cycling cadence (lower plot) achieved by subject A during first attempt.

Figure 5.9 shows stimulation intensity (pulsewidth) and cycling cadence during the first attempt. Unaided pedalling was achieved for approximately 70 seconds, with a maximum cadence of 60rpm. When the maximum pulsewidth of 150μs was reached and cadence began to lower, suggesting the onset of fatigue, the attempt was ceased and followed by a period of rest. To counter the apparent fatigue, during the second attempt, maximum pulsewidth was raised to 200μs. As can be seen in figure 5.10, three short periods of pedalling (unaided) were accomplished with maximum intensity being reached each time. The total pedalling time amounted to approximately one minute on this attempt, with a maximum cadence of 60rpm seen again. Due to time constraints, only one session was undertaken.

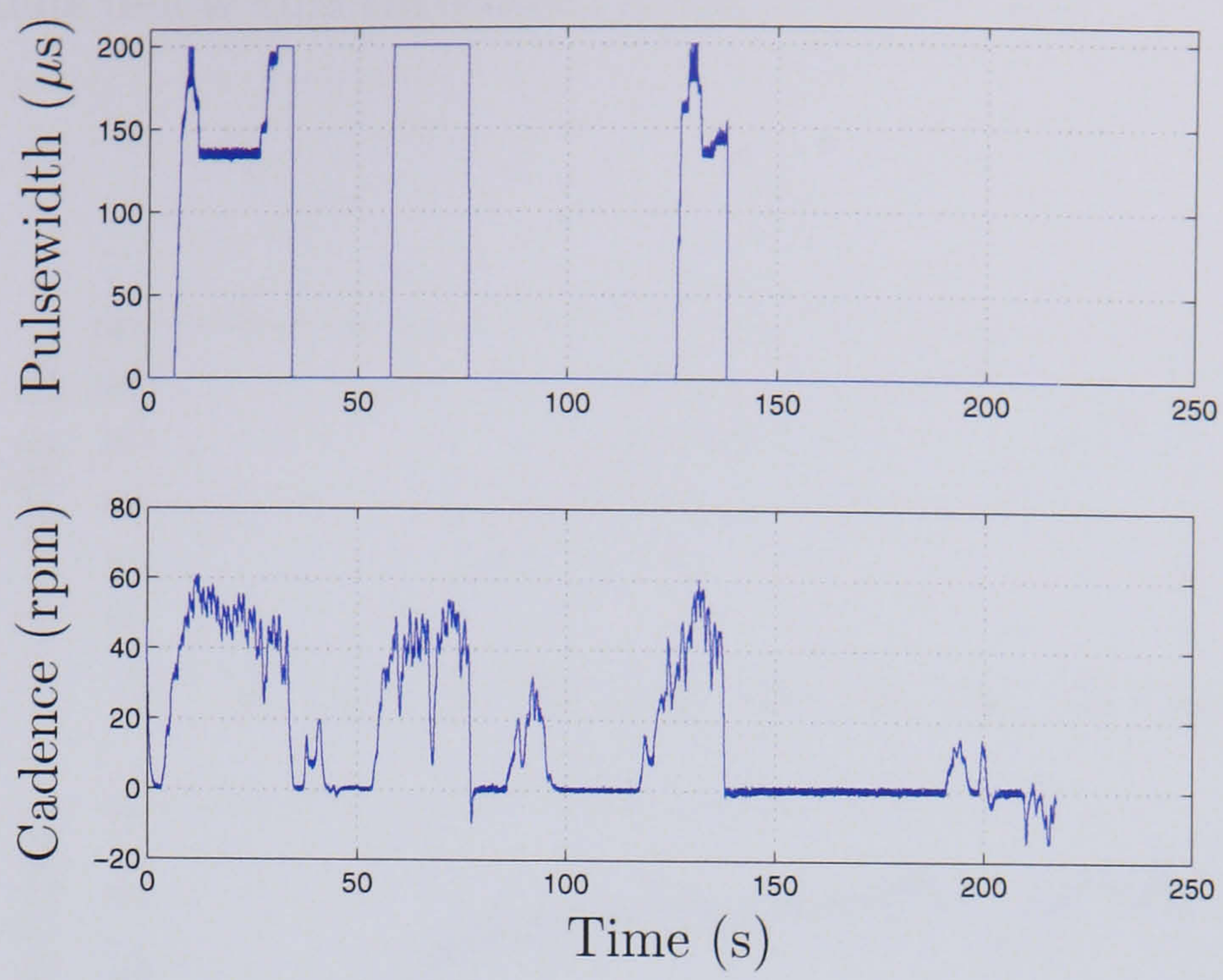

Figure 5.10: Stimulation intensity (upper plot) and cycling cadence (lower plot) achieved by subject A during second attempt.

Subject B

No significant adjustment was required during subject B's (figure 5.11) seating session. Medica orthoses were chosen as they provided better ankle security in this instance.

Figure 5.11: Subject B on paediatric FES-cycle system.

Several cycling attempts were made over the course of two separate sessions using the stimulation parameters shown in table 5.4. On every occasion, when the pulsewidth was increased to a particular level (around 112μs), the subject felt discomfort and exhibited lower-limb spasms, at which point stimulation was reduced (figure 5.12). Although there was a significant contribution by the stimulated muscles to the total torque at the pedals below this threshold, it was not sufficient to turn the legs unaided at any point.

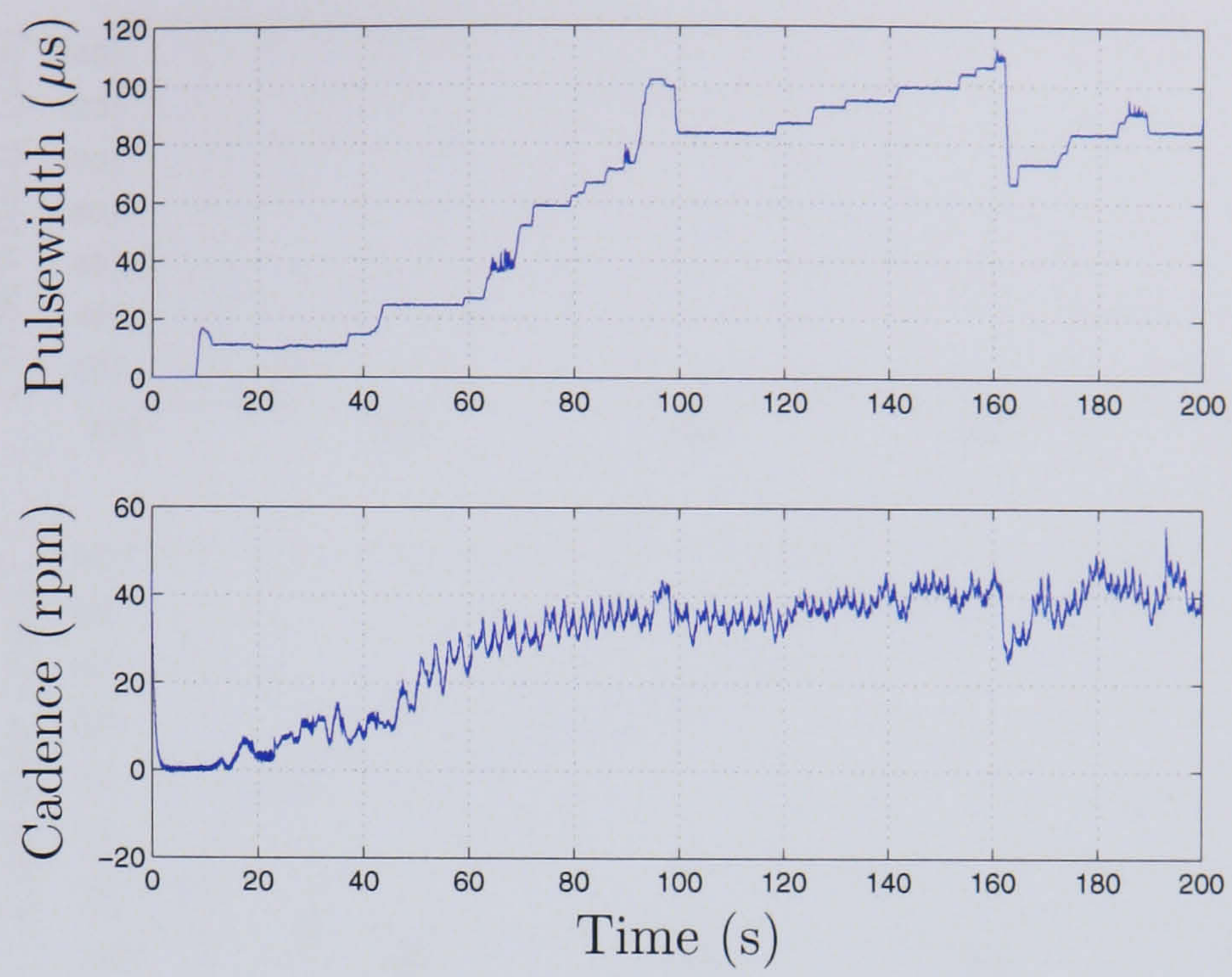

Figure 5.12: Example of stimulation intensity (upper plot) and cycling cadence (lower plot) achieved by subject B during second session.

Subject C

Figure 5.13: Subject C on paediatric FES-cycle system.

The full range of modifications, described in section 5.2, were available during experiments carried out with subject C and tested during the seating session. A combination of the larger seat and Medica orthoses proved to offer superior comfort and range of motion (while also reducing setup time during the actual cycling session), when compared to the original versions, and were therefore chosen (figure 5.13). In addition, the subject had difficulty remaining still during testing, therefore, a waist safety belt was included to ensure balance would be maintained.

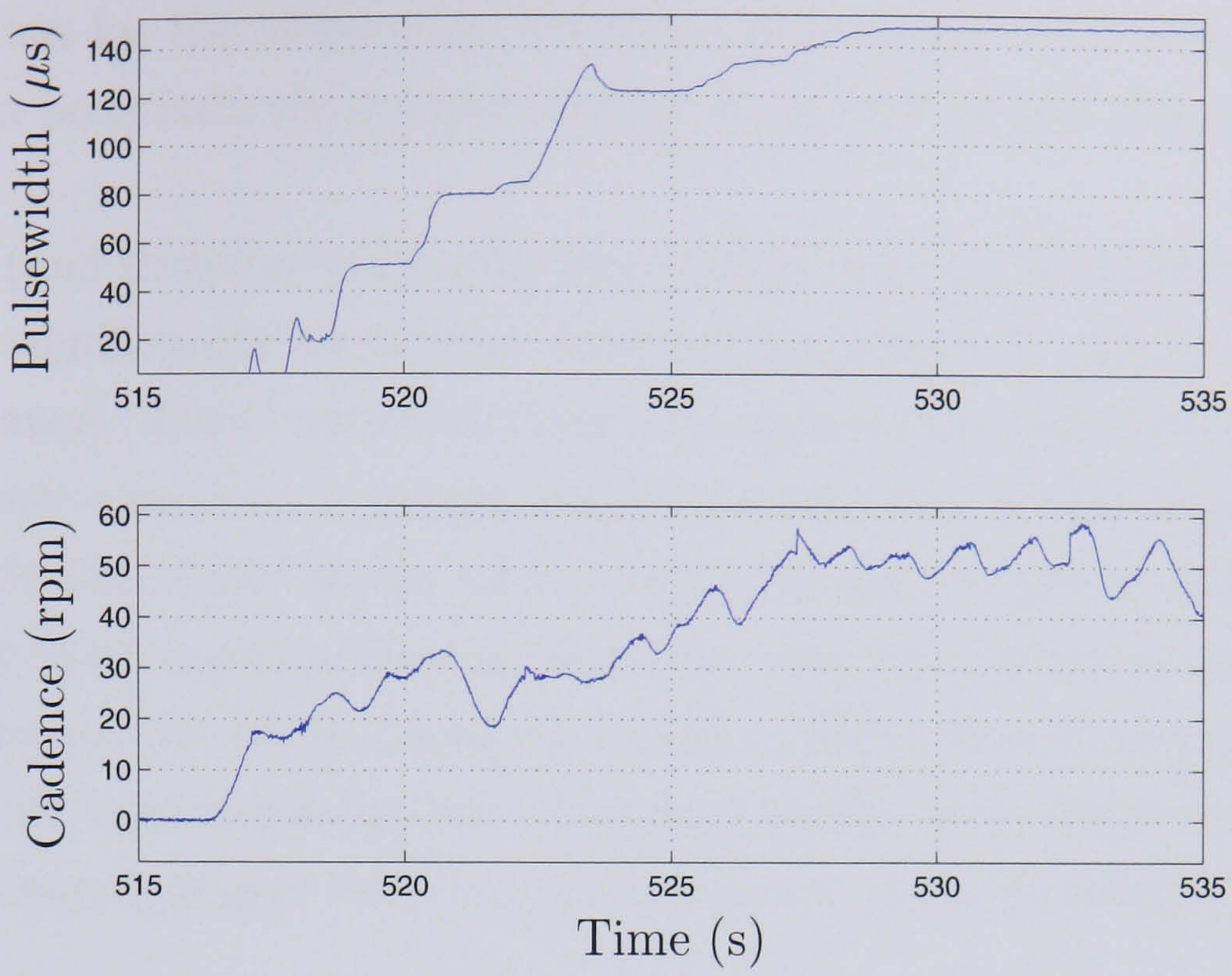

Figure 5.14: Example of stimulation intensity (upper plot) and cycling cadence (lower plot) achieved by subject C during the second session.

One cycling session was carried out, during which the quadriceps and hamstrings were stimulated. The gluteal muscles were omitted because on this occasion electrodes were applied while the subject was seated on the trike. During this session, several brief periods of unaided pedalling were achieved (an example is shown in figure 5.14). However, a significant bout could not be accomplished because spasms in the subject's right leg were intermittently affecting free cycling motion.

5.5 Discussion

Experiments involving paediatric spinal cord injured subjects were carried out to investigate the feasibility of FES-cycling within this population and the performance of a new system designed for that purpose. Of the three subjects who successfully completed seating sessions, one pedalled unaided for a significant period of time (over two minutes during two separate attempts) while the tricycle was placed on a stationary trainer.

All subjects were untrained at time of testing and had very limited experience with electrical stimulation of their lower-limbs. This may account, in part, for the relatively short lengths of unaided, stimulation-induced, cycling seen and the observed intolerance to high intensity stimulation, shown by one of the participants. A complete explanation for the latter issue, however, is probably more complex, with likely influences from both individual experimental setup and subject physiology.

Current levels (and therefore maximum stimulation intensity available) for both subject B and C were significantly lower than those set for subject A, who cycled successfully without assistance. These initial settings (in conjunction with the other stimulation parameters) were chosen to replicate maximum intensity values employed previously using a separate stimulator device with differing output waveform characteristics from the one used in these experiments and, therefore, may not reflect the optimum levels on our system. Irrespective of this, however, neither subject B or C was able to sustain (or even reach in the case of the former) maximum levels, while those that were attained were not sufficient to propel their legs independently for a significant period of time.

In the case of subject C, the influence of spasms, which did not appear to be triggered by the level of stimulation intensity and are of unclear origin, caused the session to be ended. Due to time constraints, only one session could be carried out, and as no other problems were apparent, a more successful attempt may have been possible at a later time. In addition, only the quadriceps and hamstrings were stimulated during the session, and therefore, the full range of muscle groups were not employed. Cycling attempts involving subject B were made over two different days. In each case a threshold stimulation level was reached which caused significant discomfort and eventually a rise in blood pressure. The reason for this is unclear, and perhaps more familiarisation time would have helped. However, the injury levels of both subjects B and C (C7 and C8/T1 respectively) are high enough that the influence of any dysreflexic behaviour (in reaction to the stimulation) cannot be precluded.

Aside from investigating the efficacy of this system as a suitable FES-cycling device for spinal cord injured children, the testing also provided essential information required for the development of appropriate FES-cycling methods within this population. Moreover, necessary data were obtained which would lead to adaptation of the initial design criteria and, subsequently, the modifications described in section 5.3.2.

A separate seating session prior to attempting cycling was required for all subjects in order to find the optimal configuration of equipment for providing most security and good cycling motion. A necessity during these experiments, because it formed an important part of development, this process involved patience (over a relatively long period of time from a young child's point of view) on the subject's part while adjustments were made. Ideally this should be done as fast as possible and notably, with subject C (the only one to use the fully modified setup described in section 5.3.2). a satisfactory setup was found very quickly. The latter subject was the only one to use a safety belt during experiments. However, the omission of this for previous subjects was only because several people were close by at all times to ensure stability. Thus, for general use, it would be advisable to use a security belt at all times.

Overall, the system performed well during cycling experiments. All subjects appeared happy and comfortable on it, found the trike-based design appealing, and expressed a large desire to attempt mobile cycling (all providing sufficient motivation to hold interest during setup time!). Subject A required the shortest hip joint to crank centre distance, and therefore probably represents the lower limit of size (see table 5.3) for an individual who can safely use the system.

Seven of the initially recruited ten subjects were unable to fit securely on the system in its original configuration. This was chiefly because their trunk and thighs were too large to fit safely between the handlebars and/or free cycling motion was not achievable. However, where analysis was possible, seat to pedal distance was seen to be satisfactory. Thus, although further testing involving these subjects would be required, the modifications made to seat and steering arm should allow them to use the tricycle safely in the future.

5.6 Conclusions

A new tricycle-based paediatric FES-cycling system, which is capable of both stationary and mobile use, has been developed. Initial testing within the target population indicates that the device is suitable for spinal cord injured children and could offer a low-cost appealing option for both exercise and recreation.

Using the system, a two minute bout of successful electrical stimulation induced cycling was carried out by a T4/T6 (complete) subject, who was untrained at time of testing.

Although this is a very short period, the attempts were the first by any subject on this system and, had time allowed it, there is nothing to suggest further, more extensive cycling sessions would not have been possible. Although attempts with subsequent subjects did not prove to be as successful, the major influencing factors appeared to be health related. Moreover, maximum stimulation intensity levels, reached by them, were significantly lower than subject A's (less than half when compared with the second attempt) suggesting more familiaration time using our stimulator, to potentially gain a higher tolerance, might have been beneficial.

Whilst FES-cycling has been demonstrated, the limited extent of this is probably symptomatic of the specific issues (unique to the paediatric spinal cord injured population) highlighted during the literature analysis, and, thus, the development of a system which could meet those challenges, and methods for implementation using it, is perhaps the more significant contribution.

Based on feedback from those involved in testing, the device proved very popular and provided high motivation to take part in experiments. With the FES-technology and instrumentation employed already having been proven on adult systems and adaptation to a child's version fairly straightforward, the mechanical aspect of the development process presented the most challenges. Here, the major finding was that a modular approach, where a range of seating and orthotic equipment can be quickly and easily interchanged, appears to offer the highest degree of flexibility and, therefore, most chance of successful operation in a population who have such a large variance in anatomical characteristics.

In this respect, the trike-based design has been shown to be advantageous. Having a standard mechanical device at the heart of it means the system can be easily updated using a vast range of bicycle parts. It is noted, however, that there is a limit to this in connection to compatible child-size versions (hence the reason that our system required a few custom-made components which would allow us to tap into training and seating equipment originally designed for adult cycles). From the financial point of view, basing the system around an existing, and already proven, device is also advantageous. There is possibly a danger of an FES-cycle system becoming an exclusive thing, where purchase and maintenance costs make ownership untenable for some potential subjects. Although the FES and instrumentation equipment will always be specialised, if the majority of the system's mechanical parts are cheap, have a proven reliability and are easily maintained, then the overall costs should be lowered. The latter point is of course not a new observation in assessing the performance of this type of system. However, together with the fact that (unlike many commercial systems) it closely resembles that which an able-bodied person might use, it is one which is particularly relevant to children (and something highlighted by those involved in our testing).

Thus far, only unloaded stationary cycling has been attempted. In this setup the rider is essentially working only against the combined weight of their legs, pedal/orthoses arrangement and rear wheel. There is not sufficient data to be definitive, and the performance of subject A does suggest she may have been able to propel the cycle on a flat surface very briefly, but based on our findings (i.e. that only brief, unloaded, cycling has been demonstrated), it appears that practical mobile cycling with untrained paediatric SCI subjects is not possible using the current set up.

However, as the system itself is ready and capable of this modality, and our experiments showed that a subject may be secured adequately, providing the rider has undergone a sufficient muscle training period and learned how to use the throttle safely, mobile cycling should be feasible.

For those potential users who are untrained (and/or fatigue quickly) and to aid progress during stimulation familiarisation, some form of controlled pedalling assistance, that could be reduced over time, is desirable, and probably a necessity (at least initially) for practical mobile cycling in this population. In addition, when attempting to quantify the effects of training, the ability to passively turn the legs and then augment the total torque at the pedals with stimulation-induced muscle contraction allows for a larger measurable range of potential power output with which to perform standard exercise tests. This technique (as demonstrated by Hunt et al. [43]) has been shown to be particularly useful when dealing with a population who exhibit vastly reduced workrates when compared with their able bodied peers, an issue which is, again, even more pronounced in children.

In an attempt to address these points by providing an initial training facility, as well as both an exercise and mobile cycling test bed, a second, separate system with an auxiliary motor and further instrumentation, has been developed. A description of this will be given in the sequel.

6 FES-cycling for the Child with a Spinal Cord Injury - Development of a Motorised Test Bed

The main contribution presented in this chapter is the development of a paediatric FES-cycle system which may be used as a test bed for investigation into exercise characteristics and facilitate the development of control methods for mobile FES-cycling and initial training in the paediatric spinal cord injured population. The aims and objectives for achieving this are set out in section 6.1. A detailed description of the system is given in section 6.2, while experiments carried out to verify sensor and system-integration operation are reported in 6.3. Finally, a discussion of the device, and its place in the targeted research climate, along with conclusions drawn are given in sections 6.4 and 6.5, respectively.

6.1 Aims and Objectives

The findings presented in the previous chapter indicate that untrained children who attempt FES-cycling may require pedalling assistance in the initial stages of stationary cycling and certainly for significant mobile bouts. However, as previously mentioned, these results are based on limited data and experiments which were influenced by health issues. The latter issue may, of course, be characteristic of this population but either way, it is clear further data concerning their FES-cycling capabilities are required. Moreover, analysis of the relevant literature suggests there is a general lack of understanding of exercise capacity in this population, thus a fully controllable (in terms of cadence and power output) FES-cycling system with sensors capable of quantifying some of the unknown capabilities could perhaps assist in providing further knowledge.

We propose the development of a new motorised paediatric FES-cycle test bed which may be used to perform detailed investigations into the training and exercise capabilities of spinal cord injured children. The device should provide an adequate environment in which appropriate control strategies for both exercise testing and mobile cycling may be developed, while also doubling as a training facility for individuals who require motor assistance. These goals are addressed through the following objectives:

(i) Modify a standard child's tricycle to be suitable for use by a paediatric SCI subject and with equipment necessary for FES-cycling.

(ii) Modify the paediatric FES-cycle system with an auxiliary motor and suitable instrumentation for power measurement.

(iii) Develop interface equipment for motor and sensor apparatus so laptop-based monitoring and control is possible.

(iv) Carry out experiments to validate additional instrumentation and associated data acquisition processes.

6.2 System Design

The following section will delineate a new FES-cycling testbed which is suitable for spinal cord injured children. Detailed descriptions of major parts are given, along with an explanation of the various operational layouts possible.

6.2.1 Overview

The system is based on the non-motorised version described in the previous chapter. and thus incorporates the same FES-technology and safety/security equipment. with the necessary modifications. Broadly, a hub motor located in the rear wheel and directly coupled to the front chainset may be employed to drive the pedals/legs. Motor speed is controlled using either a throttle potentiometer (similar to that used for stimulation) or laptop while power comes from a 24V battery/controller pack. A torque sensor, attached to the crank shaft, allows for force measurement at the pedals, which (together with pedalling cadence) can subsequently be used to calculate power output.

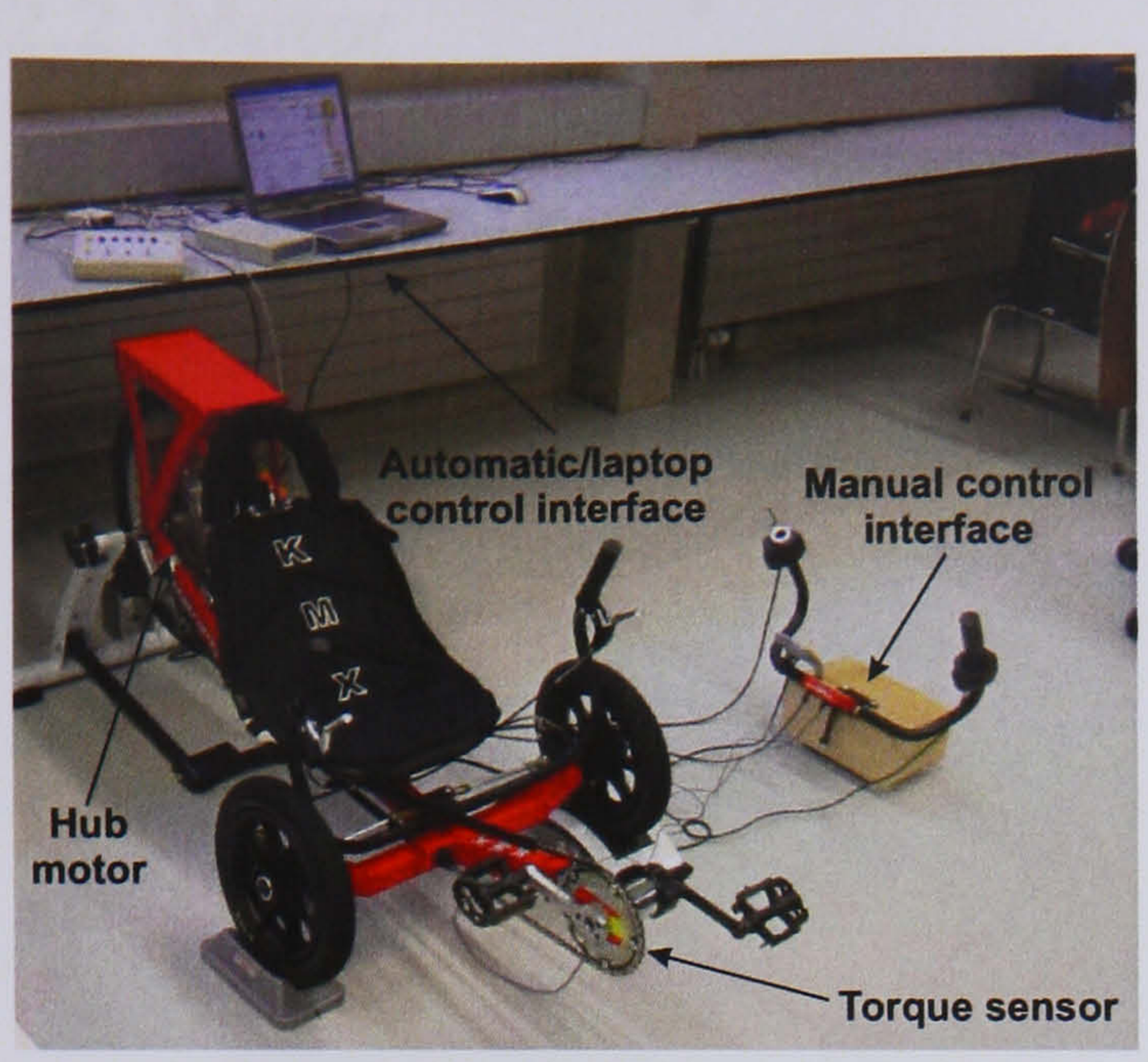

(a) Experimental.

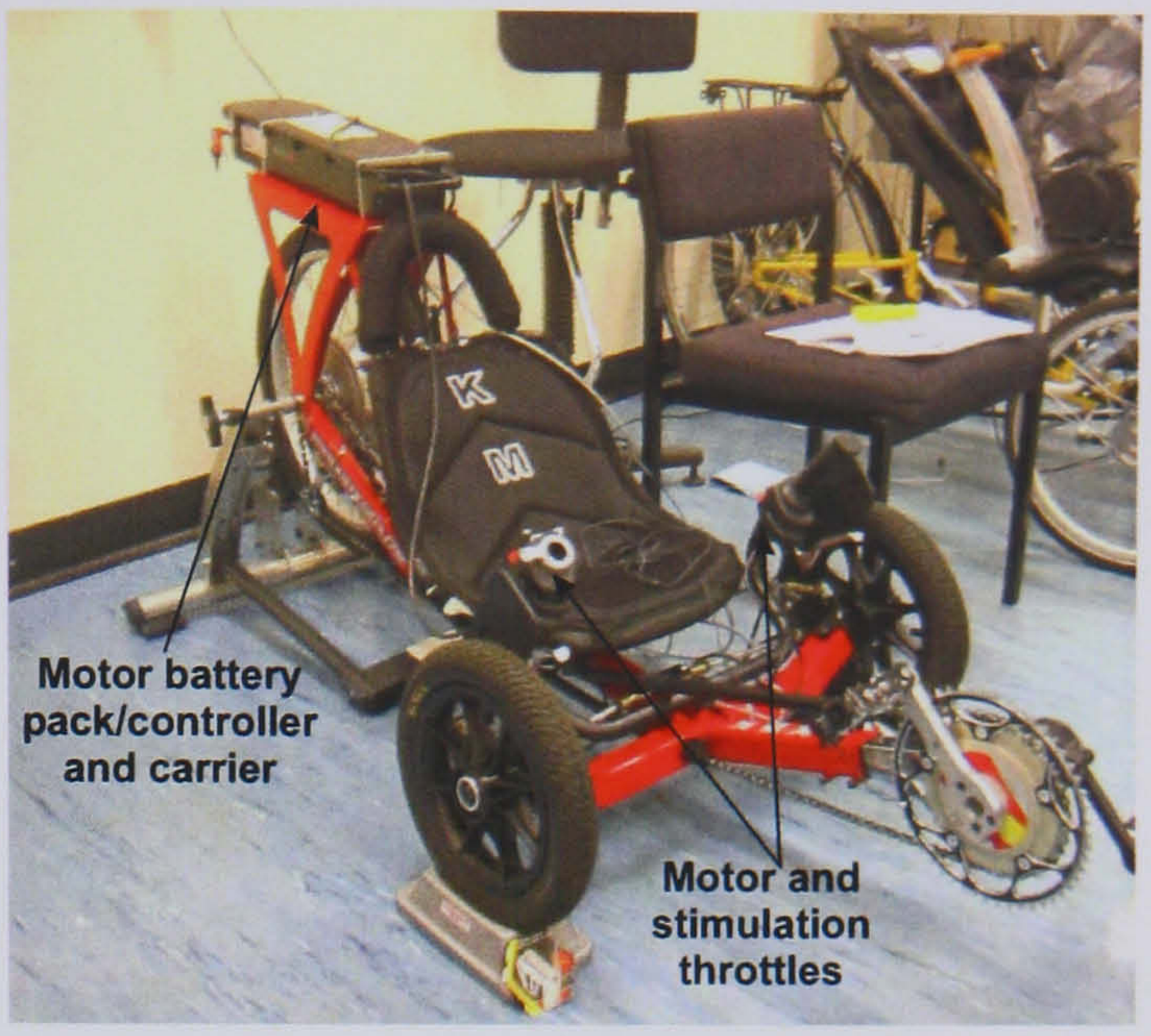

(b) Training/mobile.

Figure 6.1: Operational layouts of motorised paediatric FES-cycling system.

Two operational layouts are possible with the device and are illustrated in figures 6.1(a) and 6.1(b). For testing and development, control of stimulation and motor speed is taken away from the rider and can be implemented through either a manual (open-loop) or automatic (closed-loop) approach. In the former case, an operator has control over both throttles and can use a combination of displays from the torque sensor, cycle trainer and laptop software (figure 6.2). For automatic control, motor speed, and/or stimulation intensity may be passed to the laptop. In addition to this experimental setup, both throttles can be attached to the handlebars and the battery/controller pack placed on a supporting frame at the tricycle rear so mobile cycling is possible.

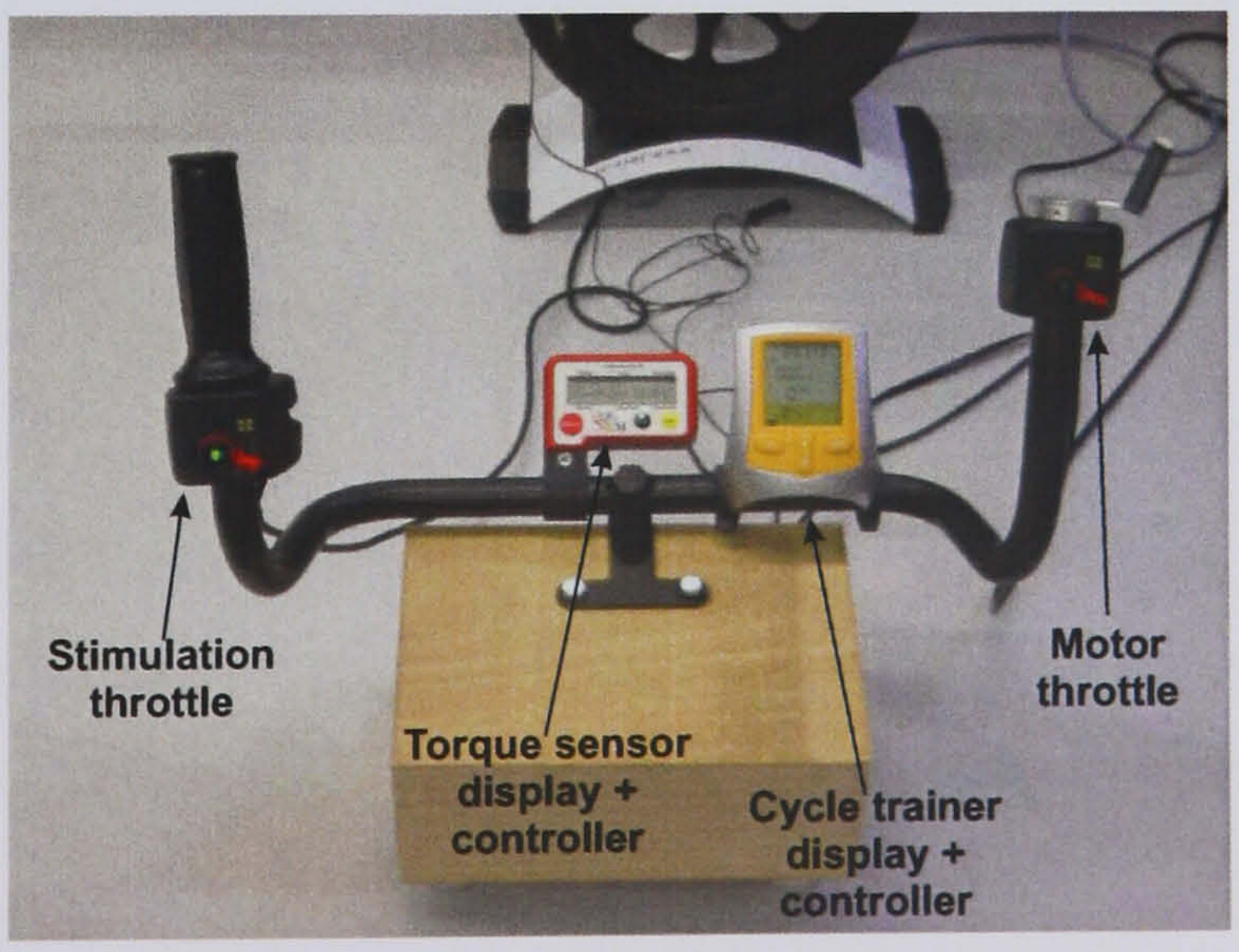

Figure 6.2: Control interface for open-loop/manual operation.

6.2.2 Motor

A 200W DC hub motor[1] (specifications given in table 6.1) was chosen to provide auxiliary power to the device because of its compactness and reliability. Part of the tricycle's rear wheel, it is spoked directly into the rim and clamped to the rear fork via a connecting arm (figure 6.3(a)).

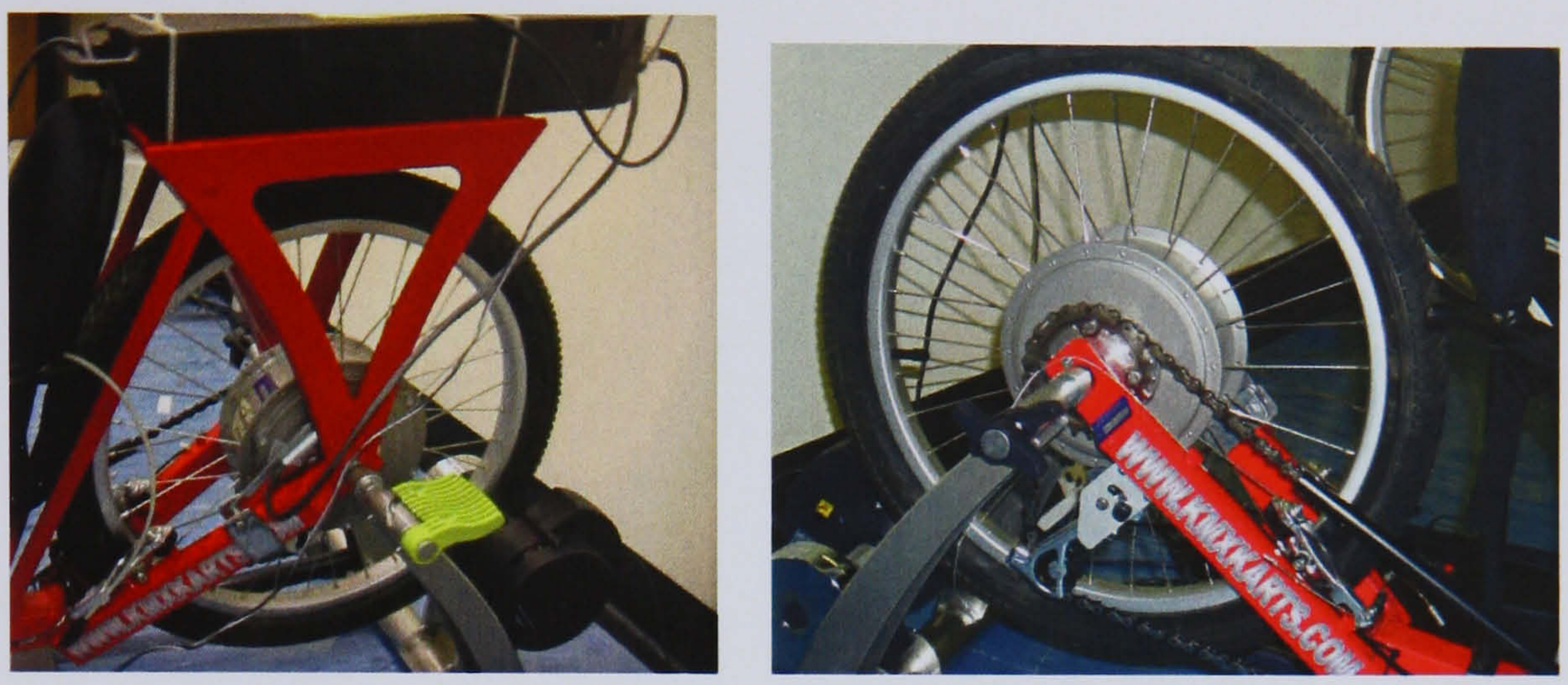

(a) Left hand view showing connecting arm/clamp, battery pack and carrier. (b) Right hand view showing fixed cog and derailleur.

Figure 6.3: Hub motor and attachments.

Part	*Dimensions* (cm)	*Weight* (kg)	*Power rating* (W)	*Voltage* (V)
Motor	Diameter - 17.6 Width - 8.8	2.76	200 (continuous) 400 (peak)	24
Battery pack/ controller	42 x 14 x 7	5	-	24

Table 6.1: The Heinzmann hub motor system - specifications.

Normally a standard freewheel cassette is attached to the axle. However, as we wish to drive the pedals using the motor and the hub is significantly wider than that on a standard wheel, a single speed, fixed gear setup was adopted (figure 6.3(b)). To achieve this, a single sprocket was fixed to a second cog (which acts as a spacer) using grub screws round its perimeter, then both were attached to the side of the hub using a suitable adhesive (an approach used because of the difficulties involved in drilling or

[1]Heinzmann GmbH, Schönau, Germany. http://www.heinzmann.de/

welding the stainless steel motor case). Finally, to ensure that chain tension is sufficient, a custom derailleur which is fixed in one position but can also be adjusted for different front boom lengths, was attached to the right rear fork.

The rechargeable battery cells (nickel-cadmium) and power control electronics are located in a plastic case mounted on a custom made carrier above the rear wheel and attached to the axle. The battery case also contains a master on/off power switch and sockets with which to connect the motor, charger and throttle. Motor speed is adjusted proportionally by the motor controller based on the voltage read from an accompanying thumb throttle potentiometer, similar to the twist version used for stimulation intensity control. It too may be mounted on a handlebar and has a switch on the side. However, in this case it is simply used as an on/off selector for the motor.

6.2.3 Torque Sensor

To calculate power output at the pedals, the original chainset is replaced with a torque sensor (SRM professional version[2]) which is mounted on the crank shaft, as shown in figure 6.4. Broadly, the sensor system (specifications are shown in table 6.2) consists of two main components: a sensor/chainset arrangement and display/controller. The instrumented chainset, which contains strain gauges, measures torque applied to the crank arm and the velocity at which it turns. The latter information is obtained using a reed switch located on the trike frame. Data are transmitted to (and recorded on) a display and control unit, which may be mounted on the handle bar.

Figure 6.4: Torque sensor with custom-made crank arm.

[2]Schoberer Rad Messtechnik, Königskamp, Germany. http://www.srm.de/

Sensor type	*Operating range*	*Accuracy*
Torque - four strain gauges (wheatstone bridge configuration) Cadence - contact reed switch	Power: 0 - 4800W Cadence: 20 - 255rpm	±2.5%

Table 6.2: SRM torque sensor - specifications.

The sensor was originally designed for adult bicycles and thus the supplied crank arms (165mm) were too long for our system. To rectify this, a custom 125mm version was manufactured and attached to the chainset, while a standard arm of equal length was located on the other side. This was the only modification required to fit the sensor to the tricycle. However, a full calibration of both it, and the associated data acquisition apparatus was performed. Details of these experiments are given in section 6.3.

6.2.4 Data Acquisition and Control

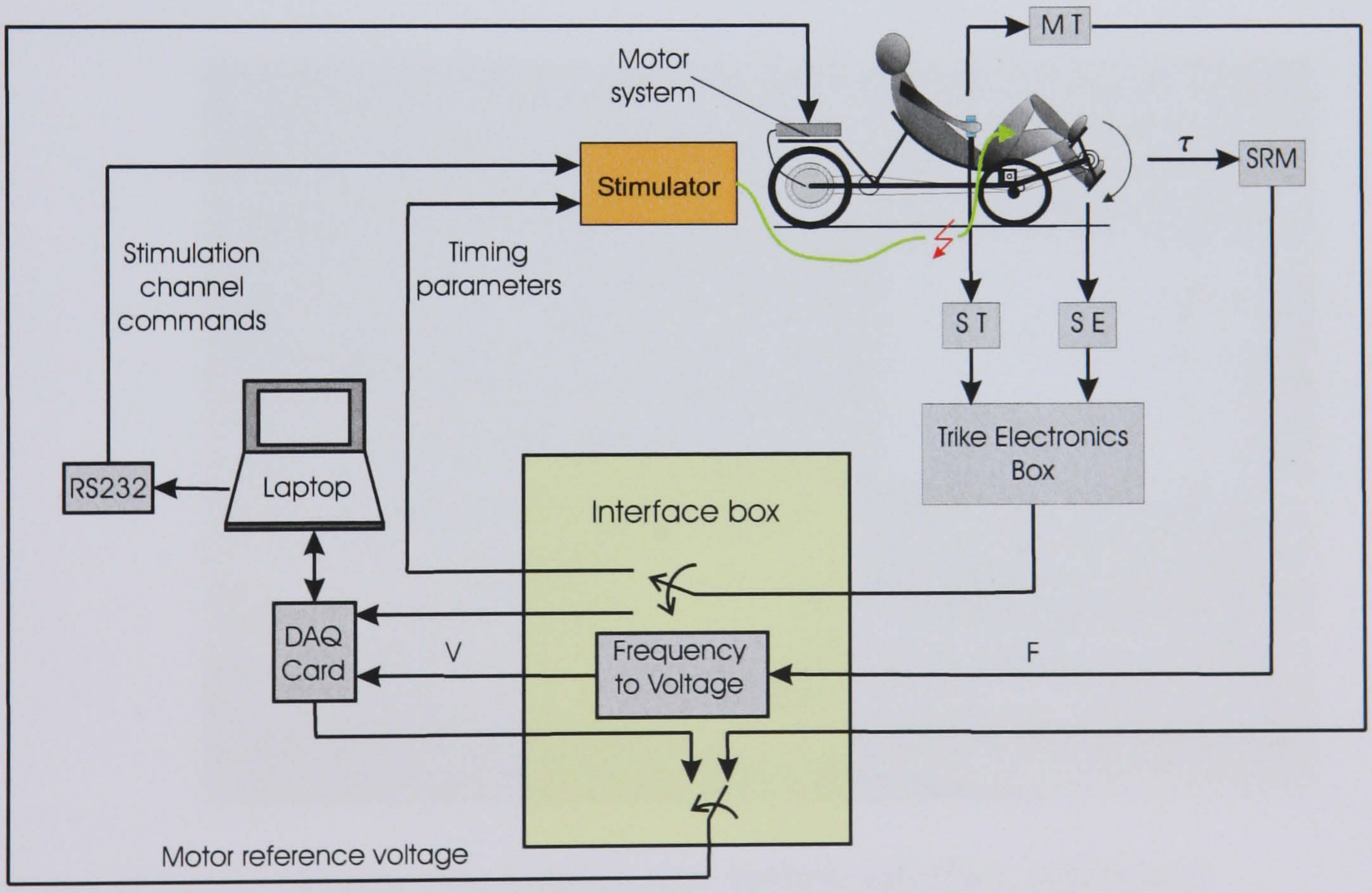

Figure 6.5: Schematic showing interface box function in the motorised tricycle system. MT - motor throttle, ST - stimulation throttle, SE - shaft encoder, SRM - SRM torque sensor, τ - torque, V - voltage, F - frequency, DAQ - data acquisition.

A schematic illustrating the setup for open and closed loop control of both stimulation and motor speed, in addition to all interface equipment used, is shown in figure 6.5. A custom-made interface box links the system's sensors and control throttles to the laptop, stimulator and motor. Shaft encoder and stimulation throttle data can either be sent to the stimulator directly (then used by its internal cycling algorithm) or to the laptop using a switch on the box. In the latter case, individual channel stimulation commands from the laptop-based cycling algorithm are sent to the stimulator via an RS232 serial connection.

A frequency proportional to the torque generated at the crank can be obtained from the SRM controller/display unit (called the "power control") in realtime, and is passed through a frequency-to-voltage converter, located within the interface box. Both this voltage and those representing crank and stimulation throttle position are sent by the laptop using a data acquisition card (National Instruments USB-6009[3]). Finally, for control of the motor, the throttle signal passes through the interface box where a second switch may be used to choose between it and an output voltage from the laptop/DAQ card as the input to the motor system.

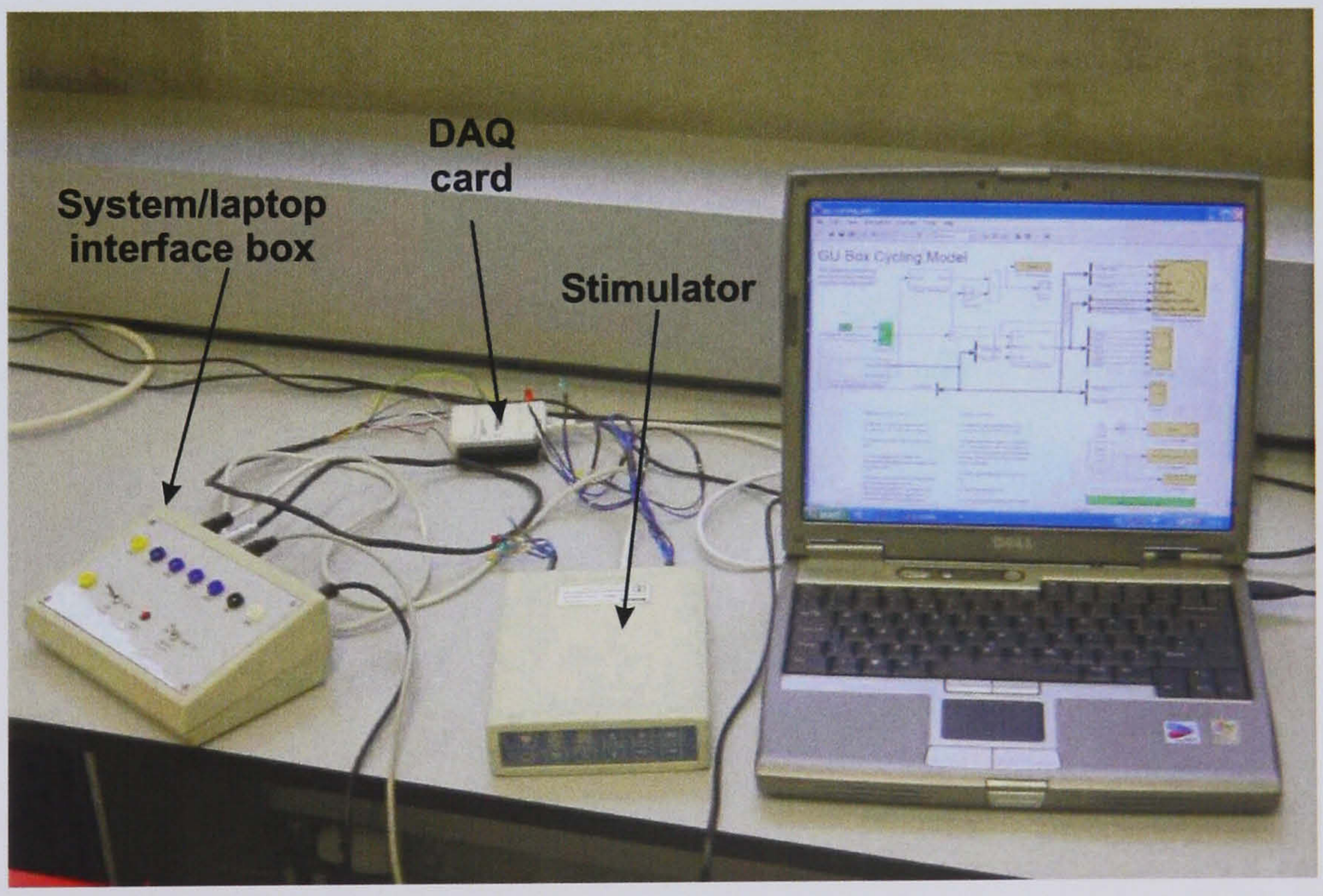

Figure 6.6: Laptop and system interface equipment.

All signals that pass in and out of the DAQ card can be utilised or set within Matlab Simulink. Thus, through using this setup, an environment is created whereby methods

[3]National Instruments Corporation, Austin, TX, USA. http://www.ni.com/

for controlling motor and stimulation can be developed. In addition, control, via the throttles, can be passed to the rider or operator using the switches located on the interface box. Thus, the change from manual to automatic control is straightforward.

6.2.5 Power Measurement

It has been shown that through accurate control of cadence and power output FES-cycling can be used to facilitate exercise testing within the adult spinal cord injured population [43]. Considering the comparatively low power outputs reported in this group, such testing is made possible by lowering the workrate baseline and, thus, increasing the functional range for exercise using FES-cycling.

When the pedals are driven by the motor with no stimulation applied (and therefore no work input from the legs), a resistive torque caused by factors such as joint stiffness and friction in the mechanical system will result in an observed negative power level, based on the torque measured at the crank. As stimulation is initiated and raised to a level sufficient to overcome this resistance, the power output will rise to 0W. Beyond this, the legs will begin to contribute to the mechanical work done against the load.

It is this "negative workrate" region which enables the baseline for exercise testing to be lowered. The resulting increase in functional range could also be beneficial for training of those with severe muscle atrophy (or who have difficulty in tolerating adequate levels of stimulation) and thus allow a larger number of potential candidates, who are untrained, to use the system. Therefore, based on initial testing described in the previous chapter, it would appear to be a particularly desirable capability for a paediatric FES-cycle system. Moreover, the ability to quantify performance within this range could facilitate the measurement of small improvements in training outcomes, such as strength, that previously would not have been possible.

To achieve these goals it is imperative that our system can provide precise torque and cadence measurements (the product of which will give power output) in realtime. Cadence may be accurately derived from crank position and is already used for control of stimulation (as shown in the previous chapter). Acquiring instantaneous torque data for realtime software-based control requires a series of custom hardware and software components. In order to test these, the sensor system has been fully calibrated and verified through experiments which will be discussed in the following section.

6.3 Torque Sensor Calibration

A series of experiments has been undertaken to calibrate and verify the torque measurement setup. The procedure undertaken and results found are given here.

6.3.1 Methods

Aims and Objectives

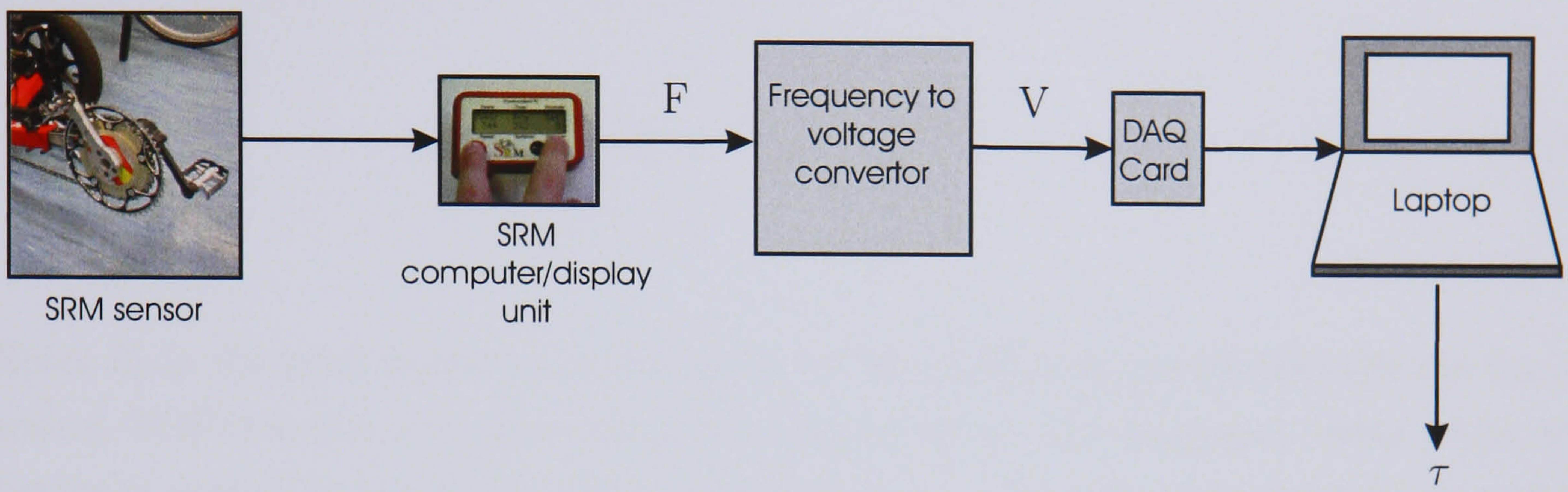

Figure 6.7: Torque measurement setup. τ - torque, F - frequency, V - voltage.

Figure 6.7 illustrates the process involved in acquiring realtime torque data. As described previously, a frequency which is linearly related to the torque generated at the pedals (based on a predetermined slope) can be obtained from the SRM "power control" unit. This frequency is converted into a voltage between zero and five using a custom-made converter. The range used and minimum value read into this converter can be tuned, but it is designed to read between approximately 100 and 600Hz. This gives a functional torque range of roughly 6 to 26Nm, or a power range of -31 to 135W (which encompasses reported performance of spinal cord injured individuals comfortably). The voltage output is sampled by a DAQ card and processed by control software on the laptop. At this point, the process is reversed to obtain the frequency, corresponding torque and power.

Several variables are involved in the entire process. Thus, the aim of the following experiments was to calibrate these parameters and validate the approach through the following objectives:

(i) Calibrate the slope value used for the frequency to torque transformation.

(ii) Determine absolute values for frequency to voltage parameters.

(iii) Verify sensor and software accuracy using known weights.

Torque/Frequency Slope Calibration

The slope value used to convert the sensor's measured frequency to a corresponding torque can be found using the following expression:

$$slope = \frac{F_p - ZOPM}{(M \times g \times r)} \tag{6.1}$$

Here, F_p is the peak frequency value given as the crank arm passes through the horizontal, ZOPM is the zero offset frequency measurement (the frequency value when no torque is applied to the crank), M is a known mass, g is the gravitational field strength (taken as 9.81) and r is the length of the crank arm.

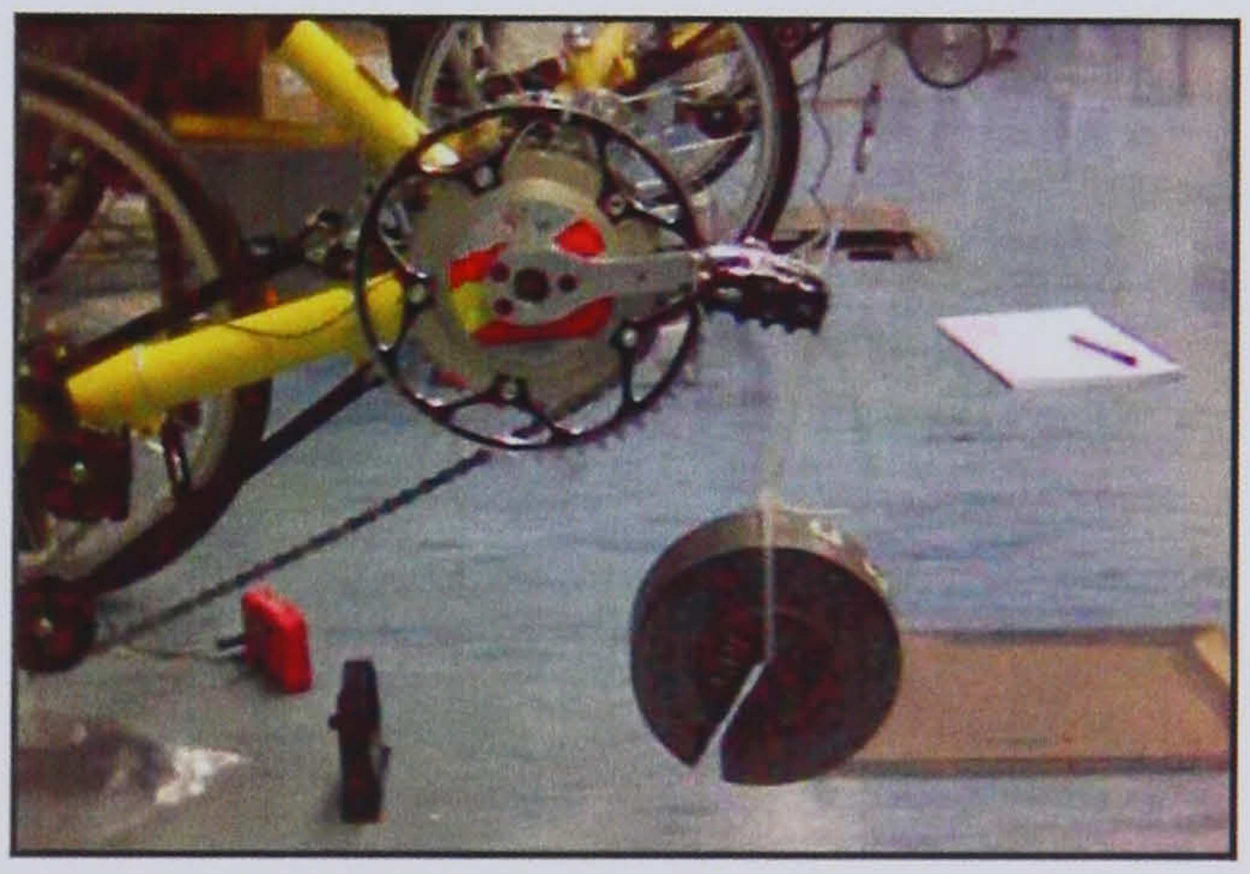

Figure 6.8: SRM sensor with weight hanging from pedal.

A known mass (measured using a Mecmesin digital force gauge[4], model BFG200N) was hung from the right, then left crank arm (figure 6.8) three times to obtain values of F_p. This peak value was found by rotating the rear wheel to pass the crank arm through the horizontal repeatedly. On each occasion the ZOPM value was recorded before applying the weight. The observed data were used in equation (6.1) to obtain a

[4]Mecmesin limited, Slinfold, UK. http://www.mecmesin.com/

slope for both the right and left side, with the mean of the two giving the final value.

This process was repeated on three different days to allow for changing environmental conditions (such as temperature).

Determination of Frequency to Voltage Parameters

On the laptop, the voltage signal (V) from the frequency-to-voltage converter is normalised between zero and one volt then used with the now determined slope and ZOPM values in the following expression to calculate torque (τ):

$$\tau = \frac{(V \times F_r) + F_0 - ZOPM}{slope} \tag{6.2}$$

F_r and F_0 are the frequency range and minimum value used by the converter. Although they were designed to be approximately 500 and 100Hz respectively, absolute values were determined to give a more accurate torque measurement.

To do this, peak values of V were recorded as the crank arm was passed through the horizontal, first with no torque applied and then with a known mass hanging from the crank arm (giving the variables V_1 and V_0). As the corresponding torque with no load applied (τ_0) is zero and $\tau_1 = M \times g \times r$, equation (6.2) may be rearranged to give:

$$F_0 = ZOPM - (V_0 \times F_r) \tag{6.3}$$

and,

$$F_r = \frac{(\tau_1 \times slope)}{(V_1 - V_0)} \tag{6.4}$$

Thus, using equations (6.3) and (6.4), values for F_0 and F_r could be determined.

Validation of Sensor and Software

To verify the sensor measurement and data acquisition process, all parameters were used to calculate the torque applied when hanging three known masses (table 6.3) from the right and left crank arms.

Mass (kg)	*Expected torque* (Nm)
2.007	$\tau_1 = 2.46$
5.007	$\tau_2 = 6.14$
10.01	$\tau_3 = 12.27$

Table 6.3: Masses used and torques expected ($\tau_1 - \tau_3$) for sensor validation experiment.

Each mass was measured using the digital force gauge mentioned previously, then multiplied by g and r ($r = 12.5$cm) to obtain $\tau_1 - \tau_3$. Just as during the determination of frequency to voltage parameters, peak sensor-measured torque values were recorded as each pedal was passed through the horizontal (crank arm/pedal to the front) while a weight was hanging from it.

Verification of Complete System Operation

As a final step, tests were undertaken to ensure the complete system integration functioned correctly. All possible layouts (as depicted in figure 6.5) were checked including observing and recording all sensor data, controlling the motor from both throttle and laptop, and initiating stimulation (while observing activation timing) during cycling with dummy loads.

6.3.2 Results

Torque/Frequency Slope Calibration

The slope calibration procedure described above was carried out using a mass of 5.007kg attached to a crank arm 12.5cm long. ZOPM and F_p values found during all three tests are shown in tables 6.4 to 6.6.

Measurement	*Right ZOPM* (Hz)	*Left ZOPM* (Hz)	*Right F_p* (Hz)	*Left F_p* (Hz)
1	194	194	287	291
2	194	194	290	291
3	194	194	288	291

Table 6.4: ZOPM and F_p values from test one. Temperature: 24°C.

Measurement	*Right ZOPM* (Hz)	*Left ZOPM* (Hz)	*Right F_p* (Hz)	*Left F_p* (Hz)
1	193	193	289	290
2	193	193	289	291
3	193	193	289	292

Table 6.5: ZOPM and F_p values from test two. Temperature: 22.5°C.

Measurement	*Right ZOPM* (Hz)	*Left ZOPM* (Hz)	*Right F_p* (Hz)	*Left F_p* (Hz)
1	194	194	290	292
2	194	194	290	293
3	194	194	290	293

Table 6.6: ZOPM and F_p values from test three. Temperature: 23°C.

The final slope value used for subsequent experiments was calculated as:

$$\text{slope} = 15.8\text{Hz/Nm}$$

Left, right and mean values for all experiments, as well as the percentage variation from both the factory setting (17.4Hz/Nm) and previous test, as calculated using expression 6.1 are given in table 6.7. SRM state that a percentage variation in slope value of more than 5% between tests is significant and that if the change is below this value an average should be taken. Although all values found during our experiments were significantly different than the factory specified, the mean did not vary more than 5% between tests. Thus, the average of the three means was chosen as the final slope (15.8Hz/Nm).

test	*Right Slope* (Hz/Nm)	*Left Slope* (Hz/Nm)	*Mean* (Hz/Nm)	*Variation from factory specified*	*Variation from previous test*
1	15.37	15.8	15.59	-10%	-
2	15.64	15.97	15.8	-9.2%	+1.35%
3	15.8	16.24	16.02	-7.93%	+1.39%

Table 6.7: Slope values and percentage variation for all tests. Factory specified slope: 17.4.

Determination of Frequency to Voltage Parameters

	Torque (Nm)	*Voltage* (V)
Unloaded pedal	τ_0: 0	V_0: 0.182
Loaded pedal	τ_1: 6.138	V_1: 0.369

Table 6.8: Torques and corresponding peak voltages used for frequency-to-voltage parameter determination.

Peak voltages, V_0 and V_1, were found by applying torques τ_0 and τ_1 and passing the crank arm through the horizontal position (table 6.8). These values were then used in equations (6.3) and (6.4) to obtain:

$$F_0 = 98.61\text{Hz}$$

$$F_r = 518.6\text{Hz}$$

Validation of Sensor and Software

The experimentally found values of slope, F_0 and F_r were inserted into a simulink model, which is based on equation (6.2). Torque values were then calculated from the input voltage and current value of ZOPM (194Hz) while three known weights were hung from the crank arm.

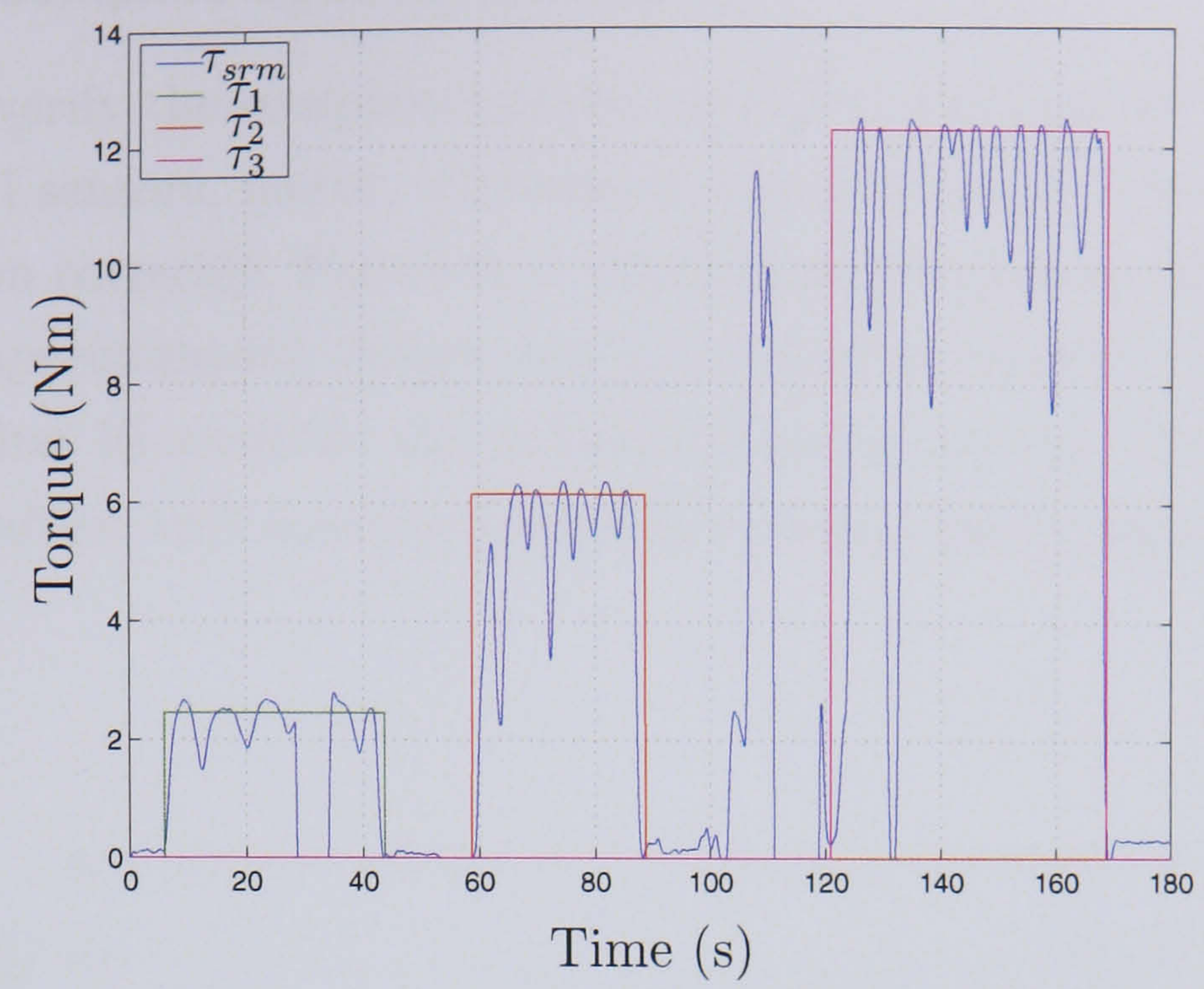

Figure 6.9: Expected/calculated (τ_1 - τ_3) and measured (τ_{srm}) torque with weight hanging from left crank arm.

Figures 6.9 and 6.10 show measured torque, τ_{srm}, using the model as the pedals are passed through the horizontal repeatedly with each weight (represented by the expected torques, τ_1 - τ_3, described in section 6.3.1) hanging from them. In all cases, the observed peak torque matched the expected value closely.

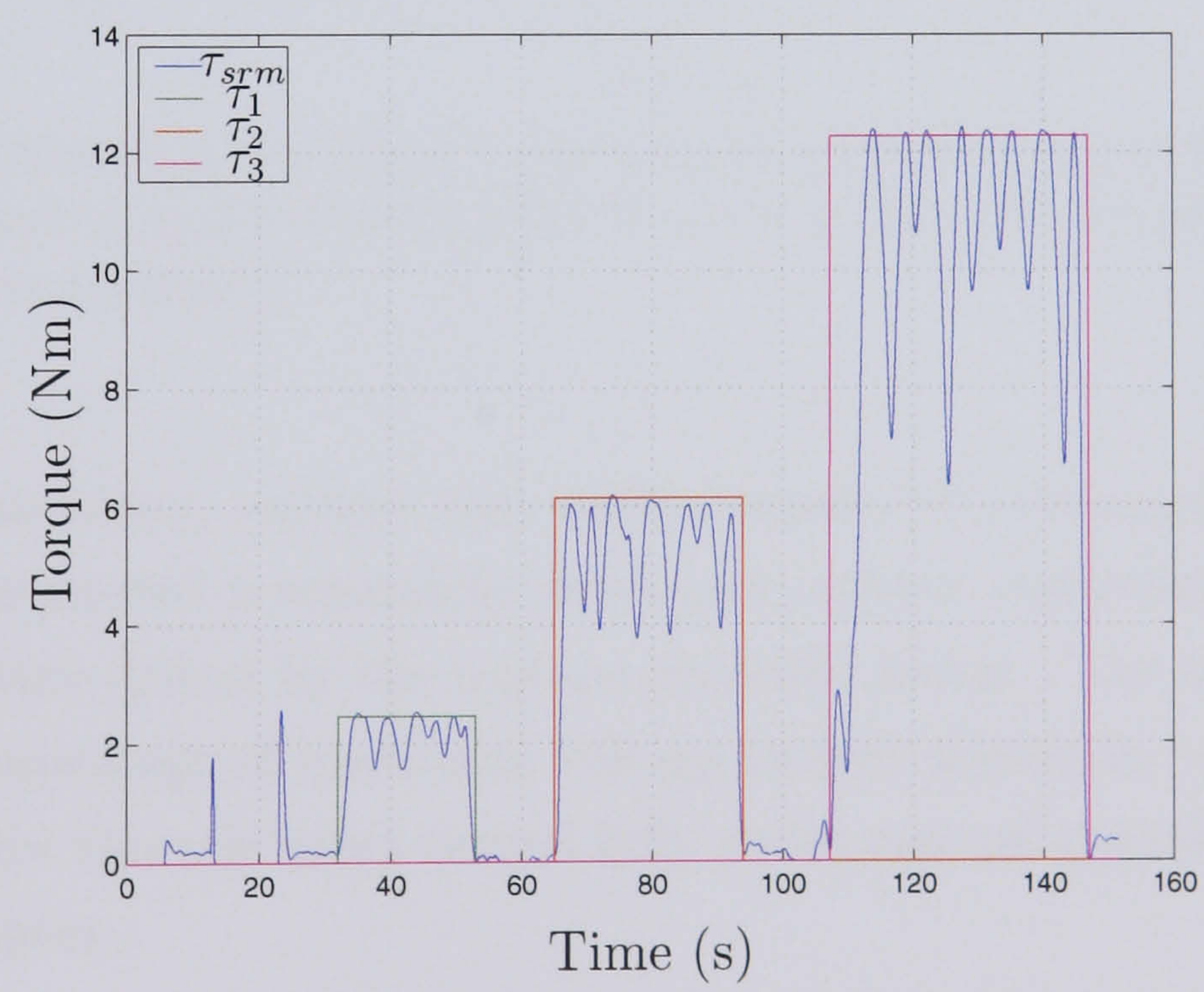

Figure 6.10: Expected/calculated (τ_1 - τ_3) and measured (τ_{srm}) torque with weight hanging from right crank arm.

Verification of Complete System Operation

Experiments to verify the complete system operation were carried out as described in section 6.3.1. All sensors, motor, stimulation equipment and control layouts were observed to function correctly. Figure 6.11 shows measured torque and calculated power at a cadence of approximately 50rpm during a period of passive cycling (driven by the motor over the first 10 seconds) and subsequent active period. The negative workrate area discussed earlier, and possible using this system, can be seen during the passive period.

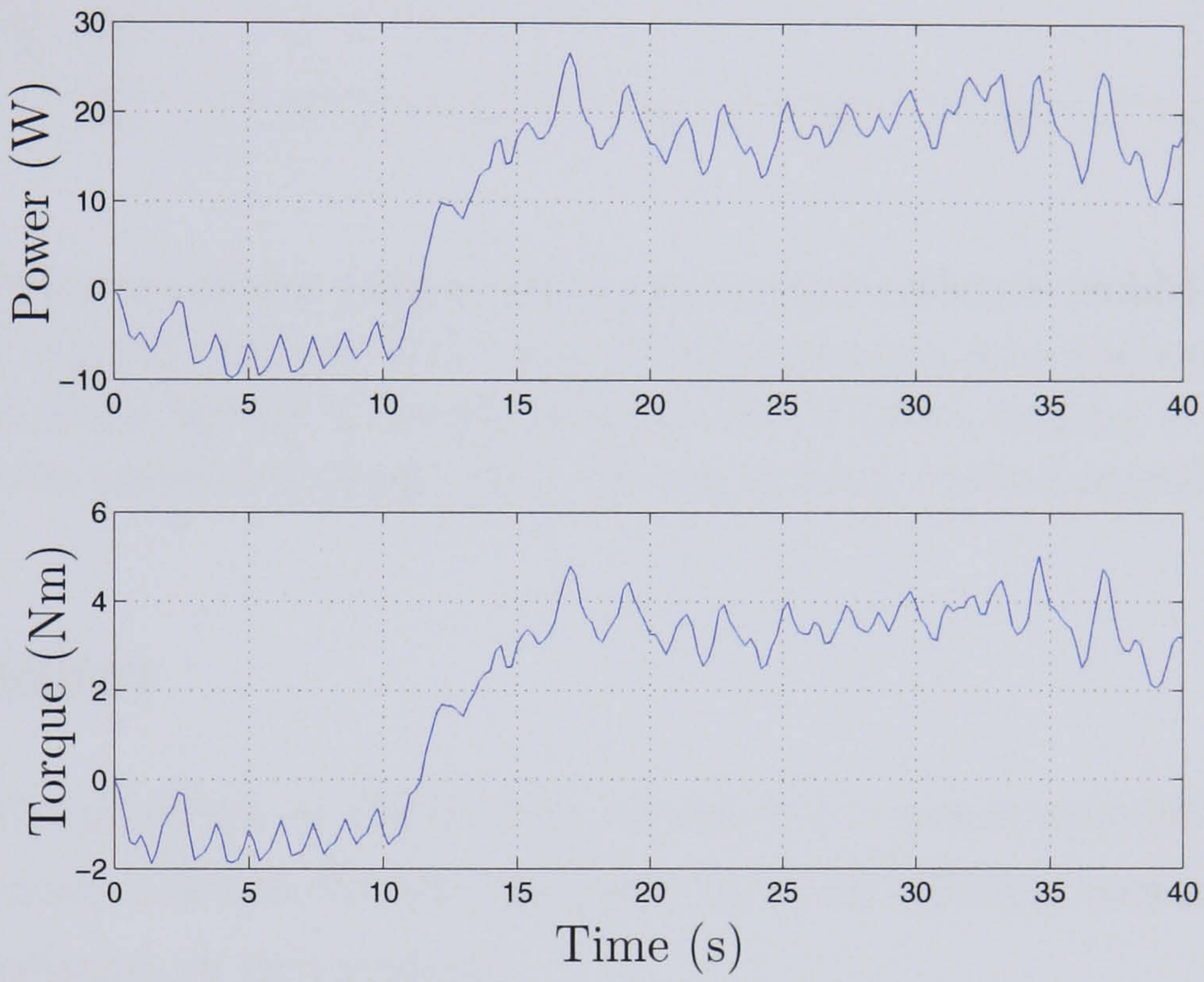

Figure 6.11: Calculated power (upper plot) and measured torque (lower plot) during a period of motor-driven passive cycling (first 10 seconds) and subsequent active cycling.

Figure 6.12 shows power, cadence and control signal data obtained during an experiment which incorporated a separately developed cadence controller. During this test, the rider's legs were driven by the laptop-controlled motor. The motor control signal represents the percentage of maximum voltage (where maximum voltage would correspond to the motor throttle being turned fully under manual control) sent to the motor system by the laptop.

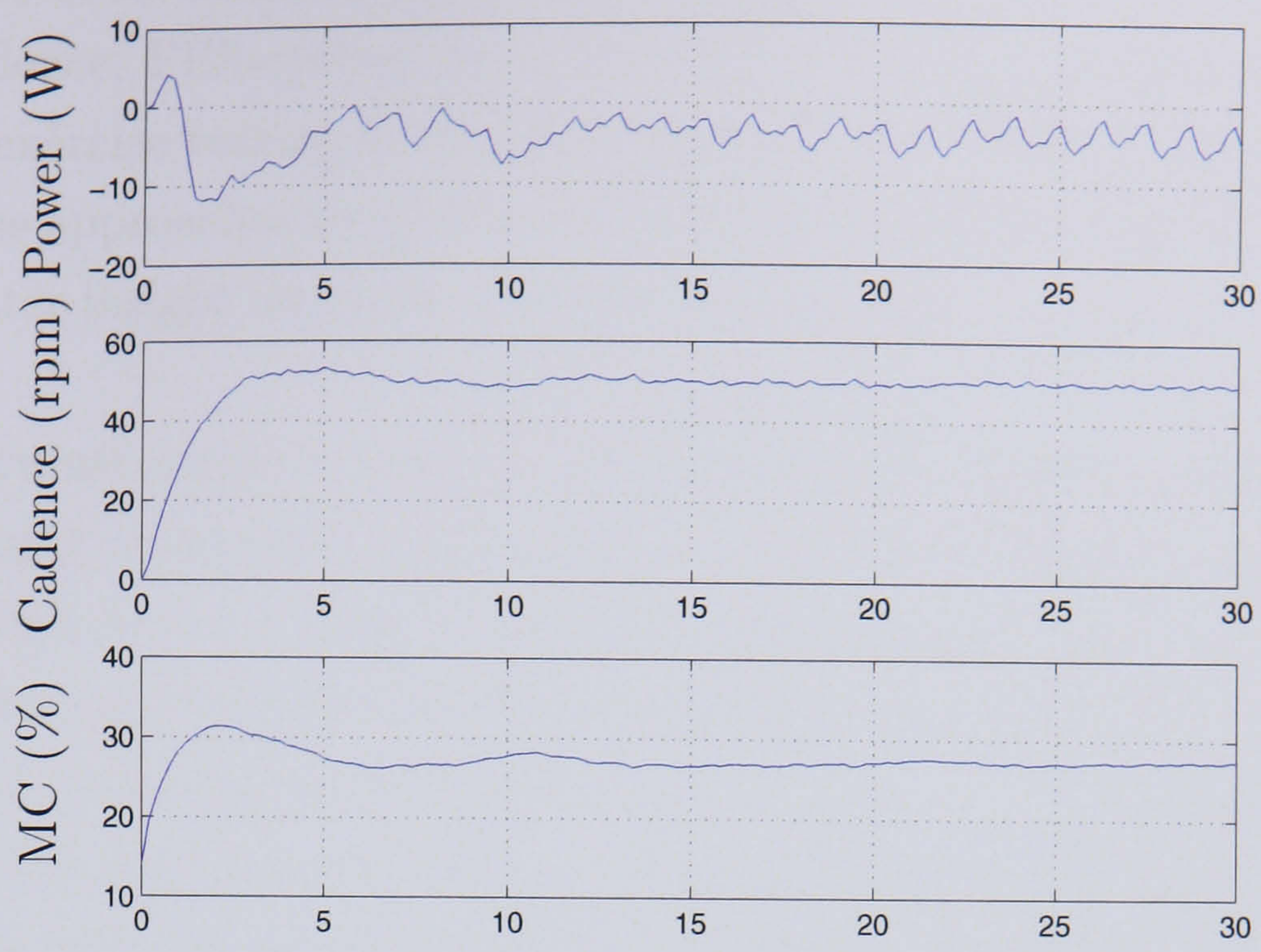

Figure 6.12: Calculated power (upper plot), measured cadence (middle plot) and control signal (expressed as a percentage between zero and maximum voltage) sent from laptop to motor system (lower plot), during a period of motor-driven passive cycling. MC - motor system control signal.

6.4 Discussion

In addition to the prospect of developing methods for motor-assisted mobile cycling, there are three main reasons for the inclusion of a controllable motor and force measuring instrumentation in this system:

- As indicated by initial testing within this population, potential subjects may require familiarisation time to reach sufficient levels of stimulation intensity. Motor assistance during this initial exposure, which can be reduced as stimulation toleration increases, could allow for a smooth transition period.

- With the system described in chapter 5, subjects must have sufficient muscle strength to overcome the mechanical impedance associated with the rider/tricycle system to achieve cycling at all. As many of this system's potential users will have not only severely atrophied, but also underdeveloped musculature, they may well be unable to meet this criterion. Therefore, in the initial stages of training such individuals, assistance would be a necessity.

- Through use of an auxiliary motor and suitable control strategies to govern power output and cadence, FES-cycling has been used previously to facilitate standard cardiopulmonary exercise testing in the adult spinal cord injured population. Therefore, replicating these approaches on a device suitable for paraplegic and tetraplegic children could give greater insight into their exercise capabilities.

In all cases, accurate measurement of both torque and cadence is required for control purposes or simply to quantify what could be very small effects of training. The approach of deriving cadence from a sampled crank position, used by our system, has been successfully employed for accurate stimulation control in many devices and gives accurate data on pedalling speed within a control-strategy-software development environment. We have demonstrated through the experiments in section 6.3 that accurate values of torque may also be measured and processed to obtain power output in real-time. Thus, together with the ability to control auxiliary motor speed (and therefore amount of pedalling assistance) through providing a reference voltage from the DAQ card, laptop-based closed-loop power and cadence control strategies can be created and implemented. In addition, this control can also be applied manually as use of the interface box allows for a flexible layout whereby motor speed and stimulation intensity are easily passed to the throttles.

As the device incorporates all the security and orthotic modifications described in chapter 5, it should be suitable for a spinal cord injured child to use. Rider safety is obviously of the utmost importance. Therefore, the relative power output of the motor (which is driving the legs) comes into question when considering the particularly high lower-limb bone fracture risk, generally seen in the target population. For this reason, maximum voltages (which are proportional to motor speed) sent to the motor system under laptop control will be carefully limited both within software environments and through the use of an external voltage converter. The latter device is currently under development and is specified for a voltage range limit which is approximately 40% of maximum. Although this value will be adjustable, levels used for motor-driven passive cycling at 50rpm during verification experiments (as illustrated in figure 6.12) were within this range. Thus, a 40% maximum should be both practical and safe for children.

Where younger children are concerned, it would be advisable to ensure motor and stimulation throttles are not under their control, but stop buttons for both devices are still easily within reach (the inclusion of a second "emergency stop" button for this purpose is also planned). This point also highlights some of the practicalities of mobile cycling under manual control. Although both throttles, motor controller/battery and stimulator may be mounted on the tricycle easily, the prospect of governing two throttles whilst also steering presents difficulty. One option for the system in this configuration could be for the motor to be used only as an aid to overcome initial inertia or when the legs have fatigued. However, as the addition of the motor system substantially increases the weight of the tricycle (and consequently the mechanical work that the rider must do to propel themselves), automatic cadence control strategies which distribute work between the legs and motor using only one throttle may have the best chance of success.

6.5 Conclusions

A new motorised FES-cycle system for spinal cord injured children has been developed. The device is designed to provide a platform from which further development of suitable FES-cycling methods, for training and mobile cycling, within this population may be undertaken. It also provides an opportunity to develop and carry out suitable control strategies for standard cardiopulmonary exercise testing (such as a constant load or incremental approaches). Moreover, when compared with our non-motorised system the additional instrumentation and increased range of functional workrate available should allow the FES-cycling/exercise capabilities of paraplegic and tetraplegic children to be quantified in greater detail.

We have demonstrated that accurate instantaneous torque data can be obtained and processed in a software environment that already contains necessary pedalling cadence information (the product of these two variables giving power output) and from which realtime control of motor speed and stimulation may be exercised. Although the next step will be to develop appropriate strategies which utilise these variables in a closed-loop manner (for optimum accuracy), the flexibility of the system's setup allows simple manual control to be employed and, thus, it is ready to be used by its target population.

The tricycle can currently be set up for mobile use under manual control. However, the practicalities of this (especially with younger children) mean that the system probably has more to offer as a development tool for future mobile control strategies rather than for recreation at this time.

As a practical stationary training ergometer, the motorised system should be seen not only as an evolution of the non-motorised version, but also as a second option that could offer an introductory or transitional period of FES-cycling to those who require pedalling assistance or stimulation familiarisation time. Thus, even though there will undoubtedly be subject-specific hurdles to overcome (because of the highly variable nature of the population), we surmise that between the two systems there will be enough flexibility to allow a substantial increase in the participation of paediatric spinal cord individuals.

7 Conclusions and Recommendations for Future Work

The technique of utilising controlled artificial electrical stimulation pulses to induce cycling has been used now for over two decades. During that time, several systems have been developed and numerous studies undertaken which have demonstrated this modality as a method with the potential to increase fitness and improve health in individuals with a spinal cord injury. Moreover, its ability to be used for recreation makes it an attractive tool for achieving these goals.

Although the work reported in this thesis is split into two different research foci (using a limb-mounted sensor and PDA-based system for FES-cycling, and developing FES-cycling methods and equipment for the paediatric SCI population), in our opinion, both represent paths that the common theme (FES-cycling) must undertake for it to progress as a practical rehabilitation and exercise technique available to as many potential beneficiaries as possible.

7.1 FES-cycling - Moving Forward

With FES-cycling still being primarily laboratory-based, a move to employ modern sensor and computing technology (which is significantly more compact, and perhaps more user friendly) would seem an important step to advancing its progression into the clinical environment and toward practical home use.

Our investigations into using a multi-functional PDA-based FES system and limb-mounted sensor for FES cycling (chapter 4) have yielded two novel contributions:

(i) Two new stimulation activation control strategies which utilise a limb-mounted sensor have been developed. Through manipulating hip angle data which are measured using a limb-mounted sensor, we have shown that a corresponding crank position (which can subsequently be used as a reference for stimulation activation timing) can be estimated relatively accurately by two different approaches. Both techniques have been tested through simulation, then verified using experimentally found data offline. and finally, incorporated into models which calculate crank position in realtime on the PDA-based system.

(ii) The new angle conversion approaches have been incorporated into FES-cycling control strategies which can be run in realtime on the PDA-based system. In addition. a third strategy employing a "traditional" approach (whereby crank position is measured directly) has also been developed and integrated into the same device. All three techniques have been shown to produce practical stimulation activation times when implemented on a recumbent tricycle.

As described in section 4.5, further work involving alternative sensors is required to fully establish the origin of an observed measurement error and either compensate for or eliminate this to increase both angle conversion algorithms' accuracy. Providing there is accurate sensor measurement, however, we have shown that practical stimulation activation times can be achieved based on an estimated crank position. Moreover, the system's range of capabilities means that all three strategies could be implemented using either surface or implanted stimulation (although further testing with dummy loads is required to ensure the sample rate issues previously discussed do not impede successful operation). Also, if the two hip-angle-based approaches were further modified with some form of on-screen stimulation intensity control (as mentioned in the relevant discussion section) then there would be no need to instrument the tricycle.

A possible disadvantage to this setup is that there is more body-worn equipment than used with existing approaches. However, the fact that the FES-device in question can be used for a whole range of applications (and, thus, cycling may not necessarily be the main reason an individual owns one) means donning and doffing may not be such a big issue for those who use it, particularly those who have an implanted stimulator. The idea of miniaturising and consolidating FES technologies is one possible direction which could help the progression of FES-cycling as a practical technique. However, in terms of increasing the potential benefits from using it, progress in the areas of stimulation pulse behaviour and delivery is equally consequential.

Although reported benefits of FES-cycling in the adult spinal cord injured population are significant and encouraging, it is still evident that relatively small training returns accompany large efforts on behalf of the rider. It could be speculated that the most influential limiting factors are the delivery methods and nature of artificial stimulation pulses. Surface stimulation, although non-invasive, is still a rather crude approach where charge is passed over a relatively large area and high number of motor units, some of which (when activated) could induce antagonistic muscle contraction. Implanted stimulation may offer more accuracy but delivery of pulses using either method is still vastly inferior to the fatigue-retarding abilities of the central and peripheral nervous systems under volitional control.

Recent work involving the investigation of stimulation pulse trains has shown that utilising variable frequency train (or VFT) techniques may offer a way of reducing the rapid fatigue seen during FES applications. In a study by Janssen et al. [86], one of these techniques was implemented in new FES-cycling stimulation patterns and compared with a standard constant frequency train . Results were inconclusive as to the effectiveness of this new pattern on cycling performance. However, in a more recent study by Scott et al. [87] implementation of another VFT approach, during repeated isometric contraction of the quadriceps, yielded a 14% improvement (in terms of the number of times a target force was reached) when compared with standard constant frequency techniques. Thus, there may be scope for improving the performance FES-cycling using such techniques in the future.

7.2 FES-cycling in the Paediatric Spinal Cord Injured Population

It is unfortunate that, in general, FES technologies have not been employed in the paediatric spinal cord injured population as prolifically as with adults and teenagers. Our opinion, however, is that even though the challenges to be faced are bigger, children have potentially the most to gain from such technology, in particular FES-cycling.

Thanks to modern medical interventions, children who sustain spinal injuries will live a near-normal lifespan. However, this also means that they will be subject to all the primary and secondary health complications discussed in chapters 2 and 3 the longest. Thus, when considering the subsequent social and economic costs involved, undertaking a modality such as FES-cycling with a view to maintaining or improving health throughout life could be extremely beneficial. Moreover, the recreational qualities of cycling mean it is ideally suited to a population for whom availability of and participation in social activities is somewhat limited.

Given that a potential candidate may still be growing and developing, it could be speculated that the regenerative processes involved during this time might assist in improving upon the training returns seen in adults during an FES-cycling intervention. Even if training benefits can only be replicated, such improvements may be more consequential to the child with a spinal cord injury given that the health complications seen in this population are often more severe than in adults.

Through investigations into the development of methods and equipment for FES-cycling within the paediatric spinal cord injured population, the following novel contributions have been made:

(i) A tricycle-based FES-cycle system which incorporates a range of seating and orthotic/safety equipment for increased flexibility has been developed (through testing with 10 paediatric spinal cord injured subjects) to be suitable for use by a child with a spinal cord injury (chapter 5).

(ii) FES-induced pedalling has been demonstrated on our system by a seven year old untrained T4/T6 (motor complete) subject. In addition, methods for safely undertaking stationary FES-cycling sessions within the paediatric SCI population have been developed (chapter 5).

(iii) A second, motor-integrated, paediatric FES-cycle device has been developed to allow a greater number of potential subjects to take part, in addition to providing a test bed for future investigations (chapter 6).

Although only one subject has cycled for a significant period of time using our non-motorised system, the experience gained with others provided data which were vital to the development of what, we hope, is now a "child proof" device. Moreover, the experiments undertaken supplied us in part with impetus for the motorised system development. In addition to allowing a larger proportion of the population to undertake FES-cycling through providing controlled assistance, it is hoped this second device can be used to quantify and gather information concerning this population's exercise and training capabilities. To this end, planned future work will include pilot testing of the motorised system with paediatric SCI subjects to verify safe and correct operation.

When comparing our system with other approaches (including those presently available for use by children), it is our opinion that a tricycle-based one which revolves around a standard device is an extremely attractive option for its target population. Although not without its limitations (the need for transfer for example), it is hoped the combination of low-cost, pleasing aesthetics and the potential for mobile recreational cycling will encourage more children to participate in future FES-cycling interventions.

Incorporation of FES-cycling into the rehabilitation process following a spinal cord injury is a major goal. Although placement within the clinical environment is undoubtedly an important part of this, the wishes of those who undertake it are crucial to success and "in the clinic" is not necessarily where they wish to be. This is especially true for children. Moreover, reported evidence on health benefits suggests that training intensity levels must be sustained in order to maintain gains. If this is the case, then the recreational qualities of FES-cycling could offer the necessary motivation. However, for this to be achieved, the technology and methods involved must be straightforward and robust enough. Thus, it is probably most important that future FES-cycling development is aimed at improving practicality with a view to home use.

Bibliography

[1] D. Grundy and A. Swain, *ABC of Spinal Cord Injury.* BMJ, 3rd ed., 1996.

[2] A. B. Jackson, M. Dijkers, M. J. Devivo, and R. B. Poczatek, "A demographic profile of new traumatic spinal cord injuries: change and stability over 30 years," *Arch Phys Med Rehabil*, vol. 85, pp. 1740–1748, Nov 2004.

[3] V. R. Hentz and C. Leclercq, *Surgical Rehabilitation of the Upper Limb in Tetraplegia.* W.B. Saunders, 1st ed., 2002.

[4] B. Cirak, S. Ziegfeld, V. M. Knight, D. Chang, A. M. Avellino, and C. N. Paidas, "Spinal injuries in children," *J Pediatr Surg*, vol. 39, pp. 607–612, Apr 2004.

[5] P. L. Jacobs and M. S. Nash, "Exercise recommendations for individuals with spinal cord injury," *Sports Med*, vol. 34, no. 11, pp. 727–751, 2004.

[6] C. A. Glass, *Spinal Cord Injury - Impact and Coping.* BPS Books, 1st ed., 1999.

[7] R. R. Seeley, T. D. Stephens, and P. Tate, *Essentials of Anatomy and Physiology.* McGraw-Hill, 4th ed., 2002.

[8] G. J. Tortora and S. R. Grabowski, *Principles of Anatomy and Physiology.* Wiley, 9th ed., 2000.

[9] C. Stevens, S. Durham, L. Eve, and D. Ewins, "Preliminary findings of a study of the effect of functional electrical stimulation on the gait of children with cerebral palsy," in *Proc. 6th Ann. Conf. Int. Functional Electrical Stimulation Soc., (Cleveland, USA)*, pp. 85–87, 2001.

[10] S. C. Lee, S. K. Stackhouse, T. A. Ronan, K. W. Parker, J. J. McCarthy, S. A. Binder-Macleod, and B. T. Smith, "Preliminary results of percutaneous neuromuscular electrical stimulation for strength training in children with cerebral palsy," in *Proc. 8th Ann. Conf. Int. Functional Electrical Stimulation Soc., (Queensland, Australia)*, pp. 252–255, 2003.

[11] C. M. Gregory and C. S. Bickel, "Recruitment patterns in human skeletal muscle during electrical stimulation," *Phys Ther*, vol. 85, pp. 358–364, Apr 2005.

[12] J. S. Petrofsky, H. Heaton, and C. A. Phillips, "Outdoor bicycle for exercise in paraplegics and quadriplegics," *J Biomed Eng*, vol. 5, pp. 292–296, Oct 1983.

[13] K. Hunt, T. Schauer, N. Negård, W. Stewart, and M. Fraser, "A pilot study of lower-limb FES cycling in paraplegia," in *Proc. 7th Ann. Conf. Int. Functional Electrical Stimulation Soc., (Ljubljana, Slovenia)*, 2002.

[14] T. Perkins, N. de N. Donaldson, R. Fitzwater, G. Phillips, and D. Wood, "Leg powered paraplegic cycling system using surface functional electrical stimulation," in *Proc. 6th Ann. Conf. Int. Functional Electrical Stimulation Soc., (Cleveland, USA)*, pp. 36–39, 2001.

[15] C. A. Phillips, D. Danopulos, P. Kezdi, and D. Hendershot, "Muscular, respiratory and cardiovascular responses of quadriplegic persons to an F. E. S. bicycle ergometer conditioning program," *Int J Rehabil Res*, vol. 12, no. 2, pp. 147–157, 1989.

[16] P. B. Arnold, P. P. McVey, W. J. Farrell, T. M. Deurloo, and A. R. Grasso, "Functional electric stimulation: its efficacy and safety in improving pulmonary function and musculoskeletal fitness," *Arch Phys Med Rehabil*, vol. 73, pp. 665–668, Jul 1992.

[17] K. E. Sloan, L. A. Bremner, J. Byrne, R. E. Day, and E. R. Scull, "Musculoskeletal effects of an electrical stimulation induced cycling programme in the spinal injured," *Paraplegia*, vol. 32, pp. 407–415, Jun 1994.

[18] N. Hjeltnes, A. K. Aksnes, K. I. Birkeland, J. Johansen, A. Lannem, and H. Wallberg-Henriksson, "Improved body composition after 8 wk of electrically stimulated leg cycling in tetraplegic patients," *Am J Physiol*, vol. 273, pp. 1072–1079, Sep 1997.

[19] H. L. Gerrits, A. de Haan, A. J. Sargeant, A. Dallmeijer, and M. T. Hopman, "Altered contractile properties of the quadriceps muscle in people with spinal cord injury following functional electrical stimulated cycle training," *Spinal Cord*, vol. 38, pp. 214–223, Apr 2000.

[20] T. W. J. Janssen, R. M. Glaser, and D. B. Shuster, "Clinical efficacy of electrical stimulation exercise training: Effects on health, fitness and function," *Topics in Spinal Cord Injury Rehabilitation*, vol. 3, no. 3, pp. 33–49, 1998.

[21] M. L. Sipski, J. A. Delisa, and S. Schweer, "Functional electrical stimulation bicycle ergometry: patient perceptions," *Am J Phys Med Rehabil*, vol. 68. pp. 147–149, Jun 1989.

[22] S. F. Figoni, R. M. Glaser, D. M. Hendershot, S. C. Gupta, A. G. Suryaprasad, M. M. Rodgers, and B. N. Ezenwa, "Hemodynamic responses of quadriplegics to maximal arm-cranking and FNS leg cycling exercise," in *Proc. 10th Ann. Conf. Int. IEEE Engineering in Medicine and Biology Soc., (New Orleans, USA)*, 1988.

[23] S. P. Hooker, S. F. Figoni, M. M. Rodgers, R. M. Glaser, T. Mathews, A. G. Suryaprasad, and S. C. Gupta, "Physiologic effects of electrical stimulation leg cycle exercise training in spinal cord injured persons," *Arch Phys Med Rehabil*, vol. 73, pp. 470–476, May 1992.

[24] P. D. Faghri, R. M. Glaser, and S. F. Figoni, "Functional electrical stimulation leg cycle ergometer exercise: training effects on cardiorespiratory responses of spinal cord injured subjects at rest and during submaximal exercise," *Arch Phys Med Rehabil*, vol. 73, pp. 1085–1093, Nov 1992.

[25] T. Mohr, J. Pødenphant, F. Biering-Sørensen, H. Galbo, G. Thamsborg, and M. Kjaer, "Increased bone mineral density after prolonged electrically induced cycle training of paralyzed limbs in spinal cord injured man," *Calcif Tissue Int*, vol. 61, pp. 22–25, Jul 1997.

[26] J. Raymond, G. M. Davis, and M. van der Plas, "Cardiovascular responses during submaximal electrical stimulation-induced leg cycling in individuals with paraplegia," *Clin Physiol Funct Imaging*, vol. 22, pp. 92–98, Mar 2002.

[27] D. Theisen, C. Fornusek, J. Raymond, and G. M. Davis, "External power output changes during prolonged cycling with electrical stimulation," *J Rehabil Med*, vol. 34, pp. 171–175, Jul 2002.

[28] R. M. Glaser, S. F. Figoni, S. R. Collins, M. M. Rodgers, A. G. Suryaprasad, S. C. Gupta, and T. Mathews, "Physiologic responses of SCI subjects to electrically induced leg cycle ergometry," in *Proc. 10th Ann. Conf. Int. IEEE Engineering in Medicine and Biology Soc., (New Orleans, USA)*, 1988.

[29] R. M. Glaser, S. F. Figoni, S. P. Hooker, M. M. Rodgers, B. N. Ezenwa, A. G. Suryaprasad, S. C. Gupta, and T. Mathews, "Efficiency of FNS leg ergometry," in *Proc. 11th Ann. Conf. Int. IEEE Engineering in Medicine and Biology Soc., (Seattle, USA)*, 1989.

[30] K. K. BeDell, A. M. Scremin, K. L. Perell, and C. F. Kunkel, "Effects of functional electrical stimulation-induced lower extremity cycling on bone density of spinal cord-injured patients," *Am J Phys Med Rehabil*, vol. 75, no. 1, pp. 29–34, 1996.

[31] S. A. Bloomfield, W. J. Mysiw, and R. D. Jackson, "Bone mass and endocrine adaptations to training in spinal cord injured individuals," *Bone*, vol. 19, pp. 61–68, Jul 1996.

[32] S.-C. Chen, C.-H. Lai, W. P. Chan, M.-H. Huang, H.-W. Tsai, and J.-J. J. Chen, "Increases in bone mineral density after functional electrical stimulation cycling exercises in spinal cord injured patients," *Disabil Rehabil*, vol. 27, pp. 1337–1341, Nov 2005.

[33] P. Eser, E. D. de Bruin, I. Telley, H. E. Lechner, H. Knecht, and E. Stüssi, "Effect of electrical stimulation-induced cycling on bone mineral density in spinal cord-injured patients," *Eur J Clin Invest*, vol. 33, pp. 412–419, May 2003.

[34] M. Kjaer, G. Perko, N. H. Secher, R. Boushel, N. Beyer, S. Pollack, A. Horn, A. Fernandes, T. Mohr, and S. F. Lewis, "Cardiovascular and ventilatory responses to electrically induced cycling with complete epidural anaesthesia in humans," *Acta Physiol Scand*, vol. 151, pp. 199–207, Jun 1994.

[35] D. J. Pons, C. L. Vaughan, and G. G. Jaros, "Cycling device powered by the electrically stimulated muscles of paraplegics," *Med Biol Eng Comput*, vol. 27, pp. 1–7, Jan 1989.

[36] R. M. Glaser, W. P. Couch, T. W. Janssen, J. W. Almeyda, D. D. Pringle, S. R. Collins, and T. Mathews, "A development system to enhance FES leg cycle ergometer technology," in *Proc. Ann. Conf.Rehabilitation Engineering and Assistive Technology Society of North America., (USA)*, 1996.

[37] N. Donaldson, T. A. Perkins, R. Fitzwater, D. E. Wood, and F. Middleton, "FES cycling may promote recovery of leg function after incomplete spinal cord injury," *Spinal Cord*, vol. 38, pp. 680–682, Nov 2000.

[38] J. S. Petrofsky, "New algorithm to control a cycle ergometer using electrical stimulation," *Med Biol Eng Comput*, vol. 41, pp. 18–27, Jan 2003.

[39] J. S. Petrofsky, C. A. Phillips, H. H. Heaton, and R. M. Glaser, "Bicycle ergometer for paralyzed muscle," *J Clin Eng*, vol. 9, pp. 13–19, Mar 1984.

[40] K. F. Eichhorn, W. Schubert, and E. David, "Maintenance, training and functional use of denervated muscles," *J Biomed Eng*, vol. 6, pp. 205–211, Jul 1984.

[41] G.-C. Jang, J.-J. J. Chen, C.-T. Shih, and T.-C. Huseh, "Design of FES-cycling system and its stimulation patterns," *Chinese J. Med. Biol. Eng.*, vol. 13, pp. 305–315, Dec 1993.

[42] M. Gföhler, M. Loicht, and P. Lugner, "Exercise tricycle for paraplegics," *Med Biol Eng Comput*, vol. 36, pp. 118–121, Jan 1998.

[43] K. J. Hunt, B. Stone, N.-O. Negård, T. Schauer, M. H. Fraser, A. J. Cathcart, C. Ferrario, S. A. Ward, and S. Grant, "Control strategies for integration of electric motor assist and functional electrical stimulation in paraplegic cycling: Utility for exercise testing and mobile cycling," *IEEE Transactions on Neural Systems and Rehabilitation Engineering*, vol. 12, no. 1, pp. 89–101, 2004.

[44] K. Chen, S.-C. Chen, K.-H. Tsai, J.-J. J. Chen, N.-Y. Yu, and M.-H. Huang, "An improved design of home cycling system via functional electrical stimulation for paraplegics," *International Journal of Industrial Ergonomics*, vol. 34, pp. 223–235, 2004.

[45] C. Fornusek, G. M. Davis, P. J. Sinclair, and B. Milthorpe, "Development of an isokinetic functional electrical stimulation cycle ergometer," *Neuromodulation*, vol. 7, pp. 56–54, Jan 2004.

[46] J. S. Petrofsky and J. Smith, "Three-wheel cycle ergometer for use by men and women with paralysis," *Med Biol Eng Comput*, vol. 30, pp. 364–369, May 1992.

[47] T. Angeli, M. Gföhler, T. Eberharter, and L. Rinder, "Tricycle for paraplegics using functional electrostimulation," *Med. Biol. Eng. Comp.*, vol. 37, pp. 326–327, 1999.

[48] R. M. Glaser, J. A. Gruner, S. D. Feinberg, and S. R. Collins, "Locomotion via paralyzed leg muscles: feasibility study for a leg-propelled vehicle," *J Rehabil R D*, vol. 20, pp. 87–92, Jul 1983.

[49] R. B. Stein, D. Roetenberg, S. L. Chong, and K. B. James, "A wheelchair modified for leg propulsion using voluntary activity or electrical stimulation," *Med Eng Phys*, vol. 25, pp. 11–19, Jan 2003.

[50] H. Berkelmans, D. Thijssen, P. Heesterbeek, B. van Ginneken, M. Hopman, D. van Kuppevelt, and J. Duysens, "Physiological responses after 4 weeks training with a hybrid FES tricycle in spinal cord injured individuals," in *Proc. 9th Ann. Conf. Int. Functional Electrical Stimulation Soc., (Bournemouth, UK)*, pp. 174–175, 2004.

[51] J.-J. J. Chen, N.-Y. Yu, D.-G. Huang, B.-T. Ann, and G.-C. Chang, "Applying fuzzy logic to control cycling movement induced by functional electrical stimulation," *IEEE Trans Rehabil Eng*, vol. 5, pp. 158–169, Jun 1997.

[52] M. Gföhler and P. Lugner, "Dynamic simulation of FES-cycling: influence of individual parameters," *IEEE Trans Neural Syst Rehabil Eng*, vol. 12, pp. 398–405, Dec 2004.

[53] T. A. Perkins, N. de N Donaldson, N. A. C. Hatcher, I. D. Swain, and D. E. Wood, "Control of leg-powered paraplegic cycling using stimulation of the lumbo-sacral anterior spinal nerve roots," *IEEE Trans Neural Syst Rehabil Eng*, vol. 10, pp. 158–164, Sep 2002.

[54] J.-J. J. Chen, C.-T. Shih, D.-G. Huang, N.-Y. Yu, M.-S. Ju, and T.-C. Huseh, "Development of FES-cycling system with closed-loop control," *Chinese J. Med. Biol. Eng*, vol. 14, pp. 195–209, Sep 1994.

[55] J.-J. J. Chen and N.-Y. Yu, "The validity of stimulus-evoked EMG for studying muscle fatigue characteristics of paraplegic subjects during dynamic cycling movement," *IEEE Trans Rehabil Eng*, vol. 5, pp. 170–178, Jun 1997.

[56] L. R. Vialle and E. Vialle, "Pediatric spine injuries," *Injury*, vol. 36 Suppl 2, pp. B104–B112, Jul 2005.

[57] L. C. Vogel and M. J. DeVivo, "Etiology and demographics," in *The Child With a Spinal Cord Injury* (R. R. Betz and M. Mulcahey, eds.), ch. 1, pp. 3–12, American Academy of Orthopaedic Surgeons, 1996.

[58] R. J. Triolo, R. R. Betz, M. J. Mulcahey, and E. R. Gardner, "Application of functional neuromuscular stimulation to children with spinal cord injuries: candidate selection for upper and lower extremity research," *Paraplegia*, vol. 32, pp. 824–843, Dec 1994.

[59] B. Martin, "Paediatric cervical spine injuries," *Injury*, vol. 36, pp. 14–20, Jan 2005.

[60] C. d'Amato, "Pediatric spinal trauma: injuries in very young children," *Clin Orthop Relat Res*, pp. 34–40, Mar 2005.

[61] M. Moynahan, R. R. Betz, R. J. Triolo, and A. H. Maurer, "Characterization of the bone mineral density of children with spinal cord injury," *J Spinal Cord Med*, vol. 19, pp. 249–254, Oct 1996.

[62] F. Miller, "Pathologic long-bone fractures: Diagnosis, etiology, management and prevention," in *The Child With a Spinal Cord Injury* (R. R. Betz and M. Mulcahey, eds.), ch. 28, pp. 331–338, American Academy of Orthopaedic Surgeons, 1996.

[63] R. Betz, R. Triolo, V. Hermida, M. Moynahan, E. Gardner, A. Maurer, S. Cook, and J. Bennett, "The effects of functional neuromuscular stimulation on the bone mineral content in the lower limbs of spinal cord injured children," *J Am Paraplegia Soc*, vol. 14, no. 2, pp. 65–66, 1991.

[64] F. Miller and R. R. Betz, "Hip joint instability," in *The Child With a Spinal Cord Injury* (R. R. Betz and M. Mulcahey, eds.), ch. 31, pp. 353–362, American Academy of Orthopaedic Surgeons, 1996.

[65] J. P. Lubicky and R. R. Betz, "Spinal deformity in children and adolescents after spinal cord injury," in *The Child With a Spinal Cord Injury* (R. R. Betz and M. Mulcahey, eds.), ch. 32, pp. 363–370, American Academy of Orthopaedic Surgeons, 1996.

[66] M. R. Nelson, A. G. Tilbor, L. Frieden, and Q. W. Smith, "Introduction to pediatric rehabilitation," in *The Child With a Spinal Cord Injury* (R. R. Betz and M. Mulcahey, eds.), ch. 39, pp. 461–470, American Academy of Orthopaedic Surgeons, 1996.

[67] G. M. Yarkony and K. Kohlmeyer, "Functional outcomes in pediatric spinal cord injury," in *The Child With a Spinal Cord Injury* (R. R. Betz and M. Mulcahey, eds.), ch. 61, pp. 699–707, American Academy of Orthopaedic Surgeons, 1996.

[68] K. A. Johnson and S. J. Klaas, "Recreational therapy," in *The Child With a Spinal Cord Injury* (R. R. Betz and M. Mulcahey, eds.), ch. 54, pp. 619–624, American Academy of Orthopaedic Surgeons, 1996.

[69] I. González-Mueller and M. A. Kelly, "Wheelchairs and seating systems: Evaluation and training," in *The Child With a Spinal Cord Injury* (R. R. Betz and M. Mulcahey, eds.), ch. 41, pp. 483–500, American Academy of Orthopaedic Surgeons, 1996.

[70] B. T. Smith and E. R. Gardner, "Functional electrical stimulation," in *The Child With a Spinal Cord Injury* (R. R. Betz and M. Mulcahey, eds.), ch. 64, pp. 731–750, American Academy of Orthopaedic Surgeons, 1996.

[71] R. J. Triolo, "Overview of research in pediatric spinal cord injury," in *The Child With a Spinal Cord Injury* (R. R. Betz and M. Mulcahey, eds.), ch. 60, pp. 691–697, American Academy of Orthopaedic Surgeons, 1996.

[72] B. D. Popovic, J. Watt, R. Stein, J. Raso, and T. Overton, "Functional electrical stimulation in the rehabilitation of the spinal cord injured child," in *Proc. 13th Ann. Conf. Int. IEEE Engineering in Medicine and Biology Soc., (Orlando, USA)*, vol. 13, pp. 938–939, Oct 1991.

[73] B. Smith, R. Betz, and M. Mulcahey, "Reliability of percutaneous intramuscular electrodes for upper extremity functional neuromuscular stimulation in adolescents with C5 tetraplegia," *Arch Phys Med Rehabil*, vol. 75, pp. 939–945, 1994.

[74] B. T. Smith, R. R. Betz, and M. Mulcahey, "Implantable FES system for upper or lower limb function in the growing child with a spinal cord injury," in *Proc. 6th Ann. Conf. Int. Functional Electrical Stimulation Soc., (Cleveland, USA)*, pp. 82–84, 2001.

[75] T. Johnston, B. Smith, R. Betz, M. Mulcahey, and J. McCarthy, "Implanted functional electrical stimulation for upright mobility in pediatric spinal cord injury: A follow-up report," in *Proc. 28th Ann. Conf. Northeast. IEEE Bioengineering, (Philadelphia, USA)*, pp. 13–14, Apr 2002.

[76] D. Robinson, R. J. Triolo, and R. Betz, "Physiological responses to FNS exercise in SCI children," in *Proc. 11th Ann. Conf. Int. IEEE Engineering in Medicine and Biology Soc., (Seattle, USA)*, pp. 1498–1499, Nov 1989.

[77] L. C. Vogel, S. J. Klaas, J. P. Lubicky, and C. J. Anderson, "Long-term outcomes and life satisfaction of adults who had pediatric spinal cord injuries," *Arch Phys Med Rehabil*, vol. 79, pp. 1496–1503, Dec 1998.

[78] S. Simcox, S. Parker, G. M. Davis, R. W. Smith, and J. W. Middleton, "Performance of orientation sensors for use with a functional electrical stimulation mobility system," *J Biomech*, vol. 38, pp. 1185–1190, May 2005.

[79] S. Simcox, G. Davis, A. Barriskill, J. Middleton, I. Bruinsma, M. Duncan, and R. Smith, "A portable, 8-channel transcutaneous stimulator for paraplegic muscle training and mobility-A technical note," *J Rehabil Res Dev*, vol. 41, no. 1, pp. 41–52, 2004.

[80] R. Davis, J. Patrick, and A. Barriskill. "Development of functional electrical stimulators utilizing cochlear implant technology," *Med Eng Phys*, vol. 23, pp. 61–68, Jan 2001.

[81] B. T. Smith, R. R. Betz, T. Johnston, B. Benda, M. Mulcahey, R. Davis, and A. Barriskill, "Initial experiences with the praxis multi-functional implantable FES system for indibiduals with spinal cord injury," in *Proceedings FESnet 2002 1st Biannual Conference*, 2002.

[82] H. J. Luinge, P. H. Veltink, and C. T. M. Baten, "Estimation of orientation with gyroscopes and accelerometers," in *Proc. 21st Ann. Conf. Int. IEEE Engineering in Medicine and Biology Soc., (Atlanta, USA)*, vol. 2, p. 844, Oct 1999.

[83] E. S. Idsø, T. A. Johansen, and K. J. Hunt, "A simplified nonlinear biomechanical model for FES-cycling," in *Proc. 8th Ann. Conf. Int. Functional Electrical Stimulation Soc., (Queensland, Australia)*, 2003.

[84] C. G. McRae and K. J. Hunt, "Development of methods and equipment for functional electrical stimulation induced cycling for use within the paediatric spinal cord injured population," in *Proc. 4th Ann. Conf. IEEE EMBSS UKRI PG Biomedical Engineering and Medical Physics, (Reading, UK)*, pp. 7–8, July 2005.

[85] G. F. Phillips, J. R. Adler, and S. J. G. Taylor, "A portable programmable eight-channel surface stimulator," in *Proc. Ljubljana FES Conference*, pp. 166–168, 1993.

[86] T. W. J. Janssen, M. Bakker, A. Wyngaert, K. H. L. Gerrits, and A. de Haan, "Effects of stimulation pattern on electrical stimulation-induced leg cycling performance," *J Rehabil Res Dev*, vol. 41, no. 6, pp. 787–796, 2004.

[87] W. B. Scott, S. C. K. Lee, T. E. Johnston, and S. A. Binder-Macleod, "Switching stimulation patterns improves performance of paralyzed human quadriceps muscle," *Muscle Nerve*, vol. 31, pp. 581–588, May 2005.